2021

Development of a Novel In-Situ Chemical Sampler for Aquatic Systems

Alec W. Johnson
University of Montana, Missoula

Development of a Novel In-Situ Chemical Sampler for Aquatic Systems

By

ALEC WILLIAM JOHNSON

B.A. ACS Chemistry - Traditional, Concordia College, Moorhead, Minnesota, 2017

Thesis

presented in partial fulfillment of the requirements
for the degree of

Master of Science in Chemistry, Environmental/Analytical

The University of Montana
Missoula, MT

2021

Approved by:

Scott Whittenburg, Dean of The Graduate School

Michael DeGrandpre, Chair
Department of Chemistry and Biochemistry

Lu Hu
Department of Chemistry and Biochemistry

Ben Colman
W.A. Franke College of Forestry and Conservation

Johnson, Alec W., M.S., Spring 2021 *Analytical/Environmental Chemistry*

Development of a Novel In-Situ Chemical Sampler for Aquatic Systems

Chairperson: Michael DeGrandpre

Co-Chairpersons: Ben Colman, Lu Hu

There has been a long-standing need to study Dissolved Organic Carbon (DOC) within aquatic systems. DOC is an important water quality parameter that provides insights into ecological and carbon cycle processes in aquatic systems. DOC is not easily studied due to traditional, labor-intensive sampling methods. Often, optical (e.g. fluorescence) proxy estimations for DOC are used instead of directly sampling for DOC. Using either low frequency measurements or proxy estimations for DOC can lead to inadequate understanding of the natural processes that control DOC in aquatic systems.

This thesis outlines a in-situ sampler that will be capable of collecting, preserving, and storing aquatic samples, with a special focus on Total Organic Carbon (TOC). In this initial phase of development, TOC is sampled instead of DOC due to issues encountered with in-line filtration. Employing a novel "smart sampling" technique that uses conductivity as a conservative tracer, this system collects and preserves the sample in real-time. The novel technique employed by the DUCS could be expanded to sample for other important aquatic species, and such the sampler has been tentatively named the Deployable Underwater Chemical Sampler (DUCS). The high frequency datasets that can be generated using the DUCS will be able to provide greater into ecological and carbon cycle processes.

Chapters in this thesis will primarily describe the design and performance of the DUCS for TOC sampling, as well as discuss possible future improvements. The performance of the DUCS both in and outside of laboratory settings is explored. A chapter describing initial experimental design for an in-situ UV-Persulfate based DOC sensor is also included.

There was an overall average DUCS accuracy error of ~25-30% when using the DUCS for TOC sampling versus collected QC samples during deployments in the Clark Fork River (CFR). The TOC sampling uncertainty of the DUCS for these initial deployments was shown to be close to compliance for standard method 5310 and USEPA method 415.3. This data, along with data collected during lab studies, provides evidence for the effectiveness of the prototype DUCS sampling system. With future improvements, this prototype could be improved into a commercially viable sampling system.

Acknowledgements

I would like to thank the University of Montana's chemistry department, and all the great professors I have worked with, for developing my skills as a balanced chemist.

I would like to thank to my research advisor, Dr. Michael DeGrandpre for his support through my graduate experience. Through both successes and failures, he always pushed me forward with guidance and support, continuously developing a broad skillset that will be invaluable to me in the future.

I would also like to thank Cory Beatty and the rest of the DeGrandpre group for their continued support, lab expertise, and guidance during the instrument development work carried out for this thesis. I would like to give special thanks to Fischer Young for his work repairing and maintaining the Aurora TOC analyzer, which was very important in generating the data presented in this thesis.

I would like to thank Maury Valett for his support and access to his biological sciences lab, which data from this thesis heavily depended upon. I would also like to thank the rest of the Valett lab staff for their continued support and expertise, with special thanks to lab-manager Claire Utzman.

I would like to thank Lu Hu and Ben Coleman for their continued support and involvement in the success of this project as the remainder of my graduate committee.

I would like to thank Reggie Spaulding and David Podrasky, as well as the rest of the staff at Sunburst Sensors for their continued support during this thesis.

I would finally like to thank my friends and family for their support of me to this point, to whom I hope to continue to show success in my endeavors for in the future.

TABLE OF CONTENTS

Page #

Title Page…… i

Abstract…… ii

Acknowledgements…… iii

Table of Contents……...iv-v

List of Figures……...vi-vii

List of Tables……...….viii

Chapters

I. Introduction…… 1

A. Overview of the Importance of DOC in Aquatic Systems……..…….……..... 1

B. Overview of Current Methods for Monitoring DOC in Aquatic Systems…..….. 4

C. Overview of DUCS In-Situ Sampler Background and Methodology……8

II. A Deeper Look into Aquatic Sampling and DUCS Design…….……....……10

A. Overview of the status of current discrete sampling technology.....…….10

B. Overview of the status of current continuous sampling technology…… …11

C. Design Goal for the DUCS ……..……13

III. In-Situ UV-Persulfate DOC Sensor Development……..……15

A. Overview of In-Situ UV Persulfate DOC Sensor Design……....…….15

B. DOC Sensor Development – UV Source Selection…….…..……16

C. DOC Sensor Development – Method Optimization……...…….….....19

IV. DUCS Development……...…….…..……27

A. DUCS – Initial Prototype…….....……27

B. DUCS – Pump Optimization……29

C. DUCS – SAMI Mounted Model and Dedicated Software Controls…… 32

D. DUCS – Sample Filtration……..……..…….……35

E. DUCS – System Characterizations……..……....….....36

F. DUCS – Blanks…….…….....43

i. Sampling TOC Contamination (Sampler Blanks)……...43

ii. Post-Sampling TOC Contamination (Processing Blanks)……...44

G. DUCS – Standard Sampling Method…….……...……46

H. DUCS – In-Lab Sample Analysis…….....50

I. DUCS – TOC vs. DOC Sampling…….. …….53

V. Field Deployments - Data Analysis and Discussion…….……....55

A. DUCS – Field Deployment 1…….……...55

B. DUCS – Field Deployment 2……56
C. DUCS – Field Deployment 3……62
D. DUCS – Post Deployment System Optimization……68
VI. Future Work and Conclusions……77
A. Future Work……77
B. Conclusions……81
VII. Appendices……82
A. DOC Sensor Software Controls……82
B. DUCS Software Controls and Data Acquisition……85
i. DUCS Sampling Sequence – Standard Cleaning Sequence……86
ii. DUCS Sampling Sequence – Visual Indicator Loader…. ……88
iii. DUCS Sampling Sequence – Standard Sampling Sequence……91
iv. DUCS Sampling Sequence – Storage Dispense……101
C. Aurora 1030 Instrument Operation Procedure ……102
D. DUCS Additional Information……107
E. Analytical Equipment Instrumental Specs……113
F. Additional Protocols……116
i. POC/TOC Standard preparation protocol……116
ii. Small vial cleaning and conductivity analysis procedure……117
VIII. References Cited……119

List of Figures

Fig. 1 - *The relationship between the different pools making up total carbon (TC).* – ***p. 4***

Fig. 2 – *High frequency FDOM data (Vaughn et al., 2017).* – ***p. 6***

Fig. 3 – *Flourescence Index vs. DOC timeseries in separate watersheds (Hood et al., 2016.)* **– *p. 7***

Fig. 4 – *Conceptual DUCS sample collection schematic.* – ***p. 9***

Fig. 5 – *Schematic representation of sample gradient dispersion in small bore tubing (Jannasch et. al., 2004).* – ***p. 12***

Fig. 6 - *A schematic representation of the benchtop UV-PS sensor.* – ***p. 16***

Fig. 7 - *Ocean Optics developed HG-1 Mercury Argon Calibration Source.* – ***p. 16***

Fig. 8 - *Agilent developed Agilent 8453 UV Spec.* – ***p. 17***

Fig. 9 - *DOC concentration (ppm) vs. Time (min) of irradiation with the HG-1.* – ***p. 17***

Fig. 10 - *LG-Innotek developed high-powered LEUVA77M00HU00 UV-LED.* – ***p. 18***

Fig. 11 - *DOC concentration (ppm) vs. Time (min) of irradiation with the high-powered UV-LED versus HG-1.* – ***p. 19***

Fig. 12 - *% Abs Depletion / min vs. Light Source Intensity (%).* – ***p. 20***

Fig. 13 - *% Abs Depletion / min vs. Persulfate Concentration.* – ***p. 21***

Fig. 14 - *% Abs Depletion / min vs. Temperature (C).* – ***p. 22***

Fig. 15 – *Exponential experimental decay functions for KHP.* – ***p. 23***

Fig. 16 a-b – *Degradation of organics with the high-powered UV-LED* – ***p. 24-25***

Fig. 17 - *DOC (ppm) vs. Time (min) of irradiation with the high-powered UV-LED.* – ***p. 26***

Fig. 18 - *DUCS benchtop prototype design.* – ***p. 27***

Fig. 19 – *Results of sequential sample absorbance analysis for test samples stored in coil.* – ***p. 28***

Fig. 20 – *Overlay comparison between diaphragm and syringe pumps.* – ***p. 30***

Fig. 21 – *Comparison between organic and inorganic sample plugs.* – ***p. 31***

Fig. 22 – *DUCS mounted inside SAMI instrumentation housing.* **– *p. 32***

Fig. 23 - *Simplified plumbing diagram for DUCS instrumentation.* – ***p. 33***

Fig. 24 – *Mixer effectivess graphic.* **– *p. 34***

Fig. 25 - *Conductivity vs. dilution factor of 5% HCl with DI.* – ***p. 39***

Fig. 26 - *Pumping capacity characterization.* – ***p. 41***

Fig. 27 - *Conductivity measurements – standard sampling method.* – ***p. 47***

Fig. 28 – *Accuracy of volumetric deliveries in standard sampling method.* – ***p. 48***

Fig. 29 – *Gaussian modeling for estimating peak overlap between samples.* – ***p 49***

Fig. 30 – *DOC calibration curve – Aurora 1030.* – ***p. 50***

Fig. 31 – *Analysis of DOC standards collected with the benchtop DUCS.* ***– p. 52***

Fig. 32 – *TOC experiment results, in-situ.* – ***p. 54***

Fig. 33 – *Initial Deployment Picture.* – ***p. 55***

Fig. 34 – *Closed-shell DUCS with protective coverings.* – ***p. 56***

Fig. 35 – *Conductivity series for the second deployment sample set.* – ***p. 57***

Fig. 36 – *Overlay of DUCS samples against QC samples timeseries for second deployment.* – ***p. 58***

Fig. 37 – *1:1 plot of DUCS samples against QC'ed samples for second deployment.* – ***p. 59***

Fig. 38 – *Overlay of SUNA absorbance values and TOC values from DUCS for second deployment.* – ***p. 60***

Fig. 39 – *Correlation plot of DUCS samples against SUNA absorbances for second deployment.* – ***p. 61***

Fig. 40 – *Overlay of TOC samples against hydrology data for second deployment.* – ***p. 62***

Fig. 41 – *Ice over at DUCS location during third deployment.* – ***p. 63***

Fig. 42 – *Conductivity series for the third deployment sample set.*– ***p. 63***

Fig. 43 – *Overlay of DUCS samples against QC samples timeseries for third deployment.* – ***p. 64***

Fig. 44 – *1:1 plot of DUCS samples against QC'ed samples for third deployment.* – ***p. 65***

Fig. 45 – *Overlay of SUNA absorbance values and TOC values from DUCS for third deployment.* – ***p. 66***

Fig. 46 – *Correlation plot of DUCS samples against SUNA absorbances for third deployment.*– ***p. 67***

Fig 47 – *DUCS values for samples collected with standard sampling scheme, 450-m coil.* ***– p. 68***

Fig 48 – *DUCS values for samples collected with the reversed sampling scheme.* ***– p. 70***

Fig 49 – *Overlay of results presented in Fig. 47 and Fig. 48.* ***– p. 70***

Fig 50 – *1:1 plot of DUCS samples against standards for Fig. 47.* ***– p. 71***

Fig. 51 – *DUCS values for samples collected with standard sampling scheme, 150-m coil* – ***p. 75***

Fig. 52 – *Comparison between 1:1 plot of DUCS samples against for Fig. 47 and 51*– ***p. 76***

Fig. A1 - *Computer interface for the PyKloehn software.* – ***p. 82***

Fig. A2 - *Computer interface for the NoModem software.* – ***p. 84***

Fig. C1 – *Experimental results comparing DOC Curves generated on the Aurora using KHP or a less reactive DOC standard****. – p. 86***

Fic C2 – *Experimental results examining the effects of inorganic carbon matrix on Aurora analysis****. – p. 87***

Fig. D1 – *Electrical connection diagram.* – ***p. 92***

Fig. D2 – *Software specified pin-outs for valves and pump.* – ***p. 93***

Fig. D3 – *Tubing diagram and valve orientation.* – **p. 94**

Fig. D4 – *Full range of dilution curve for 5% HCl – 2nd order polynomial.* – **p. 95**

Fig D5 – *Typical dilution standard curve for 1 % HCl.* – **p. 95**

Fig D6 – *1:1 plot of TOC values for polynomial vs. linear conductivity fits.* – **p. 96**

Fig. E1 – *Aurora 1030 instrument specs.* – ***p. 97***

Fig. E2 – *F30 and InLab 751 conductivity setup specs.* – ***p. 97***

Fig. F1 – *Dilution factor standard curve for POC standard.*– ***p. 101***

Fig. F2 – S*mall vial station setup.* – ***p. 101***

Fig. F3 – *Visual indicator on coil.* – ***p. 102***

List of Tables

Table 1 - *Summary of average degradation rates observed and calculated from absorbance measurements for heated Persulfate/UV, UV-PS, UV (no PS), and PS (no UV) methodologies. –* ***p. 22***

Table 2 - *Summary of average degradation rates observed using the Aurora 1030 for a range of different organic compounds. Fischer DOC standard comes as a 1000 ppm C master solution used for calibration of DOC instrumentation. –* ***p. 24***

Table 3 - *% Recovery of DOC in acidified and unacidified river water over a 2- week timespan. –* ***p. 38***

Table 4– *Estimated power draw requirements for various stages of separated sampling as well as estimated power draw for a complete separated sample. –* ***p. 42***

Table 5– *Mass of components utilized in the full DUCS design. –* ***p. 43***

Table 6– *Sources of TOC contamination at the sampling and processing levels. –* ***p. 45***

Table 7– *Back calculating DOC concentration in measured samples (separated) using dilution factors measured using conductivity with a 1 to 5 mL dilution using a volumetric flask. –* ***p. 51***

Table 8 - *Theoretical back calculated TOC values (ppm C) for DI and 5 ppm samples collected using the standard or reversed sampling schemes. The different cases represent contamination being introduced at the processing and/or sampling levels****. - p. 74***

Table D1 – *Previous pump models used in tubing circuit.****- p. 94***

I. Introduction

A. *Overview of the Importance of DOC in Aquatic Systems*

In aquatic environments, total organic matter (TOM) consists of two operationally defined phases, particulate organic matter (POM) and dissolved organic matter (DOM). DOM is generally defined to be the fraction of the TOM that will pass through a 0.45 μm filter (Thurman 1985). POM is the fraction that is filtered out in this process. DOM, the most mobile form of organic matter, plays a crucial role in many important processes that take place in aquatic systems. For example, DOM is a significant part of microbial metabolism, which in turn affects carbon and nutrient cycling. Having accurate measurements for DOM is also important in balancing carbon budgets both globally and locally (Santana et al., 2017; Smiley et al., 2017), determining biological oxygen demand (Khamis et al., 2016), monitoring the effectiveness of disinfection processes for waste treatment (Khan et al., 1998), and ascertaining the major energy sources for heterotrophic respiration in aquatic systems (Cooper et al., 2016).

The majority of DOM in freshwater systems originates from the breakdown and solubilization of organic matter through the accumulation of vegetation and biological waste materials (Guggenberger 1994; McDowell 2003; Tate et al., 1983). The exact elemental composition of DOM is largely dependent on its origin, but carbon is always the major structural component. Due to the large amount of carbon in DOM, it is often quantified by its total carbon content and is referred to as Dissolved Organic Carbon (DOC), which is functionally defined as the Total Organic Carbon (TOC) that passes through a 0.45 μm filter. Unfiltered TOC includes Particulate Organic Carbon (POC) larger than 0.45 μm, and is used as a measure of the total amount of organic carbon in an aqueous system.

Three categories present the major fractions of classically defined DOC in aquatic systems: 1) humic/fulvic substances, 2) polysaccharides, and 3) proteins (Nebbioso et al., 2013). These groups of molecules have highly varying molecular properties and reactivities and can be further

categorized as “labile” DOM or “recalcitrant” DOM, with labile species having faster turnover rates in aquatic systems (Nebbioso et al., 2013; Schulze 2005). Differences in DOC lability is seen because DOC is a heterogeneous composite of all the possible soluble organic compounds within the ecosystem (Marschner et al., 2003). The labile fraction of DOM consists mainly of simple carbohydrate compounds such as glucose or fructose, low molecular weight organic acids, amino sugars, and small proteins (Guggenberger 1994; Kaiser et al., 2001; Qualls et al., 1992). Both humic and fulvic acids are regarded as supramolecular assemblies of up to thousands of different organic molecules, (Nibbioso 2013; Piccolo 2001) and are generally considered less labile than lower molecular weight organics. The recalcitrant fraction also consists of polysaccharides, which are the breakdown products of cellulose and hemicellulose and higher molecular weight compounds that originate from microbial degradation of plant products (2003, Benner et al., 2011; Marschner et al., 2003) and enters aquatic systems as an allochthonous DOM source. The recalcitrant fraction of DOM originating from allochthonous sources are often less readily utilized by microbial life than the fraction originating from autochthonous, or in-situ sources (Asmala et al., 2018; Hansell 2013; Kritzberg et al., 2004). Autochthonous sources of DOM, coming from phytoplankton photosynthesis, incomplete grazing of phytoplankton and lysis of bacterial cells (Thornton, 2014) typically have lower average molecular weights. These compounds constitute a more labile carbon source for heterotrophic metabolism (Jiao et al., 2010; Thornton, 2014). Although less labile than autochthonous DOM, allochthonous DOM must still be considered as net-ecosystem heterotrophy often results from the bacterial metabolism of both sources of DOM (Cole et al., 1988).

DOM, and by extension DOC, is often considered to be the most mobile and reactive component of the TOM pool. Because of this, DOC often regulates major biogeochemical processes in aquatic systems. The thermodynamically available DOC is often termed DOC quality and can affect the growth rate of organisms, with faster growth rates associated with more thermodynamically available DOC (Stewart and Wetzel, 1981; Agren et al., 2008). DOC quality can be determined using quantitative analysis as well as biological assays on DOC samples (Park

et al., 2004; Ross et al., 2013; Buffle et al. 1982). The processes affected by DOC quality include the transformation and downstream transport of essential nutrients (Schiff et al., 1990), O_2 demand (Calleja et al., 2019; Coffin et al., 1993), and complexation of environmentally important heavy metals such as Cu, Pb, Hg, and Cd (Baken et al., 2011; Yi et al., 2019). These processes can in turn affect the overall growth rates of microorganisms in these aquatic systems, altering the carbon and nutrient cycling rates that are observed (Ågren et al., 2008). They are also often utilized as the energy substrate in the microbial processing of larger more recalcitrant organics (Stewart et al., 1981). In other words, DOC is an important microbial food source. Respiration of the DOC pool by microorganisms can also lead to emissions of carbon dioxide to the atmosphere (Freeman et al., 2011; Evans et al., 2016; Lynch et al., 2010). Due to all these factors, the flux of DOC throughout aquatic ecosystems can be a significant component of carbon budgets within these ecosystems.

DOC is also able to hydrologically transport carbon between different pools in the ecosystem through downstream riverine transport. Riverine exports of DOC can impair downstream water quality and aquatic ecology (Hruska et al., 2009). While changes occur in land use, industrial and municipal waste disposal, and climate occur, measurement of response variables such as DOC in these aquatic systems will become more and more critical to document effects of these changes. For example, several watersheds have been experiencing increases in DOC transport with the increasing temperatures associated with climate change (Freeman et al., 2001; Huntington et al. 2016; McDonough et al., 2020; Ritson et al., 2014). Understanding the sources and sinks of the DOC pool are also important as they affect our understanding of Dissolved Inorganic Carbon (DIC) and alkalinity. Alkalinity can be affected by contributions of deprotonated organic acids, which can lead to misestimation of carbon fluxes, as well as overestimation of pCO_2 (Cai et al., 1998; Hunt, et al., 2011). This effect is especially important in systems where the DOC pool can be larger than the DIC pool (Wang, et al., 2013).

B. Overview of Current Methods for Monitoring DOC in Aquatic Systems

DOC has traditionally been measured in one of two ways, either 1) manual sampling for DOC with lab analysis or 2) measuring a DOC proxy such as Fluorescent or Colored Dissolved Organic Matter (FDOM or CDOM). Manual sampling of DOC is limited by location access and costs associated with labor-intensive sampling and analysis. These are some of the most common reasons behind low-frequency DOC data (Köhler et al., 2008) in studies conducted today. DOC samples that have been manually collected are typically analyzed using high temperature combustion oxidation (HTOC), or UV-Persulfate oxidation instrumentation.

There are numerous lab-based DOC/TOC analyzers on the market that utilize HTOC or UV-Persulfate oxidation (Bolan et al., 1996, Doyle et al., 2004). Measurement of DOC or TOC with these analyzers involves the removal of inorganic carbon with acid, sparging of the resultant carbon dioxide, and finally the oxidation of the remaining organic carbon. This remaining portion of organic carbon is termed Non-Purgeable Organic Carbon (NPOC). The purgeable VOC fraction is typically a very small percentage of the overall DOC pool, and often negligible (MacKinnon et al., 1979). A breakdown of the relationship between the different pools making up total carbon (TC) is shown in Fig. 1. This figure shows the fraction of organic carbon analyzed (NPOC) using a TOC analyzer which consists of DOC and POC, along with the fractions of carbon removed prior to analysis (TIC + V/POC).

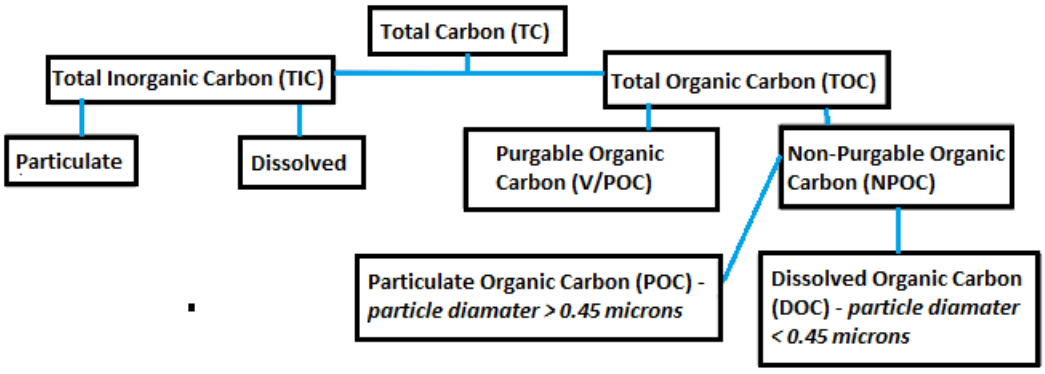

Figure 1 - *The relationship between the different pools making up total carbon (TC).*

Aquatic systems often have rapid water quality changes that are only observable with high-frequency measurements (Jollymore et al., 2012; Sobczak and Raymond, 2015; Kirchner et al., 2004). DOC concentrations in freshwater systems have been found to be highly variable over time (Zarnetske et al., 2018, Winterdahl et al., 2016). High-frequency DOC data, are valuable because they give information about biotic activity and episodic events within aquatic ecosystems. Episodic events and other short-term (e.g., diel) variability are often missed by traditional low-frequency methods of DOC sampling. Monitoring DOC as a response variable with respect to light, temperature, discharge, weather events, concentration of toxic metals, and other factors will be important for a more complete understanding of aquatic systems in the future. Many biological processes, especially in highly productive systems, will also vary significantly over short temporal scales (Johnson et al., 1994; Dickey et al., 1997; Dafner et al., 2002). It is essential to be able to frequently monitor DOC when calculating carbon fluxes in systems, which is an important part of accurately balancing the carbon budget (Battin et al. 2009).

While general trends in chemical variability can be resolved through periodic sampling (Michaels et al., 1996; Karl et al., 1996; Rebstock, 2002; Chavez et al., 1991), there remains problems associated with traditional methods of DOC sampling. These low-frequency DOC measurements can misestimate true carbon fluxes (Regier et al., 2016). Low-frequency measurements also lead to only seasonal or annual trends being analyzed. (Bishop et al., 1990; Stroheimer et al., 2013).

Proxy estimations of DOC can in part solve weaknesses associated with low-frequency manual sampling. Often these proxies are generated with previously mentioned FDOM or CDOM optical instrumentation that can be deployed in-situ. By using spectroscopic instrumentation dedicated for the analysis of either FDOM or CDOM, sample frequency for DOC can improve dramatically (Carstea et al., 2020; Tunaley et al., 2016; Saraceno et al., 2009; Dickey et al., 1997), as spectroscopic measurements are very fast.

For example, examine the high-frequency FDOM data that was collected during storm events in the Lake Champlain Basin of Vermont in the Northeastern United States (Fig. 2). This figure shows data with a measurement frequency of 15 minutes during a storm event. (Vaughan et al., 2017).

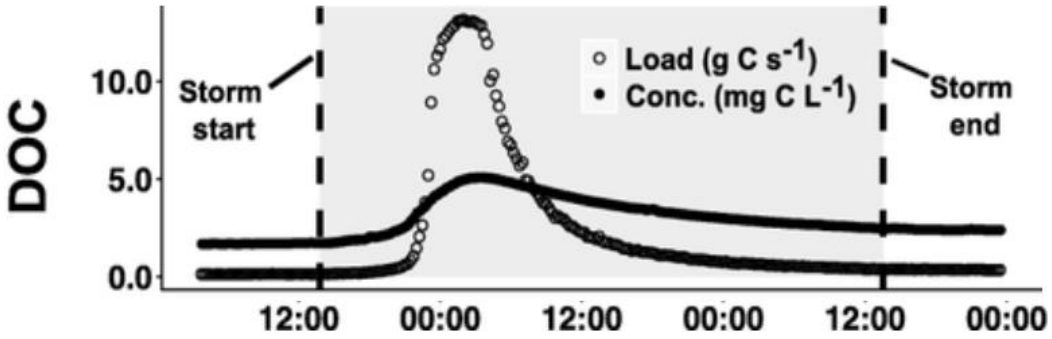

Figure 2 - *High frequency FDOM data that shows both the load and concentration changes in DOC (proxy) during an October 2014 storm event (Vaughan et al., 2017).*

"Proxy" DOC concentration values more than doubled during this event, with a steady return to baseline values over the next day. This is due to the storm event dominating riverine loads of dissolved organic carbon compared to baseflow concentrations. With traditional low-frequency monthly sampling intervals, a short-term event such as this may be completely missed. A potential return to baseline before the next scheduled sampling event would have been likely. Even with frequent, daily sampling there remains a potential to miss maximum DOC values seen during the event depending on when the sampling occurred.

These proxy estimations of DOC also have unique downsides compared to manually sampling. The relationship between FDOM or CDOM to DOC are highly site-specific, and correlations between these variables and DOC must be established at every new study site (Regier et al., 2016; Hood et al., 2016, Saraceno et al., 2017). Not only are these correlations site-variable, they are also temporally variable (Regier et al., 2016, Ferretto et al., 2016, Jaffe et al., 2008). New calibrations must be obtained frequently during deployment of an FDOM/CDOM sensor for accurate quantitation, so manual sampling must be done to determine the validity of the sensor's

dataset (Regier et al., 2016). In addition to this, these sensors must be turbidity corrected since they use optical measurements and have temperature related variability that must be accounted for as well (Saraceno et al., 2017; Downing et al., 2012). Using high-frequency sensing technology could also potentially miss important DOC quality variables, such as the humic and fulvic percentage makeup in DOM. These DOC variables can only be fully examined using high-frequency sampling technology.

In addition to increased turbidity that might accompany an event (Helton et al. 2015), the FDOM/CDOM:DOC correlation can also change during increased runoff. For example, see Fig. 3 which shows that the DOC vs. Fluorescence Index (FI) ratios change during a storm event. In multiple watersheds, there is no consistent ratio between these two measurements, both before and after the event.

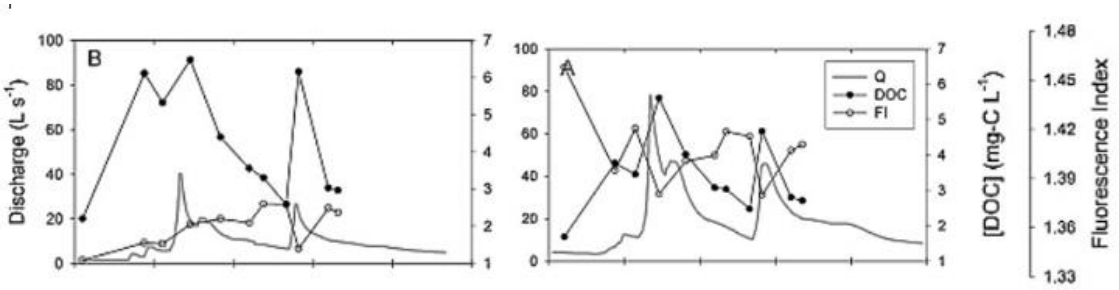

Figure 3 - *Time series of Fluorescence Index (FI) of DOC, DOC concentration and discharge at two separate watersheds (Hood et al., 2016). During the storm event, aromatic DOC mobilized from the catchment enters the stream, which increases the overall amount of DOC in the watershed while at the same time shifting the FI in each watershed.*

FI is defined as the ratio of the 450 nm and 500 nm emission values for FDOM. This measurement provides insight into whether DOC originated from autochthonous material that lacked lignin with a high FI, or allochthonous material that contained lignin with a low FI (Hood et al., 2016). In summary, while the correlation coefficients generated between FDOM/CDOM and DOC often exceed 0.80, there remains an innate uncertainty in the accuracy of these numbers since this method of measurement is still a proxy estimation (Vaughan et al., 2017; Regier et al., 2016; Tunaley, et al., 2016).

C. Overview of the Deployable Underwater Chemical Sampler (DUCS) Background and Methodology

Motivated by the factors outlined above, the original objective of this thesis was to develop a novel method for generating high-frequency in-situ DOC timeseries. This phase of the project centered around constructing a DOC analyzer that used UV-oxidation, similar to traditional lab-based technology, as there is currently no in-situ analyzer capable of direct DOC analysis. Due to a few insurmountable challenges with the development of this analyzer which will be discussed in Chapter III, this project shifted towards sampling technology. The DUCS design will be discussed primarily in Chapter IV. Using an automatic sampler for DOC monitoring will not have the temporal and spatial accuracy limitations present with optical sensing technology while having the secondary advantage of being able to directly experiment on DOC sample quality. For example, DOC quality characteristics in collected samples can be determined using chromatic fractionation or other chromatographic and biological methods (Fang et al., 2017; Yan et al., 2012). Sampling technology can also provide sample for analysis of other important aquatic species that may be linked to DOC, such as nutrients and metals. Filtration to "traditional" DOC size fractions of ~0.45 μm could not be accomplished with the simple pump technology employed by the DUCS. Therefore, the DUCS was designed to collect Total Organic Carbon (TOC) samples for in-lab analysis. The DUCS will be able collect DOC samples rather than TOC samples through future implementation of a pump capable of filtering to ~0.45 μm.

The sampler developed in this thesis uses a novel and innovative technique to preserve and store TOC samples for later analysis. Using a specially designed, valve controlled, low volume mixing loop, sample is preserved with hydrochloric acid (HCl). HCl is used as a conservative tracer of conductivity that simultaneously 1) preserves the sample 2) indicates where separate samples lie within the storage coil and 3) gives the acid dilution factor for each sample (further details in Chapter IV). Conductivity is particularly useful as a tracer for DOC/TOC because it has no carbon and can be an intimate part of the preservative itself. Conductivity values are also conservative with

dilution factor, allowing for easy back calculation of the original TOC concentrations.

Samples that have been acidified with the DUCS are dispensed into a very long, small internal diameter (ID) storage coil. Unacidified low conductivity sample is loaded both before and after the acidified sample segment to create regions of high and low conductivity, termed "peaks" and "valleys" respectively. Samples collected with the DUCS are then dispensed from storage coil to a series of small vials to be prepared for sample analysis (Appendix G). Conductivity measurements are taken in this step of the process, and discrete samples locations are determined from the conductivity peaks. Without this technique to determine sample location, there would be poor sample location accuracy in the storage coil due to less than reproducible pumping capacity. Each stored sample is then combined and diluted into a single sample for analysis. Samples are then analyzed using traditional High Temperature Catalytic Oxidation (HTOC) instrumentation, an Aurora 1030C, for direct analysis of TOC (or DOC) (Appendix E), and all relevant dilution factors are then applied to back-calculate original TOC concentrations. Fig. 4 shows a basic conceptual schematic representing the novel method of sample collection and determination utilized by the DUCS.

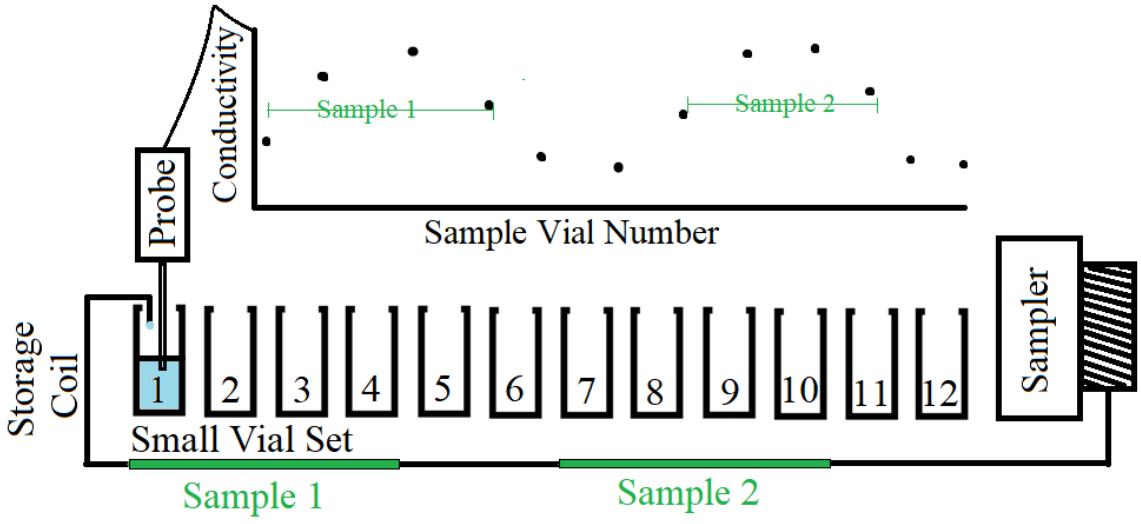

Figure 4 – *Conceptual schematic depicting sample collection and determination using the DUCS. When monitoring the conductivity of HCl acid reagent mixed with sample, individual samples dispensed from the storage coil can be determined and collected from conductivity "peaks", with "valleys" separating each sample.*

II. A Deeper Look into Aquatic Sampling and DUCS Design

A. Overview of the status of current discrete sampling technology

There are currently commercial instruments capable of sampling aquatic systems. These samplers could in part help solve the problems associated with manually sampling or using optical sensing technology for DOC data collection. For example, ISCO Teledyne, YSI and American Sigma all offer discrete samplers that have been used extensively in aquatic sampling (Wallin et al., 2015; Ensign et al., 2006; Vidon et al., 2012). However, no sampler on the market today is very useful for the high-frequency collection and storage of DOC samples. Often these samplers are utilized solely for the sampling of inorganic constituents such as metals and CO_2/O_2 in lakes and streams (Amudson et al., 2000). Many discrete sampler models are incapable of preserving degradable organics such as DOC. Preservation of DOC is required for autonomous sampling technology, due to significant microbial activity that can take place within 48 hours of sampling (Karanfil et al., 2002). Samples are typically reduced to a pH below 3.5, with pH 2.0 being the typical standard to suppress any microbial activity (Sharp et al., 1993). Studies have found that there are no significant changes in DOC concentrations for acidified samples that have been stored at approximately 4 degrees ^{o}C after sampling for periods of 2 weeks, 6-12 weeks, and 7-17 weeks (Ekstrom, 2011; Cook et al., 2016.; Carter et al., 2012).

Some of these samplers can add chemicals, such as an acid or preserving agent to suppress microbial activity, or acid can also be added to the discrete sample bottles prior to deployment (e.g. American Sigma Model 6201, Isco Model 6712). With the accurate pumping capacities of these samplers, acid concentrations can be introduced in known amounts. Despite these benefits, these discrete samplers come equipped with significant drawbacks for DOC sample collection. These samplers often are functionally limited to a maximum of between 12 to 24 samples (e.g. Sigma Model SD900, Isco Model 3700, Campbell Model PVS5120D), with many samplers only capable of collecting a single composite sample (e.g. American Sigma Model 6200, Isco Model 3710) for

a given time interval. A majority of commercially available samplers are also not well adapted for submersion in water. In addition to discrete samplers, there are continuous samplers that are not commercially available that have also been utilized for aquatic sampling that will be further discussed in the next section.

B. Overview of the status of current continuous sampling technology

The DUCS design in this thesis draws its core design concept from the osmosampler described by Jannasch et al. (2004). Osmosamplers are long-term autonomous samplers that use osmotic pumps to draw sample into long small-bore tubing (Jannasch et al., 1994, 2004; Kastner et al., 1995). The storage volume associated with an osmosampler is directly proportional to the length of tubing used. Tubing with internal diameters (IDs) of 0.8 mm and 1.1 mm stores a volume of ~0.5 mL or ~1 mL per meter respectively. A 100 meter length of 0.8 mm ID tubing is standard in the Jannasch design and holds ~50 mL of storage volume. An osmotic pump maintains a constant salinity gradient which draws sample continuously into the long bore tubing at a highly temperature dependent flowrate. The flowrate in this osmotic system is very slow, often with less than 100 uL of sample being aspirated per day to storage. The temporal resolution of the sample series within an osmotic sampler is heavily dependent upon both flow rate and the storage volume of the coil used.

Calculations show that due to molecular diffusion alone without accounting for sheering, over 99.9 percent of a step change in concentration will remain within a 20 cm section of 0.8 mm ID tubing for a month, and over 99 percent of the step change in concentration will remain within a 200 cm section of 0.8 mm ID tubing for a full year (Jannasch et al., 2004). At the end of deployment, samples from the tubing are cut into lengths representing individual 0.5 mL or 1 mL segments in the time series. Flow rates can be adjusted prior to deployment by the number of total osmotic pumps and allow for the integration of each period that each sample represents following temperature correction.

The use of small-bore tubing in this system combined with the slow flow rates of the osmotic pump minimalize sample smearing within a sample plug caused by static diffusion and sample sheer. Sheer will cause increased retention of a fraction of the intended species of interest within the tubing leading to pronounced spreading of the species in the system into successive samples (Li et al., 1974) due to interactions with the tubing wall. Within the small-bore tubing used in these osmotic systems, gradient spreading is almost exclusively controlled by molecular diffusion, as shown in Fig. 5.

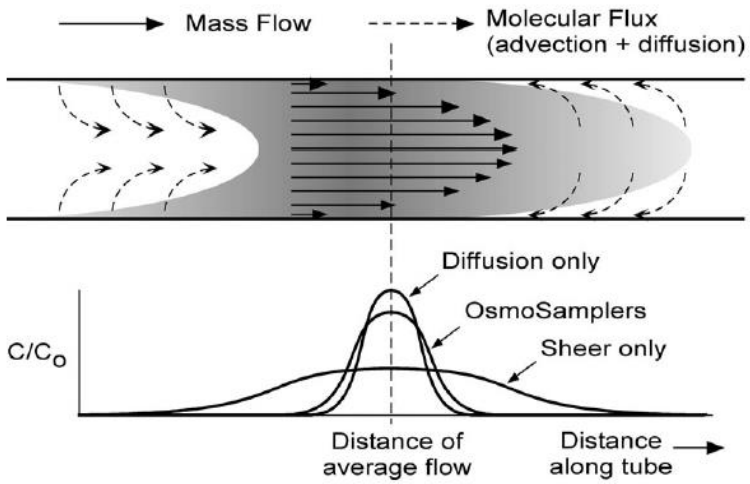

Figure 5 – *A schematic representation of overall sample gradient dispersion within small bore tubing due to static diffusion alone, or sheer, alone. Osmosamplers are shown to be a mostly diffusive system, with minimal sheering effect. (Jannasch et al., 2004).*

In situ samplers using continuous flow techniques have also been developed using peristaltic (Jannasch et al., 1986; Massoth et al., 1995), and solenoid (Amundson et al., 2000; Weeks et al., 1996) pumps. These, too, all allow high-resolution data sets to be generated, with resolution depending heavily on total available storage volume. Some of these continuous samplers, similar to the discrete samplers described above, are capable of acidifying samples – which is required for preservation of DOC samples. They are not capable of robustly mixing sample or using tracers, and instead rely on gradient dispersion for acidifying sample. This introduces a constant, acid concentration throughout the entire length of storage coil.

In addition to the fact that these samplers are not commercially available, there are a few notable problems with these samplers that render them less than ideal candidates for the generation of high-frequency DOC data. As stated above, flow rates within osmotic samplers need to be very well characterized and are strongly temperature dependent. In a system with highly varying temperatures, it is very difficult to keep track of sample location within the storage tubing with these significant temperature-dependent flow rate corrections. The osmotic, solenoid, and peristaltic samplers referred to above also are restricted to a continuous sampling method. This means they have no reliable method for introducing tracers for sample separation and determination, as described above. Instead, samples collected with current continuous sampling technology have time-averaged overlapping sample concentrations. This means the sample that is being aspirated at any given time is continuously mixing with the sample already stored in the coil. This further increases the temporal and concentration uncertainties of any sample within the coil compared to a sampler that can reliably determine where separate samples are with a tracer. This is especially important in very dynamic or complex systems. The use of a tracer also eliminates the need for temperature correcting sample location within the storage coil. Samplers developed using peristaltic or solenoid technology were developed for very short deployment periods on the order of ~24 hours constrained by very low sample capacity, which is not ideal when the species of interest requires a large initial sample volume (i.e. DOC). Finally, these systems require the destructive cutting or segmenting of the sample coil following deployment into discrete volumes. This segmenting means these samplers are only deployed once before they need to be reassembled, a time consuming and expensive process.

C. Design Goal for the DUCS

While keeping in mind the goal to generate high-frequency DOC timeseries, the primary work presented in this thesis is centered around development of an adaptable “smart sampler” prototype that would be ideal for general high-frequency sampling in freshwater aquatic systems. The DUCS uses solenoid valves and a diaphragm pump to collect samples while filtering to < 10

μm in particle diameter. The DUCS collects and preserves samples in a specially designed mixing coil loop before storing acidified samples within a long coil of storage tubing. This storage coil is similar to the storage coils used in the continuous sampling systems described above. The current standard TOC sampling method employed by the DUCS requires a minimum of ~5.5 mL of volume per sample, with the storage coil containing a maximum total storage volume of ~300 mL in the continuous storage coil loop. This allows for ~38-40 standard TOC samples after loading the visual $CuSO_4$ indicator that indicates the start of a sample set. The fastest allowable sampling frequency that can be utilized by the current model of the DUCS is ~20 minutes. Design specifications are described in greater detail in Chapter IV.

III. In-situ UV-Persulfate DOC Sensor Development

A. Overview of In-Situ UV Persulfate DOC Sensor Design

As noted above, this project's initial research was focused on developing an instrument capable of in-situ analysis of DOC using UV-LED persulfate oxidation. UV or thermally activated persulfate is commonly employed as the oxidant in dedicated TOC instrumentation. An activated persulfate solution (PS) is a strong radical-producing reagent that is known to oxidize organic contaminants (Liang et al., 2003; Todres, 2003). For this reason, it was chosen as the oxidant in this sensor technology along with a high-powered UV-LED source (low-powered compared to traditional UV sources). The UV-LED source was selected because the power requirements could potentially be low enough to be viable for field deployment. Other UV sources, such as a mercury emission line UV source and a low powered UV-LED source used during early stages of sensor development were found to be non-viable for reasons to be explained. Extensive testing found that even this final design could not completely oxidize sample DOC in a reasonable time frame, even after method optimization. The high-powered 300 mW UV source was presumably unable to degrade large, non-reactive humic and fulvic substances that traditional UV sources (up to 1000 W) would have no issue degrading (Wallace et al., 2002;. Benner et al., 1993; Gianguzza et al., 2013).

The benchtop design for this analyzer is shown in Fig. 6. Software utilized for the benchtop analyzer is discussed in Appendix A. This model mixed DOC sample with acidified persulfate reagent in a 10-mL Kloehn syringe pump chamber. This mixture was then dispensed into a flow-through, optical quartz cuvette, which is utilized as the reaction vessel, to begin the oxidation process. The cuvette and the UV-LED were enclosed in a black box. The UV source was turned on, creating radical persulfate ions which react with and oxidize DOC into gaseous CO_2, which could then be flushed with an inert gas such as N_2 to a Non-Dispersive Infrared (NDIR) CO_2 sensor.

Colorimetric methods using an indicator could also be utilized for this step. Development of the sensor was halted before progressing to the analyte detection phase.

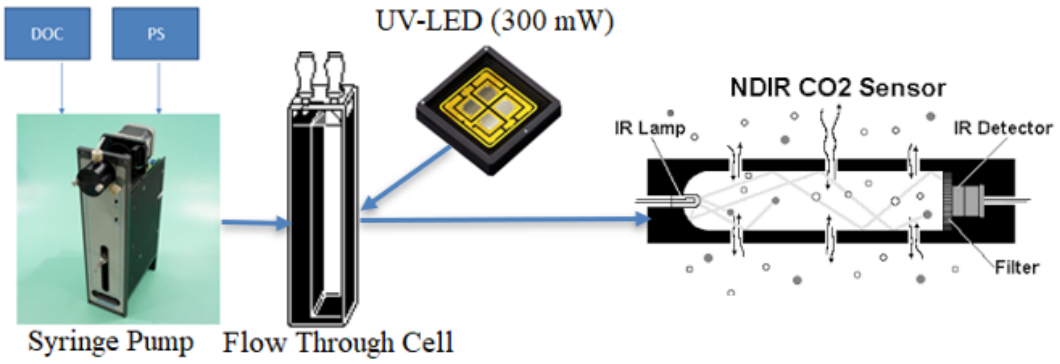

Figure 6 – *A schematic representation of the benchtop UV-PS sensor used in DOC sensor experimentation. NDIR CO_2 Sensor image was taken online from a schematic from TSI Inc.*

This method was found to not be viable for a field-deployable sensor for the reasons mentioned above and discussed further below. The following sections in this chapter will thus center around different aspects of the sensor development. Based on the results collected, development shifted to the in-situ DOC sampling system that will be discussed in detail in Chapter IV.

B. DOC Sensor Development – UV Source Selection

The first step in testing the feasibility of a DOC sensor was finding a UV source capable of degradation of DOC. The first choice for this was a mercury-argon calibration source shown in Fig. 7, as it was available conveniently in-lab.

Figure 7 – *Ocean Optics HG-1 Mercury Argon Calibration Source. This source has a 3 W emission intensity which emits Mercury and Argon source lines.*

To test whether degradation of DOC occurred, analyses of DOC containing samples were conducted on a UV-VIS spectrophotometer as shown in Fig. 8. Sample concentrations were calculated from absorbances using standard Beer's law calibration curves.

Figure 8 – *Agilent 8453 UV-VIS Spectrophotometer is pictured to the left. All UV-Vis analyses were done on the 8453 in the DeGrandpre Lab.*

For initial experimentation, a 20 ppm carbon (C) stock solution was prepared from potassium hydrogen phthalate (KHP). This solution was 10 ppm when introduced to the persulfate (PS) reagent. A stock solution of PS reagent that was 0.1M $Na_2S_2O_8$ / 1 % H_2SO_4 when mixed with C standard was also prepared. Sample analysis involved subtracting the baseline absorbance of diluted PS reagent absorbances when mixed with the C standard. Absorbance readings of 1.25, 2.5, 5 and 10 ppm C KHP standards were taken for DOC calibration. It was found that absorbance of KHP at 280 nm was linear with concentration ($R^2 = 0.99$, not shown). As the stock C solution was irradiated with the HG-1 in the presence of the PS Reagent, absorbance readings were taken at 5-minute intervals, and concentration of DOC over time was then interpolated from the KHP 280 nm regression using Beer's Law. An example of these results is shown in Fig. 9.

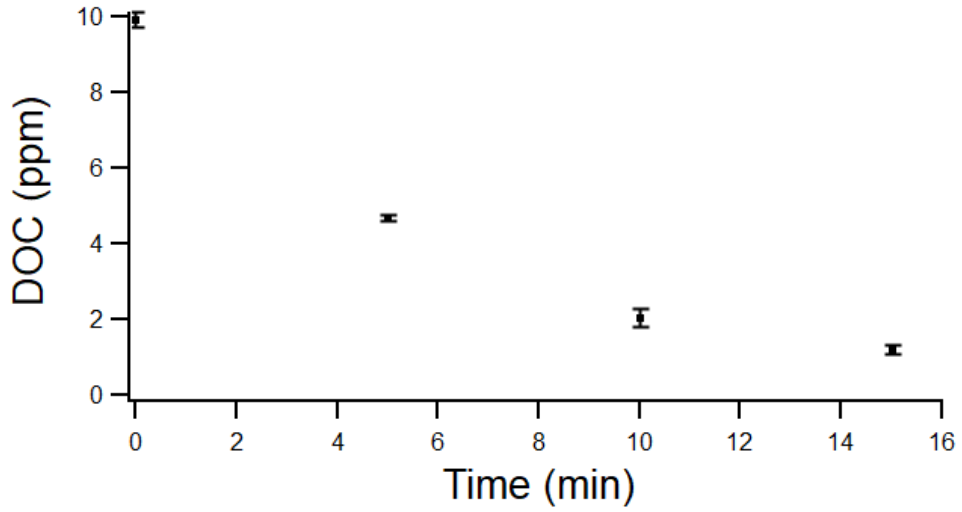

Figure 9 – *DOC concentration (ppm) vs. Time (min) of irradiation with the HG-1 light source. Irradiation intervals show (n=3) averaged readings per interval.*

The results of this experiment indicate that degradation of DOC was indeed possible. However, the greater than 15 minutes required for full oxidation of KHP was not ideal, as the HG-1 had power requirements that far exceeded those that would allow this to be utilized in a field-deployable sensor. The 9V batteries used to power this calibration source constantly dropped voltage and needed to be replaced even after a few degradation sessions. To attempt to make this type of sensor field-deployable, the power requirements of the UV source would need to be significantly decreased while still being able to degrade DOC. At this point, the feasibility of employing lower-powered UV-LEDs was evaluated. UV-LEDs have significantly lower power requirements than the traditional UV sources used in UV-persulfate oxidation, as well as the previously utilized HG-1 source. UV-LEDs also have a more compact emission envelope, therefore potentially a higher intensity over a smaller area.

The first UV-LED options explored were single diode 254 nm and 280 nm, 0.08 mW UV-LED's acquired from Sunburst Sensors. It was observed that these low-intensity UV-LED's were ineffective for the degradation of KHP. A new high-powered multi-diode UV-LED source option was then explored and is shown in Fig. 10. This UV-LED was higher-powered than any other UV-LED on the market in late 2018.

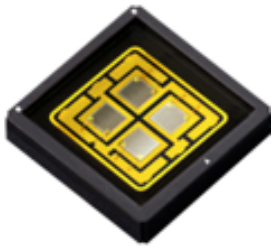

Figure 10 – *LG-Innotek high-powered UV-LED (Model LEUVA77M00HU00). This source has a 300 mW emission intensity and emits at 278 nm. Special software was developed to use this UV-LED and will be described in Appendix A.*

It was found through monitoring at 280 nm on the Agilent 8453 that the new high-powered UV-LED degraded KHP, although quite slowly compared to the HG-1 source for similar experimental conditions (10 ppm C KHP, .1M $Na_2S_2O_8$ / 1% H_2SO_4), as shown in Fig. 11.

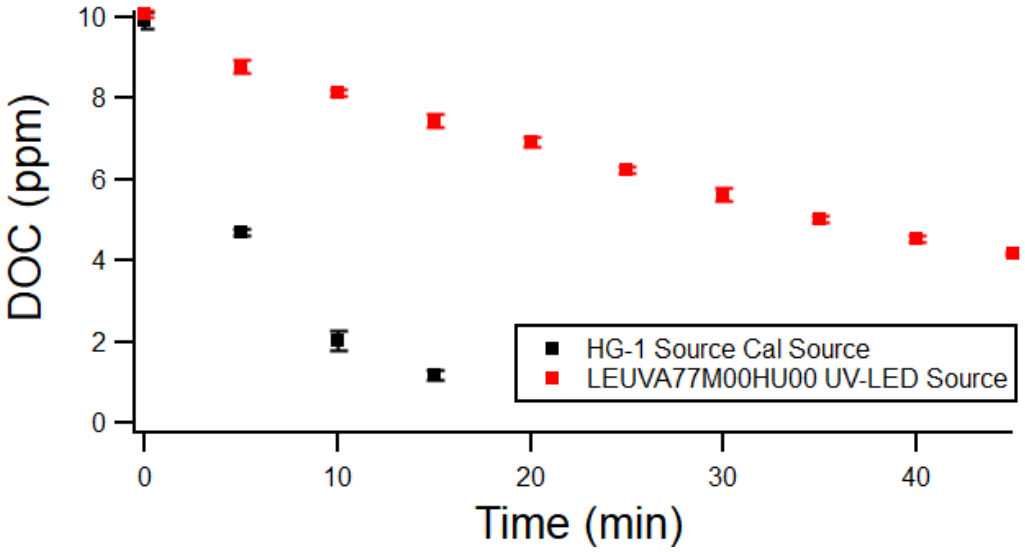

Figure 11 – *DOC concentration (ppm) vs. Time (min) of irradiation with the high-powered UV-LED. Irradiation intervals show (n=2) averaged readings per interval.*

Although DOC oxidation using the UV-LED were projected to use less overall power than the HG-1, power requirements were still high due to the long time required for full degradation of DOC sample under current conditions. Method optimization was done to attempt to decrease degradation times and power requirements to make this UV-LED source field deployable. These experiments are described in section C of this Chapter.

C. DOC Sensor Development – Method Optimization

As mentioned, if the high-powered UV-LED source were to be utilized in a field-deployable sensor, degradation times would need to be significantly decreased to meet energy requirements. This section outlines experimentation regarding method optimization to increase degradation rates of DOC using the high-powered UV-LED.

The results of an experiment looking at the effects of varying the UV-Light source between 25-100% intensity (Appendix A) under previous experimental conditions (10 ppm C KHP, 0.1M $Na_2S_2O_8$ / 1% H_2SO_4) are shown in Fig. 12. Absorbances were taken for Beer's Law calculations following 15 minute degradation periods. A power meter monitoring 278 nm was used to confirm emission intensity from the UV-LED source, with results showing close agreement with the manufacturer stated 300 mW intensity (100% = *295.4 mW*; 75% = *219.5 mW*; 50% = *148.1 mW*; 25% = *72.0 mW*). These results indicate slightly non-linear degradation rates when varying the light source intensity (Fig. 12). In future experiments with the high-powered UV-LED, light source intensity was lowered to 75% from 100% in an attempt to decrease energy requirements, due to similar degradation rates between these two intensity settings (Fig. 12). A mirror was also mounted opposite the UV-light in an attempt to refocus scattered or unreacted UV light passing through the flow-through cell; although this appeared to be ineffective in improving degradation rates.

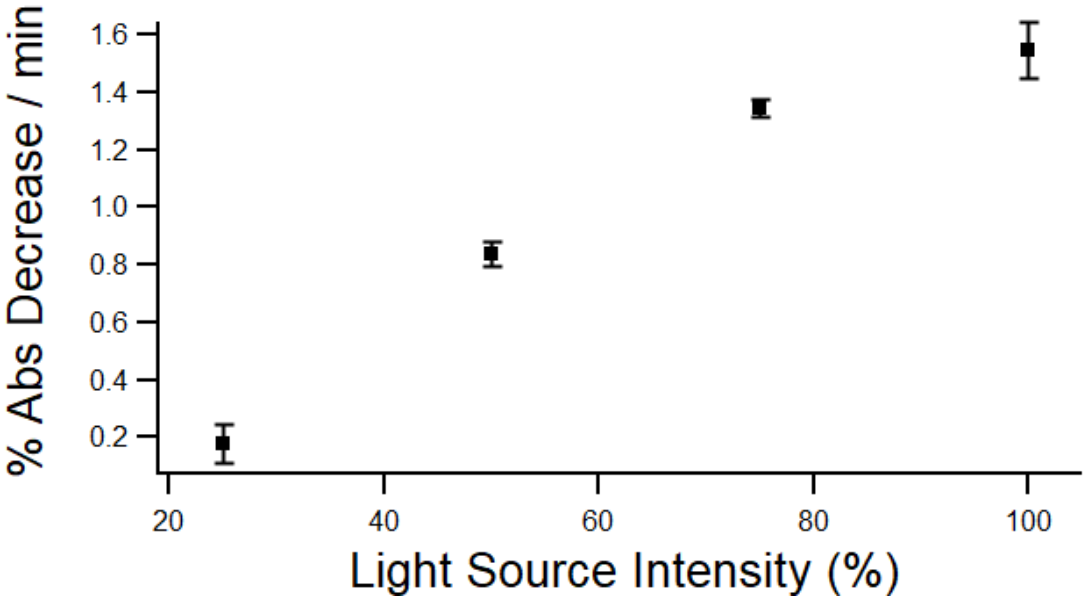

Figure 12 – *% Abs Depletion / min vs. Light Source Intensity (%). Each light source intensity result comes from the average of (n=3) degradation tests.*

Fig. 13 shows the results of an experiment examining the effects of varying the initial persulfate concentration used in degradation experiments (10 ppm C, KHP, .x M $Na_2S_2O_8$ / 1% H_2SO_4). Absorbance decreases were calculated following 15 minute degradations. The results indicate a sharp decrease in oxidative potential for the persulfate reagent after decreasing persulfate concentrations below the previously utilized 0.1 M concentration. Interestingly, it also shows similar, slightly decreased, degradative potential when increasing past 0.1 M persulfate (Fig. 13). This is likely due to increased attenuation of UV light in the more concentrated persulfate reagent forming less free radical persulfate ions to react with DOC. The results of this experiment confirm that the persulfate reagent should remain at the previously utilized 0.1M persulfate concentration. The effects of varying solution pH were also explored and found to be negligible at all low pHs (not shown), and thus the acid content of the persulfate reagent was also not altered.

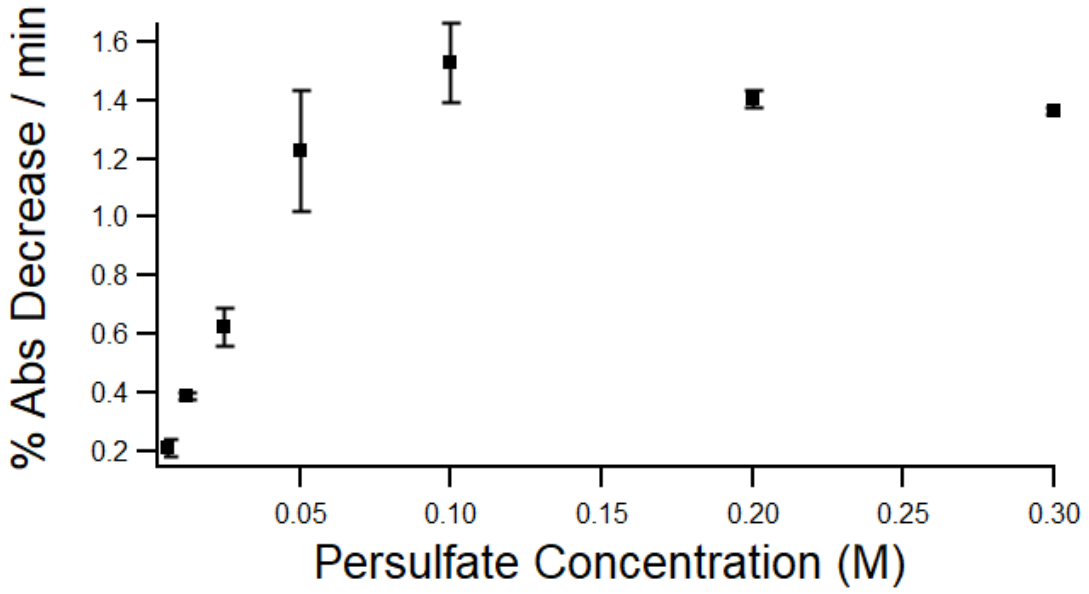

Figure 13 – *% Abs Depletion / min vs. persulfate concentration. Each persulfate concentration result comes from the average of (n=2) degradation tests.*

The results of an experiment looking at the effects of varying the temperature is shown in Fig. 14 for standard conditions (10 ppm C KHP, 0.1M $Na_2S_2O_8$ / 1% H_2SO_4). As solution temperature was increased on a hot-plate and monitored with a thermometer to reach determined

temperature, absorbance readings were taken following a 5 minute degradation period to minimize the total temperature change that occurred during the degradation. The results showed there was a slight to sharp increase in degradation rate of the oxidative reagent as temperature was increased. Samples that were heated to ~100 ºC oxidized organic carbon ~4x faster than unheated samples (10.5 vs. 2.1 % Abs Decrease /min).

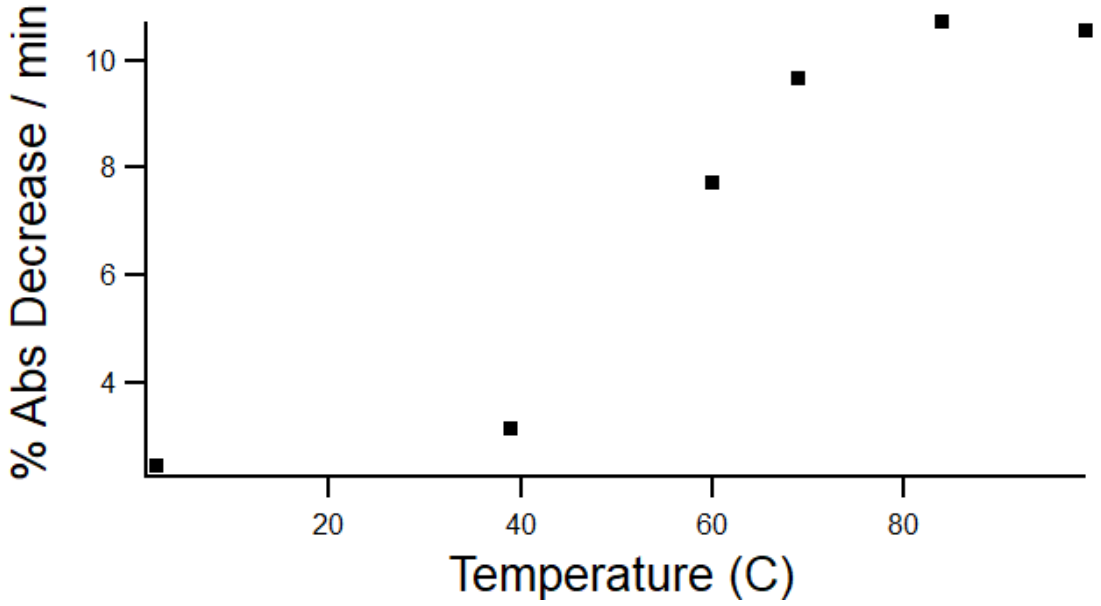

Figure 14 – *% Abs Depletion / min vs. Temperature (C). Each temperature variation result comes from 1 degradation test.*

An overall summary of maximum degradation rates achieved on KHP for the different methods used is shown in Table 1.

Table 1 – *Summary of maximum degradation rates observed and calculated from absorbance measurements for heated Persulfate(PS)/UV, UV-PS, UV (no PS), and PS (no UV) methodologies.*

Method	Degradation Rate (%Abs/min)	SD (%Abs/min)	Sample Size (n)
Heated Persulfate/UV	10.7	-	1
UV-PS	1.5	0.18	6
UV (no PS)	0.3	0.09	6
PS (no UV)	0	-	6

From these degradation rates, rate constants were set for theoretical exponential decay functions for the different methods (Fig. 15).

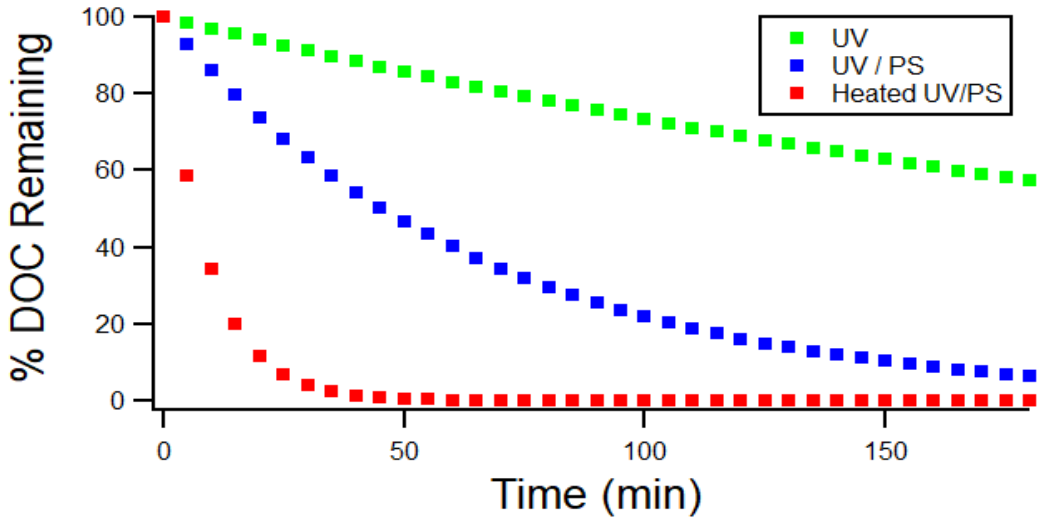

Figure 15 – *Exponential decay functions for KHP derived from maximum observed degradation rates shown in Table 1.*

It can be shown from these decay curves, that although the heated UV/PS method was the fastest method, using a UV/PS method still provided significant degradation of KHP over time. From these exponential decay curves, estimated average times to 5% remaining KHP left in solution was determined to be 200 minutes for the UV/PS method. For reference, this was 30 minutes for the heated UV/PS method, and 970 minutes for the UV method. Minimum power draw estimates for samples were then calculated assuming a 12.0 V, 250 mA power draw from the UV source. It was determined for the UV-PS method that a sample would take over 10,000 mWh of power draw per sample for degradation to < 5%, which is a significant (and impractical) power-requirement per sample for an autonomously deployed instrument.

Another problem encountered was varying degradation rates between different organic compounds. Direct analysis on the Aurora of stock DOC solutions (10 ppm C (source varying), 0 .1M $Na_2S_2O_8$ / 1% H_2SO_4) following a 15 minute degradation with the high-powered UV-LED were done. Varying the source of organic carbon led to different degradation rates (Table 2).

***Table 2** – Summary of average degradation rates observed following Aurora 1030 analysis for a range of different organic compounds.*

DOC Source (10 ppm C)	Degradation Rate (%DOC/min)	SD (%DOC/min)	Sample Size (n)
KHP	1.82	0.12	3
Glucose	2.12	0.18	3
Ethanol	0.84	0.11	3
Sigma DOC Standard	0.41	0.03	3

These varying degradation rates were problematic because KHP is an organic that has been shown to be readily oxidized by UV-PS treatment. Moving to less readily oxidized organics leads to significantly increased degradation times. The Sigma DOC standard comes as a 1000 ppm C solution containing a mixture of organics found in real-world aquatic systems including humic and fulvic acids. As such this standard degraded slowly compared to other organics (Table 2). Having varying rate constants between different organics also removes the possibility of correlating a rate of DOC degradation to actual DOC content. In addition, it was found that the formation of secondary organic structures also occurred when irradiating the Sigma DOC standard is shown in Fig. 16 (a-b).

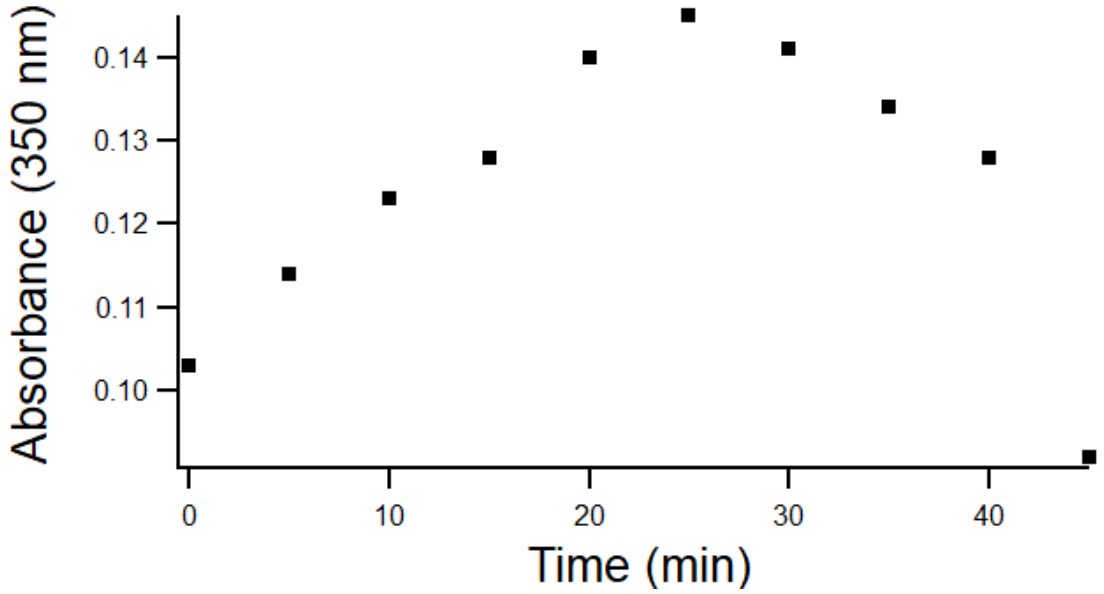

Figure 16a. – *Absorbance (350 nm) of Sigma Standard (diluted to 10 ppm C) vs. minutes of irradiation with the high-powered UV-LED.*

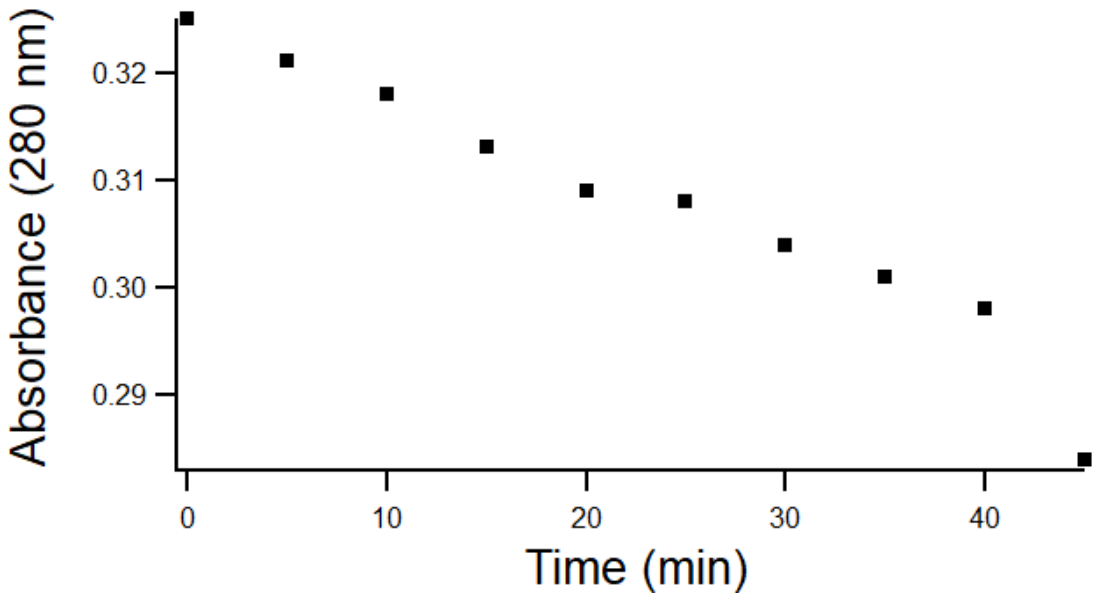

Figure 16b. – *Absorbance (280 nm) of Sigma Standard (diluted to 10 ppm C) vs. minutes of irradiation with the high-powered UV-LED.*

The 350 nm absorbance (Fig. 16a.) of the Sigma DOC standard (CAS-No. 7732-18-5) increased at first during the oxidation. However, at 280 nm (Fig. 16b.) there is only decreasing absorbance readings during the oxidation. This together indicated that some of the more labile organics were likely being degraded into intermediate species that absorbed at higher wavelengths. These intermediate organic species must then be further oxidized for full degradation, which is likely part of the reason for the slower degradation rates associated with the Sigma DOC standard. Full degradation of this standard was also shown not to occur. This was presumably due to very recalcitrant humic and fulvic acids remaining undegraded that traditional high-powered UV sources could more readily degrade. Evidence for this is shown in the long-degradation experiment of this standard shown in Fig. 17 (10 ppm C, Fischer Standard, 0.1M $Na_2S_2O_8$ / 1% H_2SO_4).

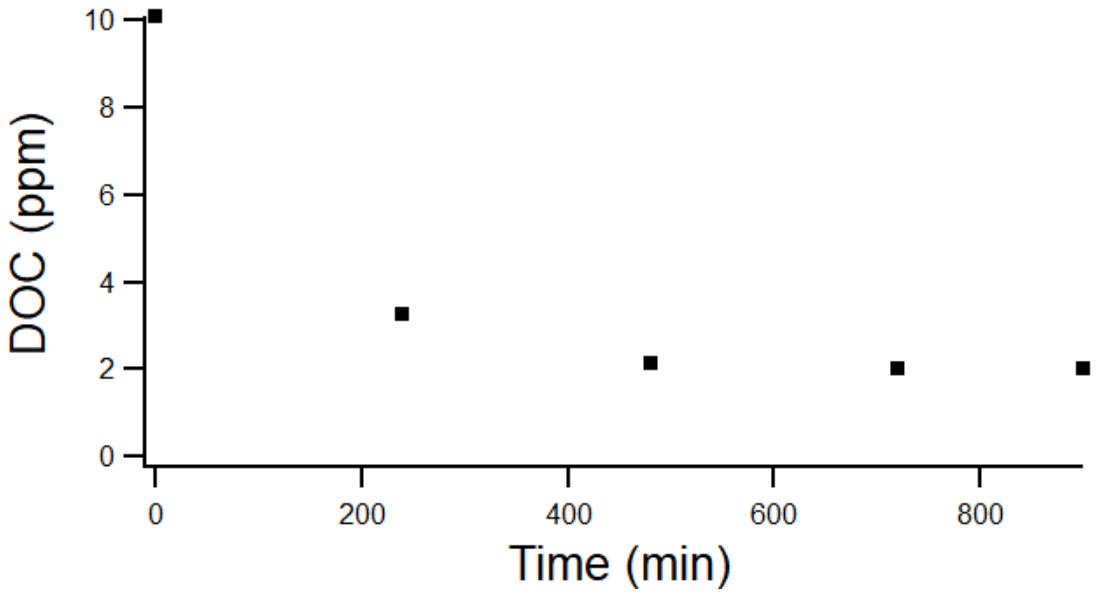

Figure 17 – *DOC (ppm) vs. Time (min) of irradiation with the high-powered UV-LED. DOC analysis was done on the Aurora 1030C. DOC was from the Fischer calibration standard.*

The results of this long-term degradation experiment show that even after the first 240 minutes of degradation, roughly 30% of the original DOC from the Fischer standard remained. Additional 240-minute degradation periods showed little to no decrease in remaining DOC (Fig. 16). This means the UV-LED would likely not fully degrade many of the organic species encountered in real-world aquatic systems. With no way of making this model field deployable without drastically increasing battery power, focus then shifted to development of the DUCS.

IV. DUCS Development

This chapter initially covers the design and in lab testing of the benchtop DUCS. It explores this initial design further through pump optimization, examining organic vs. inorganic sample tracers, and sample mixer testing. The essential components for the DUCS were then mounted and encased in watertight housing and dedicated software to control the DUCS was developed. Filtration choices for the DUCS were explored, and further system characterizations regarding the acid reagent, storage coil, sample volume, pumping capacity, power estimations, blank contamination and system mass are also described. The standard method of sampling and analysis for the DUCS was then developed and further described. This is followed in Chapter V by a real-world field deployment data analysis and discussion using the DUCS, and in Chapter VI by possible design improvements.

A. Benchtop DUCS – Initial Prototype

The design scheme utilized in the initial DUCS prototype operated using a Kloehn syringe pump (Fig. 18). The original prototype drew in 1.5 mL of sample and 1.5 mL of acid reagent for preservation. It subsequently injected this preserved sample into a 30 m (~15 mL) length of tubing for storage, with pure unacidified sample being injected between each preserved sample.

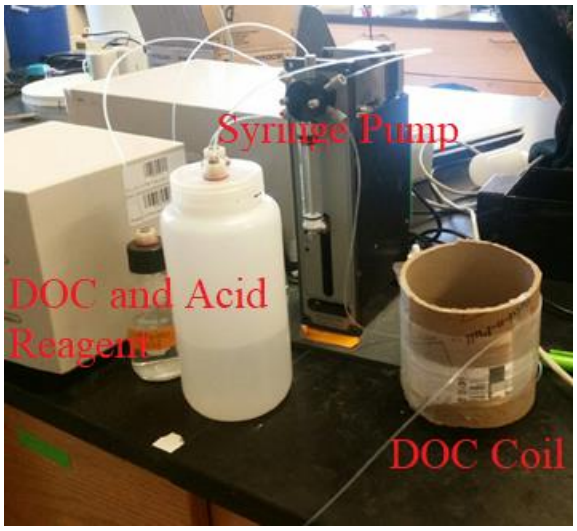

Figure 18 – *DUCS benchtop initial prototype design. Acidified DOC was injected using the Kloehn pump to the 30 m DOC storage coil.*

This electromechanical system has faster flow rates than those in the osmotic samplers to collect more sample at a higher frequency. Higher flow rates could potentially cause sheer spreading (Fig. 5) to be larger than the osmotic samplers. Initial experiments examining this effect are presented.

As an initial test food coloring dye was injected and spaced by DI. It was observed that the dye segments would not mix with each other even after travelling through the full tubing-length. This indicates sample within this tubing to be minimally diffusive and minimally sheering - at least with a short length of tubing (30 m) with low flow rates (0.375 mL/min). As another test, a 3 mL potassium hydrogen phthalate (KHP) sample and 5 mL KHP sample were injected into the storage coil with 7 mL DI separation in between each KHP sample. As sample was dispensed from the storage coil, 1 mL aliquots were diluted to 3 mL inside a 3 mL quartz cuvette and then analyzed on the Agilent 8453. Absorbance values for each sample were then plotted as shown in Fig. 19.

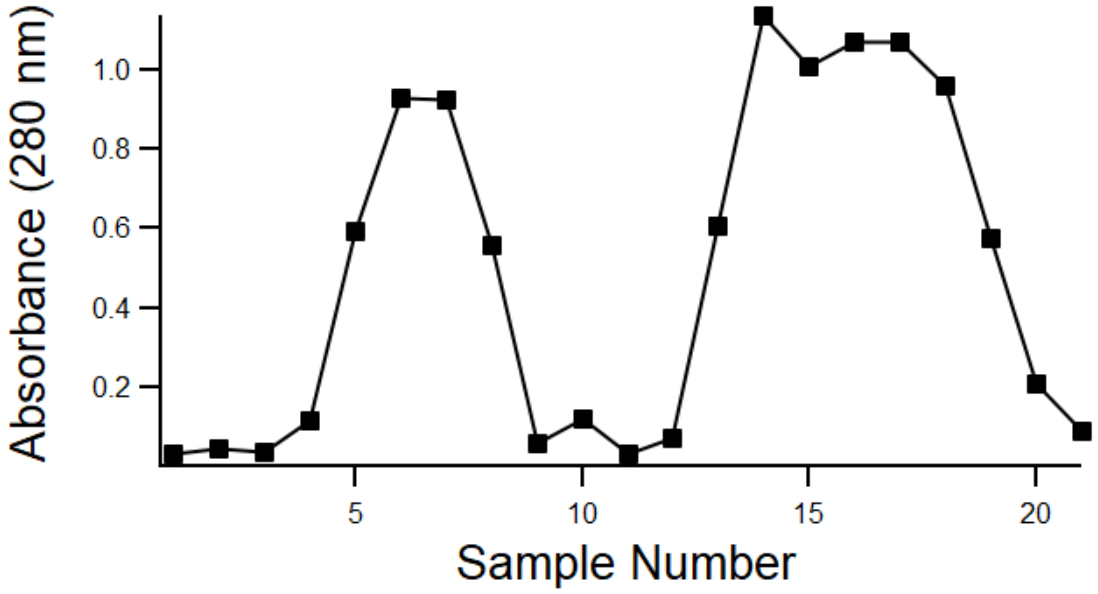

Figure 19 – *Results of analyzing 1 mL aliquots dispensed from the DOC storage coil on the Agilent 8453. During this experiment, 3 mL (left peak) and 5 mL (right peak) segments of KHP sample were injected with 7 mL DI spacing between samples.*

Ideally, the dispersion mechanics for the DUCS would not be dramatically different than those seen in the slower-flowing osmotic systems described above. The results of this experiment showed that KHP samples separated by DI did not overlap, as indicated by a return to baseline DI blank absorbance (<0.01) between these samples (Fig. 19). This demonstrates that although sample sheer is present in this initial design (note the spreading of the sample plugs), the sheering is minimal enough to prevent sample overlap with enough spacer between each sample.

This experiment (Fig. 19) provided important proof of concept that led to further development of the sampler presented in this thesis. Due to the original prototype's main flaw, specifically the bulkiness and complexity of the syringe pump (Fig. 18), system optimization was focused on using other pump designs to create a more feasible prototype.

B. DUCS – Pump Optimization

There were two primary differences between the first and second benchtop prototype models. The second design uses a smaller, more practical diaphragm pump (KNF 1.5 KPDC-M) that is more easily adapted for field deployment than the syringe pump. This diaphragm pump operates at a maximum working pressure of 85 psig. The results of experiments comparing the syringe pump and the diaphragm pump for sample injections of a DOC standard is shown in Fig. 20.

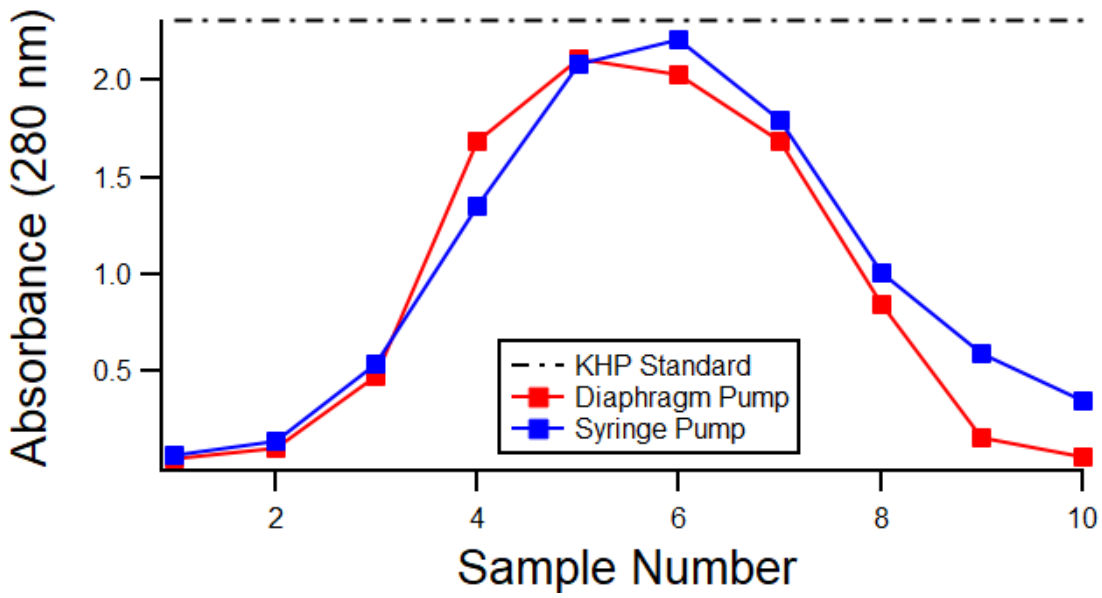

Figure 20 – *Results of overlaying the average absorbance results of (n=10) 3 mL KHP DOC samples dispensed through the storage coil with either the diaphragm pump or syringe pump. Absorbance of the KHP stock is also shown (dashed line).*

The results presented in Fig. 20 show that the diaphragm and syringe pumps similarly deliver and store organic standard. This is shown by the similarity of the absorbance peaks measured when dispensing these sample segments. Notably though, sample segments that were injected with the syringe pump took a longer time to return to DI baseline absorbance as compared to the diaphragm pump (see right side of peak). This reproducible behavior is likely due to a larger dead volume in the syringe pump setup causing residual KHP contamination. Not only is the KNF pump a less bulky field-deployable pump, it also appears to be better suited for injection of samples to the storage-coil.

Flow rates using the diaphragm pump with this coil were ~ 5 mL/min It was also found that increased flow rates set by the syringe pump (0.375 → 20 mL/min) caused increased analyte spreading for sample stored within the tubing. Flow rates within the storage coil when using the diaphragm pump were minimized through pulsed introduction of mixed sample within the programmed sampling sequence. Sample introduced using a pulsed method of pump operation had a slower flow rate on average per second of pumping (~5 mL/min vs. ~ 3.5 mL/min). This is

primarily due to the pump taking a few seconds to reach maximum flow rates during continuous pump operation. Results from another test also showed that peaks eluted immediately from the storage coil were not statistically different than peaks that had allowed natural dispersion to occur for 1 week (not shown). It was also shown that inorganic ($CuSO_4$) sample peaks eluted from the storage coil did not appear to sheer or disperse more than organic sample peaks (Fig. 21).

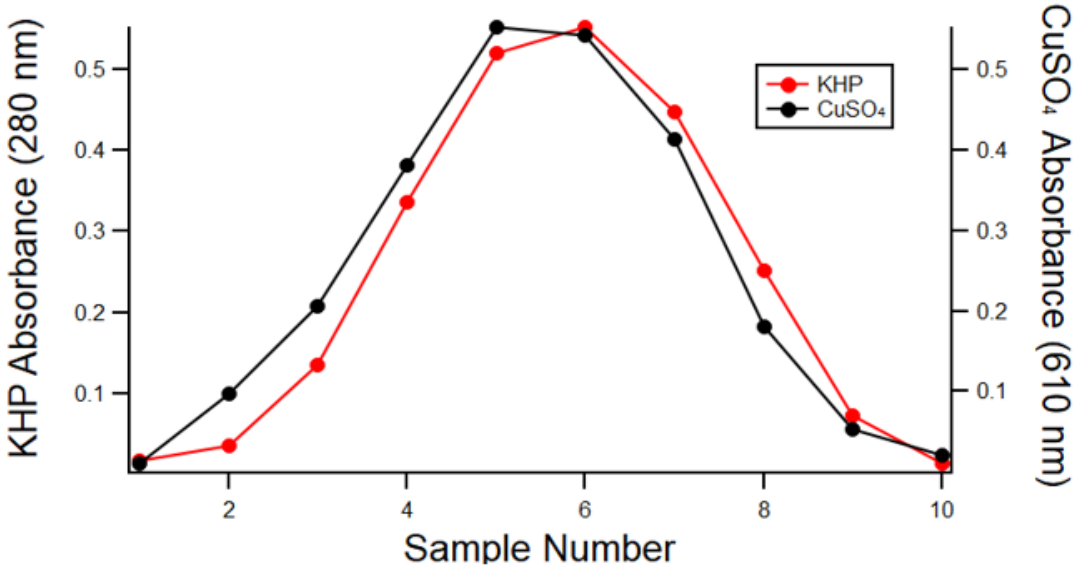

Figure 21 – *Results of overlaying the average absorbance results of (n=10) 3 mL KHP DOC samples and (n=10) 3 mL $CuSO_4$ samples dispensed through the storage coil using the diaphragm pump. $CuSO_4$ was chosen for this experiment as sample tracing was originally going to be done colorometrically using an inorganic salt.*

For this experiment, a 0.25 M copper sulfate ($CuSO_4$) solution was prepared having a similar maximum absorbance as a KHP standard. $CuSO_4$ peaks were then analyzed in a similar method to organic peaks. The results being similar provided additional evidence that the method of storage utilized for this sampling system had minimal dispersion and sample retention for a stored sample plug. It also demonstrates that inorganic tracers introduced into the sample coil will behave similarly to organic sample. Therefore, inorganic tracers such as HCl can be added to organic sample within the coil to distinguish individual samples.

C. DUCS – SAMI Mounted Model and Dedicated Software Controls

Following the development of the optimized benchtop model previously described the design for an initial model of the field-deployable prototype was undertaken. This design utilizes the housing of a repurposed Submersible Autonomous Moored Instrument (SAMI) (DeGrandpre et al. 1995) to mount the electronics, boards, plumbing and batteries (Fig. 22).

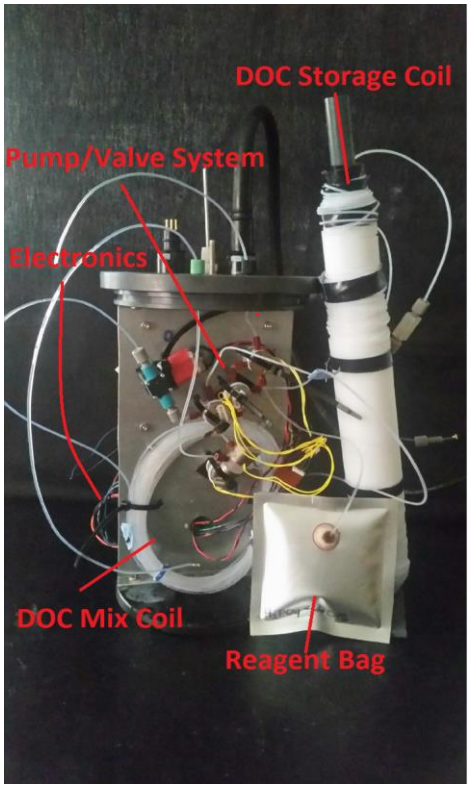

Figure 22 – *DUCS mounted inside of SAMI instrumentation housing. A more detailed description of the plumbing and electrical design is shown in Appendix D.*

As stated above, prior to storage of preserved sample, the DUCS uses a closed-loop sample mixer (shown in Fig. 23). Rather than mixing sample in a syringe chamber, this closed loop uses a series of solenoid valves before the DOC storage coil (as described below). This necessitates a flow through pump. Other pumps were also explored as potential options (Appendix D), however this pump model (KNF 1.5 KPDC) was unique in its ability to pump within the closed-tubing circuit. Using solenoid valves, these changes allow aspirated sample to be mixed internally within a closed loop sample mixer. This specialized design makes it possible to recirculate and mix sample and preservative inside the closed tubing loop using a diaphragm pump while remaining fully isolated from the storage coil (Fig. 23).

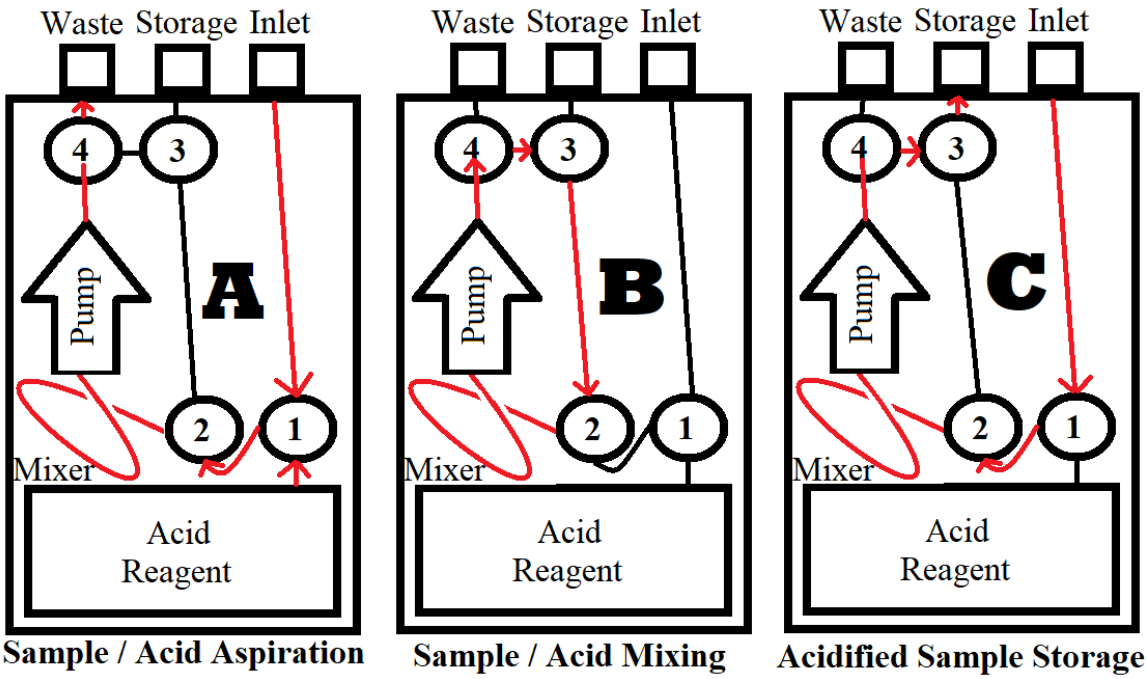

Figure 23 – *Plumbing diagram for the DUCS instrumentation. It should be noted that tubing lengths, and volumes, are not to scale in this figure. As described below, a normal sampling sequence goes through configurations A-C successively.*

Dedicated software for controlling the DUCS sampling system was then developed based on previous instrument control programs developed in the DeGrandpre lab using the programming interface TF-TOOLS for a TFX-11 data logger (Onset Corp.). The TFX-11 uses a form of BASIC (TFBASIC, programmed in TF-TOOLS) that is ideal for embedded data acquisition and hardware control for in-situ field instrumentation. In addition to controlling the sampling start time and frequency based on parameters input by the user, the software also collects time-stamped temperature (thermistor) data for each sample.

The flow paths in sequences A-C are determined by a series of solenoid valves (1-4), shown in the circles in Fig. 23 and controlled using the TFBASIC software. Configuration A is used for aspirating sample or acid. In this configuration, the software alternates valve 1 between aspirating either acid reagent or sample. All other valves remain normally closed to minimize power draw. Configuration B is the closed-circuit configuration for mixing unpreserved DOC sample with acidifying reagent. In Configuration B, valves 2, 3 and 4 are powered to form the closed circuit.

System flushing is primarily done in configuration A, before briefly changing to configuration B to flush the tubing that is only accessible in this closed-circuit configuration. Configuration C is the sequence for dispensing acidified and mixed DOC sample to storage. Configuration C is initiated after mixing in Configuration B by powering off valves 2 and 3, which allows dispensing of mixed sample to the storage tubing.

The original mixer volume was ~15 mL, but this was decreased to ~8 mL in the later stages of development to reduce flush time per sample. To test the effectiveness of the mixer, red food coloring dye was pumped to the mix coil with DI "sample" at a 50:50 ratio. When preserving sample, the mixer aspirates small segments at a set sample:acid ratio, alternating between acid or sample by pulsed activation of valve 1 (Fig. 23). The loop was then closed, and the diaphragm pump recirculated this 50:50 solution for mixing. It was visually observed that the dye was mixing as circulation occurred. As confirmation of complete mixing throughout the entire volume of the coil, 1 mL aliquots were then dispensed from the mixer and analyzed on the Agilent UV-VIS. Dilution factors were computed for each sample calculated from a standard Beer's Law absorbance curve generated for this dye (Fig. 24).

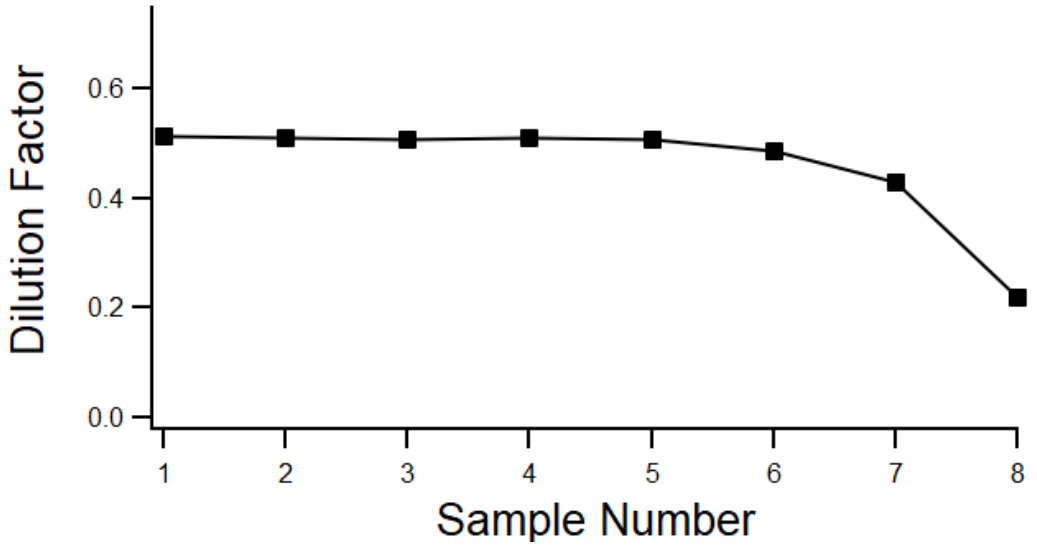

Figure 24 – *Calculated dilution factors for food coloring dye mixed with DI using the mix coil. Sample was dispensed from the 8 mL mix coil in 1 mL aliquots.*

The results from this test show that the software setting of a 50:50 mix ratio was nearly seen with an average dilution factor of roughly 0.52 (Fig. 24). The results also showed a plateau at this relative ratio for the first 5 mL dispensed from the mixer, indicating that the solution was well mixed throughout the volume of the mixer. After 5 mL, a drop off began to occur for the dilution factor in each sample. This drop was due to the DI that was being pumped into the mixer further diluting the dye within the mixer. It was also observed that the coil had not been fully flushed after 8 mL of DI had been added, indicating an additional volume must be pumped for a full mixer flush.

Following this experiment, the minimum volume required for a thorough flush of the mixer was determined. This was accomplished by dispensing DI through the coil until the baseline returned to DI absorbance values (i.e. < 0.01). From 10 trials it was determined that 14 mL was the minimum volume required for a complete return to baseline DI absorbance values within the 8 mL mixer. There is also a small section of normally closed tubing (~0.25 mL) in the mix loop that must be flushed for an effective full flush. The normal post-sampling flush sequence utilized by the DUCS flushes the tubing in the normally open and closed sections of the mix-coil loop (Fig. 23), as described above.

D. DUCS– Sample Filtration

As previously mentioned, DOC samples are traditionally filtered to 0.45 μm. This requirement was a problem for sampling with the the DUCS. Because a DOC sample must be filtered prior to acidification to prevent possible dissolution of POC, filtration at the sample inlet was required. However, attempts to implement an in-line 0.5 μm filter frit proved to be unsuccessful due to the inability of the pump to draw water through the small pore filter. A 2.5 μm filter frit was tested in-line also but was not useable for the same reason. Filtration to the 0.45 μm DOC size fraction could be accomplished through either the implementation of a dedicated pre-inlet filtration device using a secondary pump or through the implementation of a more powerful diaphragm pump. This possibility was not explored in this phase of development.

Rather, the current DUCS model incorporates a 10 μm in-line filter at the sampler intake. This allows initial filtration for any large particulate matter, and removes a fraction of microbes from collected sample, further reducing the chances of TOC loss before initial acidification. Filtration of larger particulate matter is important because this matter may cause analytic issues (i.e. incomplete oxidation) or lead to residual organic carbon contamination when using the Aurora. Since POC is sampled in addition to DOC when using 10 μm filtration, the DUCS collects Total Organic Carbon (TOC) samples. TOC samples are traditionally taken to assess the gross amount of organic matter found in natural waters and include suspended particulate, colloidal and DOC as part of the TOC measurement. TOC samples collected manually also exclude large floating vegetative or animal matter, either through an initial filtration (typically filtered to < 100 μm) or by allowing large particulates to settle out and then aspirating sample with a syringe. TOC samples exclude volatile organic matter during analysis removed during the initial TIC purge. TOC samples, like DOC samples, are acidified immediately after collection. Field collected Quality Control (QC) samples are filtered by wetting a 10 μm hydrophobic polypropylene (PPE) filter with ~1 mL of methanol, filtering 1000 mL of DI to waste, washing and drying the vacuum flask, and then filtering.

E. DUCS – System Characterizations

As stated above, samples stored within the coil are preserved with an acidic 1.370 M hydrochloric acid (HCl) solution. Early experimentation used a 0.274 M HCl solution. The concentration was increased following initial field-deployment in order to diminish the effects of residual freshwater conductivity and alkalinity on dilution factor calculations, and to reduce the possibility of increased TOC retention, which will be discussed further below. This acid solution acts as a conservative tracer (Martz et al., 2006) of conductivity when mixing. The sample to acid dilution factors from conductivity measurements for a sample can be calculated using equation 1.

$$\text{Dilution Factor, Conductivity (DFC)} = 1 - \frac{\text{Conductivity (sample)}}{\text{Conductivity (acid)}} \qquad \textit{Eq. 1}$$

The traditional acid for preserving DOC, phosphoric acid (H_3PO_4), was not chosen due to the pKa of H_3PO_4 being close to the pH of preserved sample. This means chances in pH could alter the speciation of $PO4_2^{2-}$, which could potentially change conductivity. This in turn would lead to potential inaccuracy when determining dilution factors from conductivity. Sulfuric acid (H_2SO_4) was also not chosen due to its high pKa_2 (~2). Therefore, changes in pH may also affect conductivity for H_2SO_4 similar to H_3PO_4. HCl was chosen as the acidifying reagent because it is a strong acid that has minimal oxidative potential. This ensures that HCl will remain fully dissociated and that H^+ and Cl^- ions will dominate conductivity – with other possible contributors to conductivity being negligible.

Sample that is acidified and preserved with HCl during a normal preservation sequence will remain below a pH of 2 until at a 2.0 % dilution factor from undiluted stock acid reagent. Therefore, collected sample that has at least 2.0 % of the acid reagent's initial conductivity value will be below pH 2, which is required for preservation of DOC.

To test the preservation effectiveness of 0.274 M HCl acid reagent, water was collected from the Clark Fork River and then immediately filtered to 0.45 μm through vacuum filtration and analyzed that day on the Aurora for a baseline DOC level. The river water was then split into acidified solutions (n=2) as well as unacidified solutions (n=2). The HCl was introduced to sample at a 50:50 ratio, which led to acidified solutions of pH < 2, allowing preservation to occur. Dilution factors were applied to the acidified solutions to account for the dilution with acid stock in sequential analyses. Samples were then stored at ~1 ^oC with sequential analyses performed weekly for the following two weeks to examine the % recovery of DOC in both the acidified and

unacidified solutions. Results of this test showed significantly higher % recoveries of DOC in acidified samples vs. unacidified samples. The results of this experiment are shown in Table 3.

Table 3 – *% Recovery of DOC in acidified and unacidified river water over a 2-week timespan.*

Week	% Recovery DOC (Acidified)	% Recovery DOC (Unacidified)
0	100	100
1	99.1	93.4
2	99	91.8

As mentioned above, in addition to preserving the DOC, the HCl reagent is also used as a conservative method to track dilution factor of the stock acid reagent with sample. Conductivity of undiluted acid reagent is nearly linear upon dilution with freshwater sample. Dilution factors for sample mixed with this reagent can be accurately determined by using a standard dilution curve of acid reagent with DI.

Conductivity measurements for samples eluted from the DUCS storage coil are measured using a small volume (150 μL minimum) conductivity probe (InLab 751-4) and meter (F30) both developed by Mettler Toledo. Additional instrument specifications for this probe and meter are shown in Appendix E. The conductivity of the undiluted HCl acid solution utilized with the DUCS is above the 200 mS/cm upper measuring limit allowed by the probe and meter. Upon dilution with sample and mixing, preserved sample conductivity (~60-80 mS/cm) is nearly linear with dilution factor, and under the 200 mS/cm upper limit . The conductivity of CFR water during this study was measured to be ~0.250-0.400 mS/cm from the probe and meter. This was in agreement with previously reported conductivities (Sando et al., 2016) at the USGS monitoring station #12340500. This means this acid reagent solution has an ionic strength of ~150x-200x stronger than typical UCFR conditions at the dilution factors introduced by the DUCS. Therefore, the background contribution from freshwater conductivity for samples acidified with 5% HCl leads to an error of no more than 0.7 %. There is also the potential for the consumption of HCl through neutralization of alkalinity in freshwater samples. Calculations showed that this alkalinity consumption should

not lead to more than a 0.05% change in sample conductivity in samples with ~3000 µmol/l of alkalinity. The acid solution is contained within a gas impermeable bag, with sampling requiring ~5.25 mL of acid reagent per standard sample.

Standard nanopure water collected in the DeGrandpre lab was found to have a conductivity of 3.50 uS/cm. Although conductivity vs. dilution factor is essentially linear over small ranges in dilution factor, the fit is polynomial over a wide range. This can be seen by the y-intercept not matching the nano-pure conductivity value (Fig. 25). Due to the narrow range of dilution factors introduced by the DUCS, a standard curve during the standard analysis process is generated with acid dilution factors between 0.10-0.35 and fit with a linear regression. A dilution factor standard curve for the normal dilution acid factor range introduced by the DUCS is shown below.

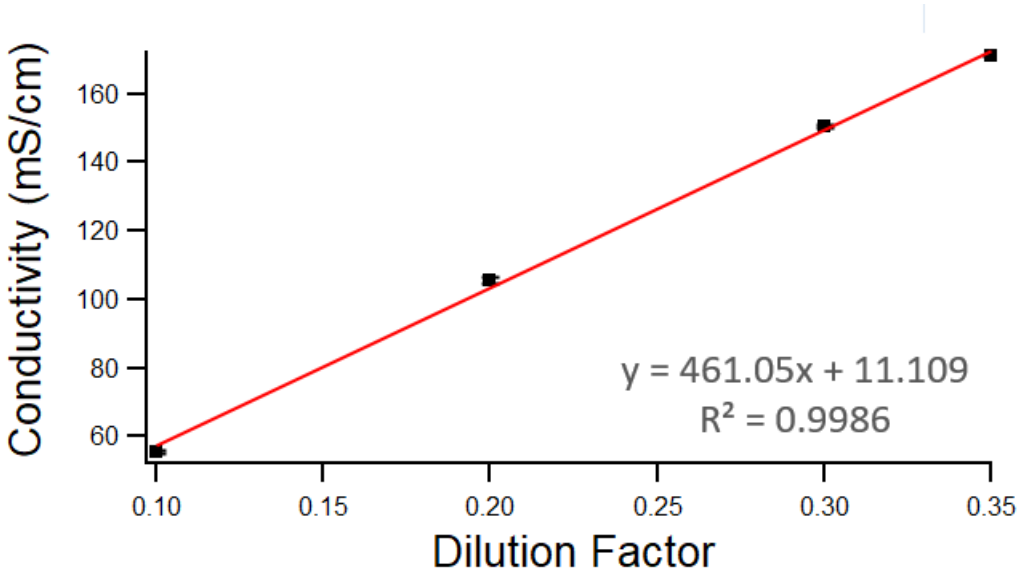

Figure 25 – *Dilution factor standard curve for typical dilutions introduced by the DUCS for 5% HCl. When using the full dilution factor range, conductivity was found to be slightly non-linear with dilution factor (Appendix D). A typical 1% HCl dilution factor standard curve used in early experimentation is also shown in Appendix D.*

Originally, tracers for dilution factor calculations were planned to be colorimetrically determined through UV-Vis absorbance (Agilent 8453). Organic dyes with very high ε's that could be used as a colorimetric tracer already incorporated carbon into their structure. When mixed with a DOC sample, baseline carbon concentration coming from an organic indicator would be equal to

or greater than the DOC sample. This additional background signal could cause inaccurate DOC measurements when analyzed on the Aurora. Organic dyes were also troublesome as they created significant residual blank DOC contamination through adsorption of the dye within the valve and tubing system. Manually taking absorbance readings for 100's of small sample segments coming the storage coil was very tedious. Additionally, no inorganic colorimetric tracer could be found that had a high enough molar extinction coefficient (ε) to effectively be used as a tracer without reaching concentrations that would not be safe for analysis on the Aurora. Colorimetric indicators also lacked the preservative nature that is present when using the current HCl reagent and would need to be spiked with an acid anyways. Consequently, the colorimetric option for determining dilution factors was abandoned. However, a solution containing copper sulfate ($CuSO_4$) is still used at a high enough molar concentration (~1 M) that it gives a visual indication as to where samples "start" as successive samples move through the coil. The $CuSO_4$ indicator is loaded into the sample coil prior to storage of any DOC sample.

Total sample volume contained in the DOC storage coil is a flexible value that can be increased or decreased as desired prior to deployment by 1) changing the length (volume) of the storage coil or by 2) increasing the total number of storage coils using valves. Further increasing the length of the current 450 m tubing may require using a similar, but more powerful, diaphragm pump. The current 450 m long storage coil is manufactured from 0.8 mm internal diameter (ID) x 1.6 mm outer diameter (OD) Polytetrafluoroethylene (PTFE) tubing. Tubing with a 0.8 mm ID can store ~0.5 mL per meter, and thus the current storage coil contains theoretically ~225 mL of allowable storage volume. Actual volume was determined gravimetrically to be ~300 mL. The discrepancy between calculated and theoretical volume could be due to either 1) more tubing delivered by the manufacturer than expected, or 2) variation in ID throughout the 450 m of storage coil. PTFE was chosen for tubing due to the combination of its 1) superior chemical resistivity, 2) low coefficient of friction (lowest of any polymer), 3) excellent UV resistance, and 4) very low gas and liquid permeability.

Further characterizations are presented in this chapter for the DUCS in its current configuration with the 450 m DOC storage coil. This was superseded by both a 45 m and 150 m coil that was used in original DUCS characterization experiments. It was found that upon implementation of the 450 m coil that when using pulsed sample dispensing flowrates through the storage coil decreased significantly from ~6 mL/min to 1.0 ± 0.1 mL/min. This was determined from gravimetric measurement of (n=15) pumps (Fig. 26). There is still some notable variability in pumping capacity over time as noted, and this variability is shown in Fig. 26. This uncertainty in the reproducibility of flow rates through the DOC sample coil is likely due to small bubbles going through the diaphragm pump. This pumping capacity variability is the reason that constant sample volumes cannot be used to segment successively stored samples (as is done in osmosamplers), and why tracers are included to determine where samples lie within the coil. In summary, the reason a tracer is needed is because pump volumes are not accurate or reproducible enough to generate reproducible dilutions of each sample with acid.

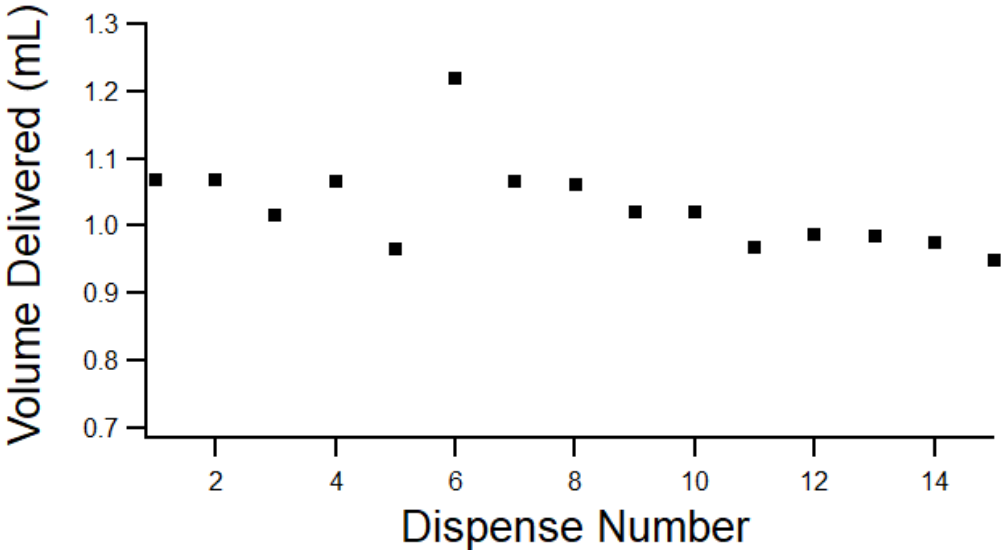

Figure 26 – *Pumping capacity characterization showing gravimetrically determined volumes of water delivered after pumping for 1 minute intervals.*

Following characterization of pumping capacity with the 450 m storage coil and adjusting software programming, the minimum power draw requirements for sampling were determined. Table 4 summarizes the estimated overall power draw per sample. The standard method of sampling (Chapter IV, Section F) collects a total of ~40 samples with current 450 m storage coil. All pumps and valves operate under standard 12V DC electrical current.

Table 4 – *Estimated power draw requirements for the sampling configurations (A-C, Fig. 23) of the standard sampling method and estimated power draw for a complete standard sample in milliWatt-hours (mWh).*

System Configuration	Current (mA)	Time (min) /Sample	Power / Sample (mWh)
A - Sample and Acid Aspiration	80	~10	160
B - Sample Mixing	110	~2	40
C - Sample Dispense and Storage	300	~5	300
Total Sample - Separated			~500

.

It was found that an average sample will require ~500 mWh of electrical energy. This is nearly 30x less power required per sample compared to the in-situ sensor that was described in Chapter III. The DUCS operates with an 18-cell alkaline D 12V battery pack with 432,000 mWh of electrical energy. Therefore, the standard 18-cell battery pack should theoretically be able to collect over 850 samples under standard operating conditions. It was found using an external power source that operating conditions must not drop below 11.2V, otherwise pumping capacity begins to diminish dramatically when using the KNF diaphragm pump. To test whether the DUCS would be able to collect a full 40 standard samples without running out of power or dropping below the minimum required system voltage, a new 18-cell battery pack was attached to the DUCS and in-lab sampling was done. It was found that the DUCS was able to readily collect all 40 standard samples with the operating life of one battery pack. Battery voltage measured using a voltmeter was determined to be 12.25 V before and 11.94 V after one 40-sample sampling cycle. This demonstrated that this battery will be sufficient for initial field deployment tests.

Prior to field deployments, it needed to be determined whether the SAMI-housing would be completely waterproof. The DUCS was closed, the lid was screwed down, and was fully submerged in a water tank located in-lab. After 24 hours of submersion, the DUCS was retrieved from the lab tank and was opened to check for water leakage. This test showed that the SAMI-housing would be waterproof, at least at shallow depths as no leakage was detected. Additionally, the mass of components used in the DUCS are shown in Table 5.

Table 5 – *Mass of components utilized in the full sampler design.*

Sampler Component	Mass (g)
DOC Coil - Loaded	2,050
Plumbing and Electronics	2,150
Battery	2,450
SAMI Housing	3,700
Full Sampler	10,350

F. DUCS – Blanks

Experiments examining sources of blank TOC contamination been carried out. Blank contamination can occur while sampling with the DUCS, or during the post-sampling processing levels. This section describes blank contamination sources at both levels. A table summarizing blanks at these levels included at the end of this section (Table 6).

i. Sampling TOC Contamination (Sampler Blank Contamination)

Early blank contamination experiments showed significant blank DOC contamination (up to 2.5 ppm C for DI collected with the standard sampling method) coming from the sampler itself. Blank contamination values were decreased significantly by 1) soaking all valve fittings in DI, 2) thoroughly cleaning the system tubing by continuously pumping 1% HCl through the valve system and storage coil for 24 hours, followed by a secondary 24 hour DI flush preparation and 3) preparation of fresh acid stock reagent prior to any new sampling session.

To examine blank contamination values following the standard cleaning procedure described above, DI water was analyzed for baseline TOC concentration and found to be 0.018 ± 0.005 ppm C[a]. Subsequent analysis runs for DI has shown consistent levels of TOC contamination. Analysis of acid-reagent blank TOC was found to be 0.029 ± 0.005 ppm C. Analysis of subsequently prepared acid-reagent batches showed consistently similar (often lower) baseline TOC contamination compared to DI (0.008-0.034 ppm C)[b]. The DI was then acidified and stored within the TOC sample coil before collection. Blank samples were collected by elution from the storage coil, and these samples were analyzed on the Aurora. The results of this experiment showed acidified blank DI sample stored within the sample coil had average values of 0.092 ± 0.007 ppm C[e]. Recent blank experimentation has shown blanks prepared identically to not have significantly different blank TOC contamination. These results showed that blanks consistently have TOC values ~4x higher than either DI or acid reagent baseline TOC. Variation in these blanks is also random in character and did not appear to be any noticeable trends when analyzing successive blanks.

DI collected from the mixer before dispensing sample to storage showed similar average values of blank contamination, with average values of 0.082 ± 0.007 ppm C[d]. Recent experimentation found these blank values to be 0.06 ± 0.01 ppm C. This again was higher than either the DI or acid reagent stock baselines, and similar to that seen from blank sample stored within the coil. This indicates that the valve and pump system is likely the primary source of contamination from the sampler itself, rather than contamination the storage coil. DI filter blanks using the inlet 10 μm in-line filter described in this chapter have also been collected and have been observed to not be significantly different than DI[c].

ii. Post-Sampling TOC Contamination (Processing Blank Contamination)

To determine blank contamination from the small vial sampling processes and secondary dilutions, DI that had not been treated with the DUCS was dispensed to a set of acid-washed and ashed small vials. Conductivity measurements were then taken for each vial with the standard method of cleaning the probe between each measurement. Sets of small vials were then combined

into larger solutions and ~ 3 mL of sample from these larger solutions were then diluted to 10 mL using a volumetric flask. Historically blanks analyzed from this procedure have been observed to have inconsistent TOC contamination levels. Blank contamination in these samples has been as low as 0.134 ± 0.008 ppm C. Blank samples prepared using the same methodology have also been seen to be as high as 0.4 ± 0.3 ppm C[f]. All glassware used for sample preparation must be acid washed and ashed to ensure blank contamination remains as low as possible. Volumetric glassware must be washed 3x with hot water and rinsed 3x with DI water following each post-sampling dilution. The source of this processing blank contamination is likely coming from a combination of the many post-sampling processing steps. Additionally, to test the efficacy of the probe cleaning process and test whether cross-contamination coming from the probe might be an issue, DI was dispensed into a series of the small vials. The conductivity probe was then dipped into 5 ppm C standard and cleaned using the standard cleaning procedure. It was then placed into a small vial containing DI, and removed. This process was then repeated for the other small vials. Analysis of DI that had been treated with this methodology was found to contain 0.5 ± 0.3 ppm C[g]. This indicates the possibility for potential carryover between sequential small vials that is not addressed during the standard cleaning process. Although there could be potential carryover between successive vials, this problem was not further addressed, as TOC concentrations for sample in any two sequential vials would very likely be close to each other and carryover would be negligible

Table 6 – *Sources of TOC contamination at the sampling and processing levels.*

Blank Contamination Summary

Sampler Level Blanks		*TOC (ppm C)*
DI Blank[a]		0.013 - 0.023
Acid Reagent Blank[b]		0.008 - 0.034
DUCS Inlet Filter Blank[c]		0.011 - 0.023
DUCS Mixer Blank[d]		0.075 - 0.089
DUCS Storage Blank[e]		0.085 - 0.099
Processing Level Blanks	*(lowest)*	*(highest)*
Small Vial Full Process Blank[f]	0.126 - 0.142	0.1 - 0.7
Cond. Probe 10 ppm Carryover Blank[g]		0.2 - 0.8

*G. **DUCS – Standard Sampling Method:** Storing a DOC sample timeseries with a tracer to determine sample locations.*

A TOC sample series can be collected with this sampling system for analysis with either standard or continuous sampling. The standard sampling method involves dispensing volumes of preserved TOC sample within the coil, with additional unpreserved TOC sample used as low conductivity "spacer regions" on either side of the acidified sample segment (refer to Fig. 4). This creates conductivity "peaks" that indicate where each sample is within the coil. Results showing the reproducibility for the standard method of sample collection and analysis for in-lab sampling is shown later in this section. The continuous sampling method will be further described in Chapter VI.

Standard samples require ~5.5 mL total volume per sample within the storage coil. This is roughly the minimum volume to achieve good conductivity peak resolution for sample determination with the current conductivity probe and meter setup. This 5.5 mL volume is prepared with ~2.0 mL of acid-preserved high conductivity sample being spaced by ~1.75 mL of unpreserved low conductivity sample spacer regions on either side of the preserved section. This allows for the collection of a maximum of ~45 samples with the current 450 m storage coil. The programming for standard sampling with the current storage coil collects 38 samples to account for variation in the pumping capacity and allowing for a set volume to store the $CuSO_4$ used to indicate the start of a sampling session. The minimum run time per sample, and thus the highest allowable frequency sample interval, is ~20 minutes per standard sample. The standard sampling method allows a sampling frequency of roughly ~4.0 hours per sample for a week-long deployment with the current storage coil. The frequency or total sample amount can be modified prior to deployment in the TFTOOLS computer interface (Appendix B).

Following deployment, sample contained within the DOC storage coil is then dispensed into a series of acid washed and furnace dried small volume vials. Aliquots of ~0.5-0.8 mL acidified sample are dispensed sequentially into small vials (Appendix G) and capped to prevent the possibility of sample evaporation. Using the conductivity probe and meter, regions of low conductivity in successive small vial samples can be determined to be sample spacer regions, and successive preserved samples can be determined from the peaks in conductivity as noted. An example of a conductivity series for the standard sampling method with DI and 5% HCl is shown in Fig. 27.

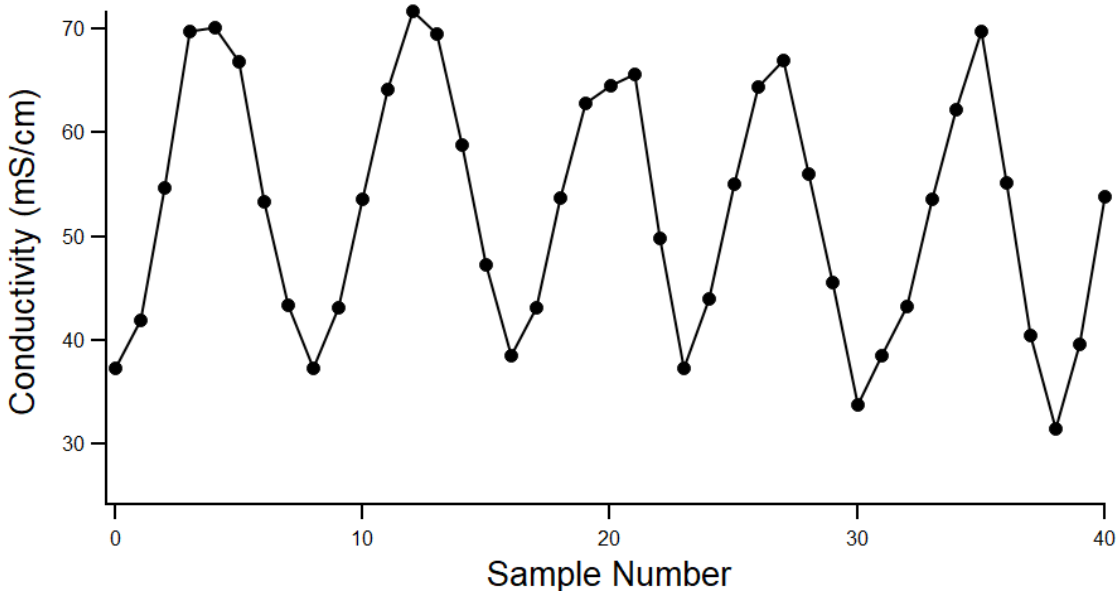

Figure 27 – *Results of conductivity measurements of DI preserved with 5% HCl with the DUCS. Samples were collected using the standard method of sample collection.*

Although the range of variability in peak maxima appears quite large (65.0-71.0 mS/cm), this is only due to small variation in the sample-to-acid ratio introduced during the mixing step. Undiluted acid stock conductivity was calculated to be ~505 mS/cm for this 5% HCl solution. This range (65.0-71.0 mS/cm) corresponds to individual samples being composed of ~12-14% acid reagent. This variability is likely explained by irreproducibility in pumping capacity (Fig. 26).

The small vials containing the ~0.5-0.8 mL aliquots are combined into a larger solution where conductivity spikes occur (i.e. highest conductivity vials). A new conductivity value is then measured for the combined samples. Using this conductivity value, an initial sample-to-acid dilution factor can be determined using equation 1. The combination of these smaller samples into a larger sample increases sample to blank ratios prior to sample analysis. For example, a 3.00 mL aliquot of sample can be aspirated from a combined solution of < 3.2 mL using 1.00 mL and 2.00 mL volumetric glass pipettes, and dispensed to a 10.00 mL volumetric flask for dilution. This step was changed to 4.00 mL using a single glass 2.00 mL pipette to reduce cleaning times between sample dilutions in later experimentation. This dilution step is a secondary dilution, and the accuracy and precision of volumetric dispenses for this step is shown in Fig. 28.

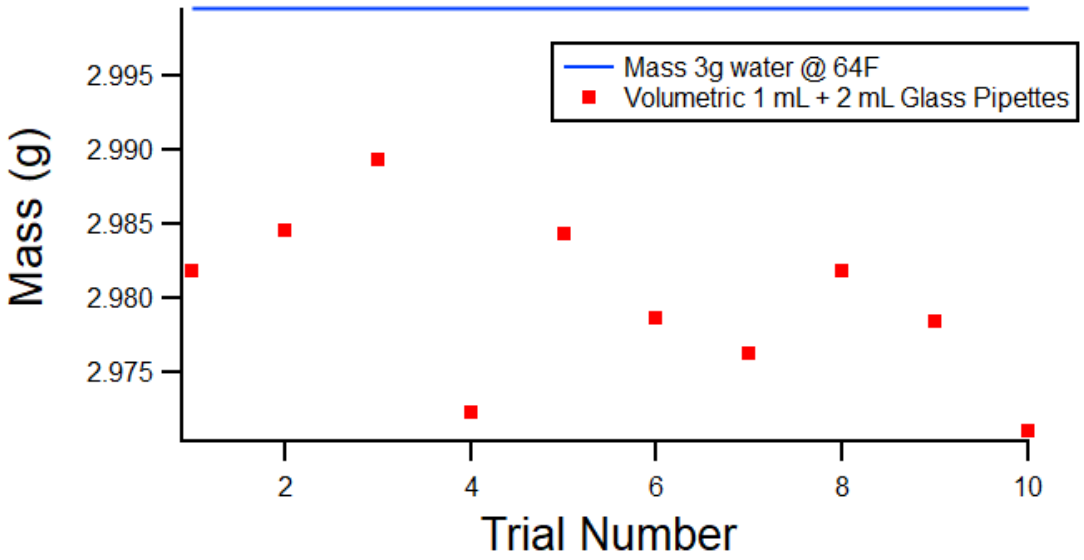

Figure 28 - *Results of successive measurements of using volumetric 1.00 mL and 2.00 mL pipettes to deliver a 3.00 mL sample. Average delivered volumes were gravimetrically determined to be 2.980 mL (±) 0.006 mL with an average error of 0.66%.*

A sample with a minimum volume of 10.00 mL is required for analysis on the Aurora using the current standard method of analysis in the Valett lab (Appendix C). Overall dilution factors can then be applied to the Aurora generated DOC using equation 2 to back calculate undiluted TOC concentrations for all analyzed samples.

$$\text{TOC}_{(\text{Undiluted})} = \frac{\text{TOC}_{(\text{Aurora})}}{\text{DFC}_{(\text{Eq. 1})}} \qquad \textit{Eq. 2}$$

It should be noted that the samples are not fully isolated due to sheering and diffusion of acid into the unacidified sample region. This causes an incomplete return to baseline conductivity between peaks, indicating there is some overlap between successive samples. However, samples are collected from the center portions of the conductivity peaks where the overlapping of samples is minimized, as shown in Fig. 29. It is possible to fully separate conductivity peaks by introducing more unacidified sample between the acidified sample plugs, but would lead to a significant loss in total samples that would fit into a set length of storage coil.

Sample that was preserved with 1% HCl was dispensed in ~0.5 mL segments from the storage coil for a higher-resolution conductivity series to accurately model the gaussian sample curves. It was found through integration of the peak collection areas (high conductivity regions) that there was no more than 0.5% sample overlap from any peak into the next peak, as is shown by the gaussian model additions for two successive peaks in Fig. 29. This can introduce a small error that increases with larger relative differences in TOC between each successive sample.

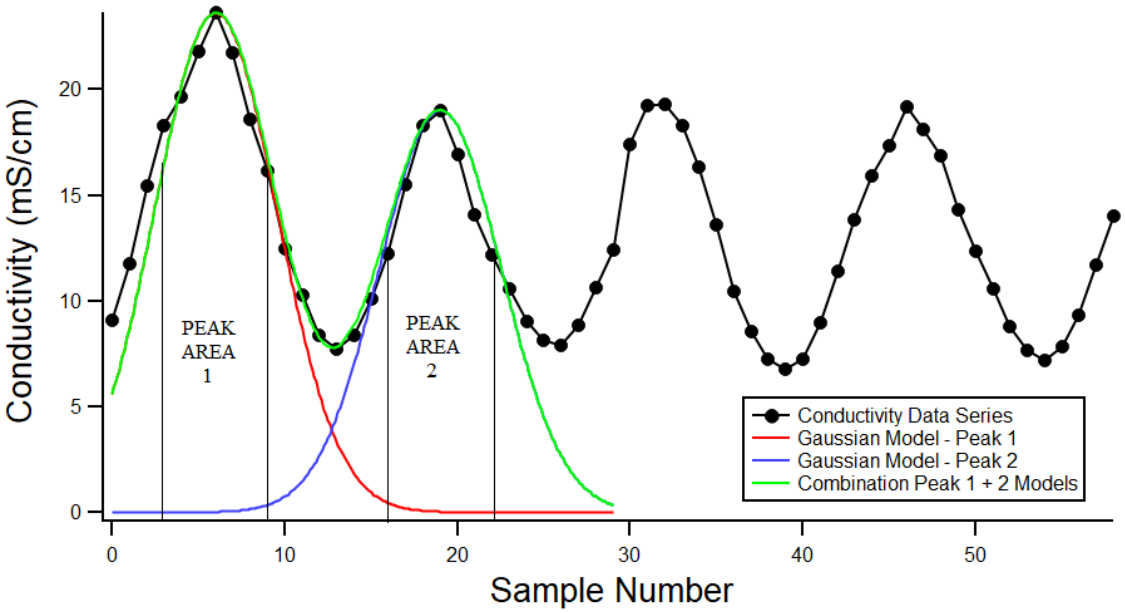

Figure 29 – *Gaussian modeling for estimating peak overlap between samples.*

H. DUCS – In-Lab Sample Analysis

For the standard method of analysis, it is assumed that HTOC values are linear with concentration (Fig. 30). This linearity means the HTOC response will decrease linearly with dilution factor. Since DOC concentrations are directly linear with dilution, dilution factors determined from conductivity (Fig. 25) can be directly applied to DOC measurements (Eq. 2). The standard method for HTOC analysis has been optimized the to minimize sample injection volumes (Appendix C).

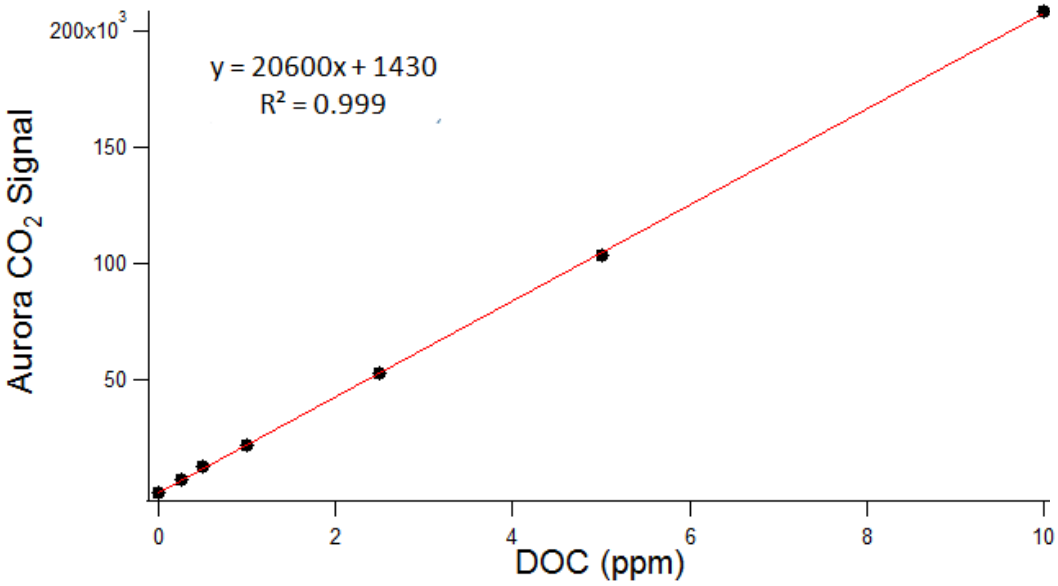

***Figure 30** – Typical calibration curve for DOC standards prepared from a 1000 ppm KHP stock solution and analyzed on the Aurora.*

Results show that HTOC response is directly proportional to DOC concentration (R^2 = 0.998). DOC stock solution was then prepared as 10.00 ppm C for in-lab sampling, with results shown in Table 7 below. This stock solution was then sampled in-lab. Following sampling, sample was dispensed to the small vials for conductivity analysis. The first five conductivity peaks were then combined into composite samples for analysis, and dilution factors with conductivity were determined using equation 1. Then, 1.00 mL was then taken from these composite samples using a 1.00 mL volumetric pipette diluted to 5.00 mL in a volumetric flask. It should be noted the current standard sample preparation procedure involves secondary dilution of volumes larger than 1 mL

(3-4 mL), rather than the scheme used in this experiment. This is to increase the sample to blank ratio. Analysis was then conducted on the Aurora, and DOC values were then determined. The dilution factors from conductivity and secondary dilution factors were then applied to the Aurora generated DOC value to get back calculated DOC values using equation 2. The overall results of applying this method for a set of Aurora 1030 generated values are shown in Table 7.

Table 7 – *Back calculating DOC concentration in standard samples using dilution factors measured measuring conductivity when doing a 1 mL to 5 mL dilution with a volumetric flask.*

Sample Number	Aurora Measured Value (ppm)	Dilution Factor (Cond)	Dilution Factor (1->5 mL)	Back-Calculated Value DOC (ppm)
Stock 10 ppm	-	-	-	10.18
1	1.669	0.7621	0.2	10.95
2	1.704	0.7650	0.2	11.14
3	1.592	0.7594	0.2	10.48
4	1.595	0.7412	0.2	10.76
5	1.715	0.7783	0.2	11.02

This shows that DOC concentrations in measured samples during this analysis were ~5.6% higher than those measured from the 10 ppm DOC stock solution. Historic data prior to development of the current standard method of analysis have seen up to 30% inaccuracy (not shown) when analyzing similar DOC stock. This overestimation was due to high sampler blanks and acid stock contaminated with high levels of DOC in addition to using a small amount of sample compared to acid during sample collection (50:50 sample to acid ratio).

Following these initial results after developing the standard method of analysis, the reproducibility of the DUCS was tested when collecting a range of DOC concentrations. DOC (KHP) stock standards were prepared as 0.5 ppm, 1.0 ppm, 2.5 ppm, 5.0 ppm, and 10 ppm DOC. In this test the standards were collected and stored during individual tests with acidified samples being separated by unacidified sample. Samples were then analyzed using the standard method of analysis described above. Results of this test are shown in Fig. 31.

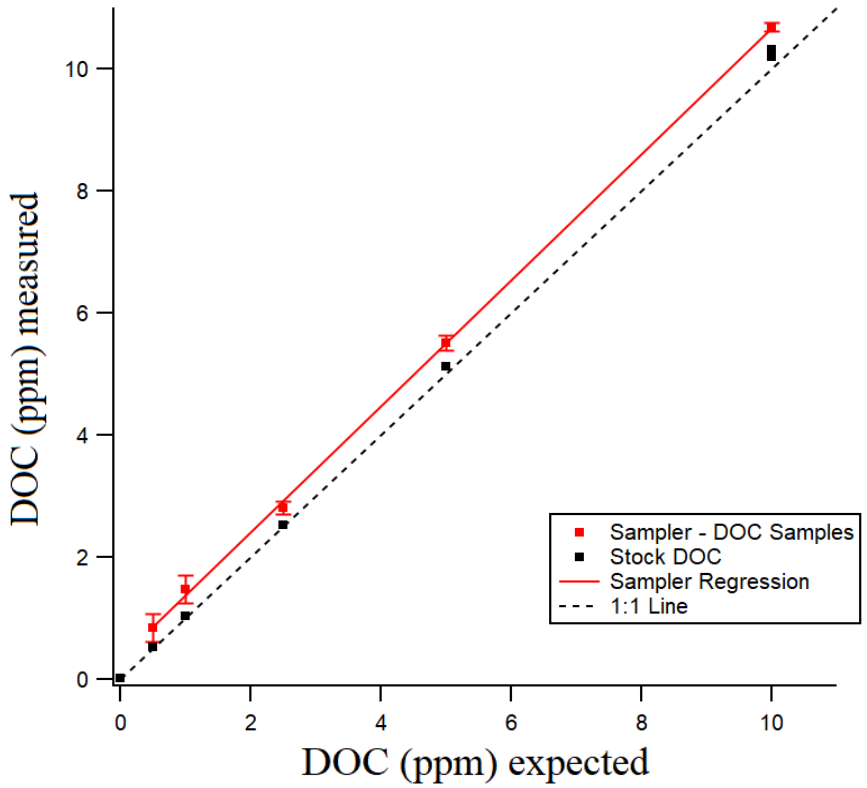

Figure 31 – *Analysis of samples stored in the storage coil using the standard method of sampling for DOC standard solutions of 0.5 ppm, 1.0 ppm, 2.5 ppm, 5.0 ppm, and 10 ppm DOC. Red dots are concentrations for samples stored using the standard method of sample collection (n=10, each concentration). Black dots are measured concentrations for stock solutions.*

There was a systematic overestimation of DOC for all standard solutions. It can also be seen that there was an increased relative range, or spread, of the measured DOC value in measurements at low concentrations (Fig. 31). This systematic overestimation causes an error that is significantly and proportionally increased in low ppm C compared to high ppm C stock solutions (42% vs. 3.2% average error for 0.5 vs. 5 ppm standards respectively). This is most likely primarily controlled by blank contamination, which leads to sample concentration overestimation (i.e. blank contamination from DUCS itself can be as high as 20% the total DOC of a 0.5 ppm DOC solution). This systematic overestimation was also indicated by the slope (1.033) near the 1:1 line in addition to the positive y intercept (0.3403). Due to these relative errors, the DUCS in its current state is likely better suited for higher DOC systems, pending further decreases in DOC blanks.

I. DUCS – TOC vs. DOC Sampling

As noted above, the issues with filtration meant that TOC (POC + DOC) sample is collected with the DUCS rather than just DOC sample. It has been observed by others that TOC samples can have uncertainties coming from sample dependent oxidation efficiency as well as issues with incomplete purging of inorganic carbon (Aiken et al., 2002). To check whether TOC sample could be analyzed similarly to a standard DOC sample, a ~10 ppm TOC standard was created using brewer's yeast (*S. Cerevisiea)* using the methodology outlined in Appendix F. This stock solution was used to create a ~10 ppm TOC in the size range between 0.45 μm-25 μm through vacuum filtration of the yeast solution. After an initial test showed that increasing the reaction time used by the Aurora to fully capture the entire TOC CO_2 peak was required, experimentation to determine the actual the concentration (in ppm C) of the stock TOC solution was conducted. This was done to determine whether the TOC calibration would be linear with dilution factor. Various dilutions of this standard were prepared and analyzed using a KHP generated calibration curve. The results of this experiment showed a linear response with TOC ($R^2 = 0.999$, Appendix F). Undiluted TOC stock concentration was determined to be 9.036 ppm C. This deviation from the expected 10 ppm C was likely due to the filter paper retaining more of the initial yeast mass than expected. The results of TOC concentrations being linear with dilution factor indicate TOC samples collected with the DUCS can be analyzed similarly to standard DOC samples on the Aurora, and that full oxidation of TOC sample is occurring. Additional experimentation described in Appendix C gives further evidence high oxidation efficiency of TOC and that full purging of inorganic carbon by the Aurora is also being accomplished.

To confirm that the DUCS was field-deployable, the full system was prepped for a full in-situ test within the lab. A TOC standard of ~4.5 ppm C was attached to the DUCS in a sealed, airtight reagent bag. This system was then submerged in a water tank and collected 24 hourly samples within the storage coil. Following the 24 hour period, the DUCS was then recovered from the water tank, opened, and examined for leaks. No leaks were found. Sample collection

timestamps and temperatures were confirmed to be operational. The samples from the coil were then dispensed into the small vials and conductivity measurements were made to confirm samples had been successfully collected. The first five small vials samples, indicated by conductivity peaks, were then combined and diluted to the minimum volumes required for analysis on the Aurora. Following TOC analysis, the appropriate overall dilution factors were then applied to Aurora generated values (eq. 2). Analysis of the prepared ~5 ppm TOC stock solution showed it to have a concentration of 4.520 ppm C. The results of analysis of the collected TOC samples are shown in Fig. 32.

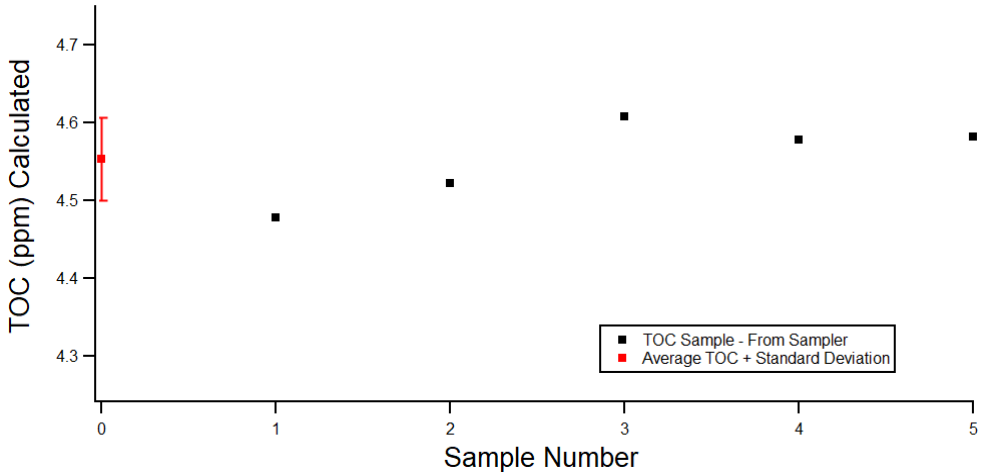

Figure 32 – *Analysis of TOC samples for the first five eluted samples from the TOC in-lab deployment experiment. Black dots represent the first five samples collected and analyzed from the sampler, with the average TOC + standard deviation of these analyzed samples being show as the red dot and whisker.*

When comparing measured vs. expected TOC values, it was found that there was an average 1.1% error in the accuracy of measured TOC samples vs. the stock solution from which the samples were drawn (4.554 ± 0.052 ppm vs. 4.520 ppm respectively). It should be noted that this error is similar in magnitude to errors shown shown previously for DOC samples (Fig. 31), as there was on average systematic overestimation of TOC vs. the stock solution. This is likely originating from the same contamination observed during standard DOC analysis. After the DUCS been confirmed to be both field-deployable and equipped to collect in-situ TOC samples, it was ready for field deployments.

V. Field Deployments - Data Analysis and Discussion

A. DUCS - Field Deployment One

The initial field deployment for the DUCS began on September 16, 2020 in the CFR at 46°51'53.7"N 113°58'39.3"W - near the Montana Technology Enterprise Center (MTEC) in Missoula, Montana. The DUCS was deployed collecting 38 samples at 2-hourly intervals for a total of ~ 3 days (Fig. 33). A black plastic bag was fitted around the storage coil to prevent the possibility of photodegradation of organics within the storage coil.

Figure 33 – *Initial deployment of the DUCS in the CFR on September 16, 2020.*

Upon recovery of the DUCS on September 19, it was noted that the visual $CuSO_4$ indicator did not make its way through the coil, indicating little or no sample flow. Upon further inspection, it was found that a few tubing loops on the storage coil had been severely crimped on the outer facing tubing, preventing flow through the storage coil. The cause was likely contact of this section of the coil with rocks in the turbulent rapids where the DUCS was deployed. To prevent similar damage to the storage coil in future deployments, a thick copper mesh was fitted and secured around the outward facing portion of the coil. The closed shell configuration of the DUCS with this mesh cage is shown in Fig. 34.

Figure 34 – *Closed shell configuration of the DUCS. A copper mesh cage surrounds and protects the exposed black plastic covered sample coil. The electronics and plumbing (Fig. 22) are sealed airtight within the SAMI housing.*

B. DUCS - Field Deployment 2

The DUCS was then redeployed on September 23, 2020 at the same location as the initial deployment. During the second deployment, 38 samples were collected at 4 hour intervals (~6 days) starting at 9:00 UTC. The DUCS was deployed alongside a Submersible Ultraviolet Nitrate Analyzer (SUNA) in order to view trends in CDOM. Discrete quality control (QC) samples were concurrently collected during corresponding sample collection times for the DUCS. QC samples were collected as early as 6:00 AM and as late as 10:00 PM local time in an attempt to capture the full range of potential diel TOC variability. The 10-μm inlet filter on the DUCS was replaced about every other day to minimize any effect of biofouling or clogging at the inlet.

Following instrument recovery, the black plastic covering was removed, and it was noted that the $CuSO_4$ indicator was on the outer shell of the storage coil which indicated proper sample flow. The $CuSO_4$ indicator was fully dispensed to waste. Sample stored in the storage coil was then dispensed to the small vials for conductivity measurements in 0.8-1.0 mL segments. The conductivity time series of this sample set was then generated (Fig. 35).

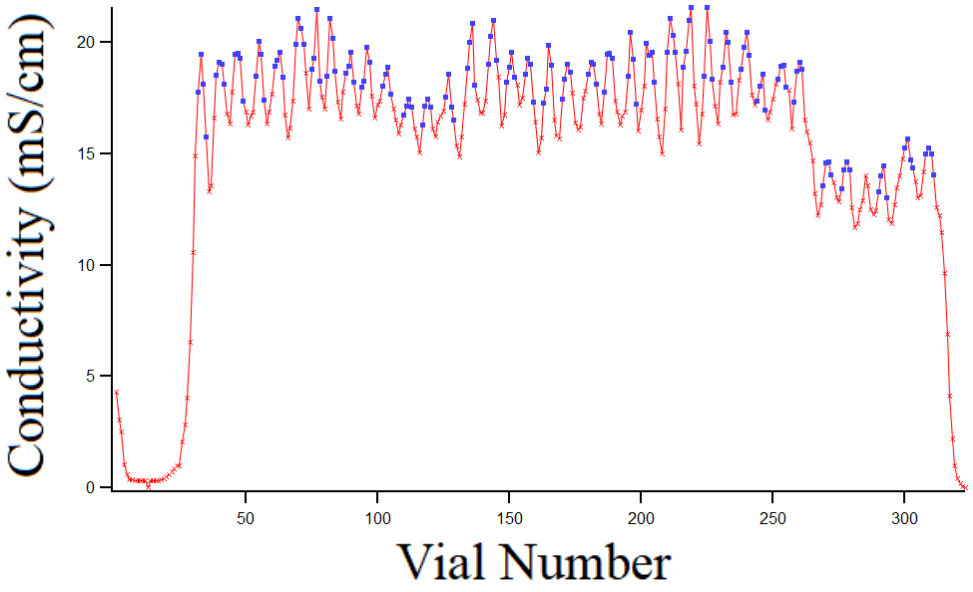

Figure 35 – *Conductivity series for the second deployment sample set. Samples combined from each peak are shown as blue dots on the red conductivity series measured for each vial. Acid reagent for this deployment was 1% HCl.*

Although the differences in peak heights past sample number ~250 showed a drop in average conductivity, this was likely due to a slightly different sample-to-acid ratio being introduced following filter replacement on Sept 28th. From this conductivity series, a total of 38 combined samples were confirmed to have been collected. The full 38 peaks collected, along with offloaded temperature and time data from the memory of the DUCS, indicated sampling occurred as expected throughout the entire course of deployment. Combined sample from these peaks was then prepared for sample analysis on the Aurora. The samples were capped in acid washed and ashed 40 mL amber vials prior to analysis. A total of 18 QC control samples were collected, filtered,

and prepared for analysis on the Aurora. Following the standard method of analysis, the dataset for the second deployment was generated, as shown in Fig. 36.

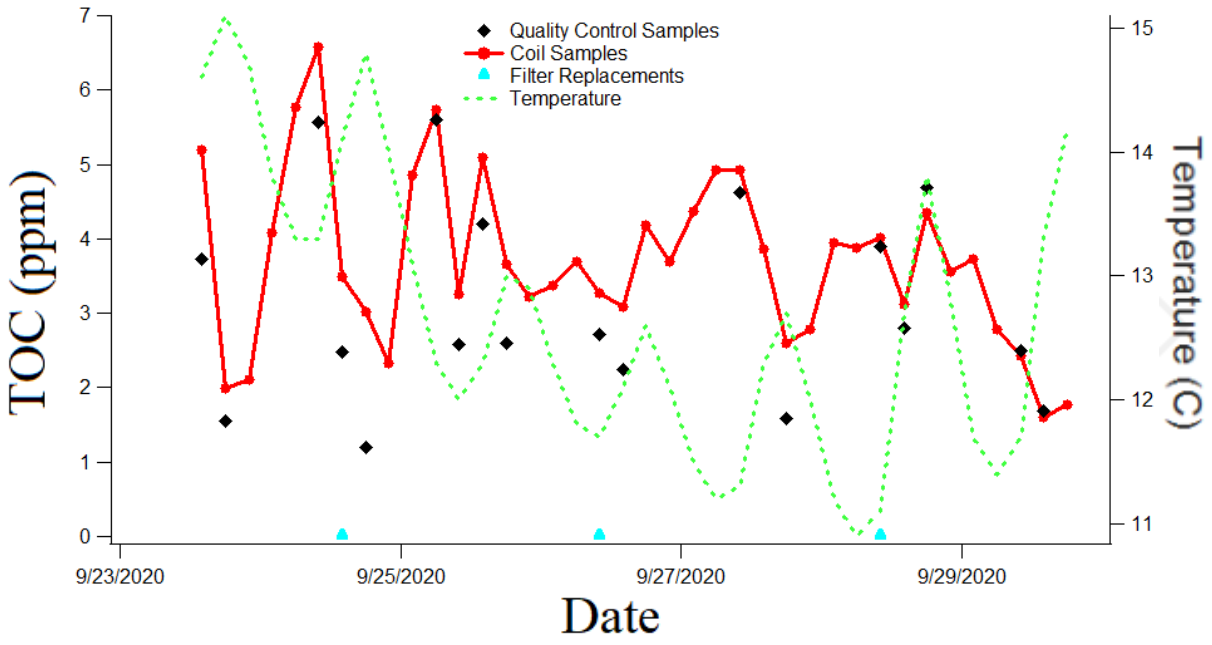

Figure 36 – *Results of samples collected with the DUCS (red circles) and QC samples (black squares). Filter replacement times are indicated by the green triangles.*

These results (Fig. 36) indicate that TOC was highly variable during the deployment with a weak diel pattern. The general downward or upward trends in TOC captured by the DUCS were also evident in the QC samples. The average sampling accuracy error when comparing between the quality-controlled samples was relatively large at ~30%. This large error could have arisen through carryover from sample to sample from TOC sticking to the tubing - increasing TOC background. This could cause DUCS data to have significantly positive error versus their respective QC sample (e.g., QC'ed Sample 5 had 165% error). TOC values were found to have little correlation with temperature ($R^2 = 0.04$). To further evaluate the accuracy of this dataset, samples from the DUCS with corresponding QC samples were plotted against each other (Fig. 37).

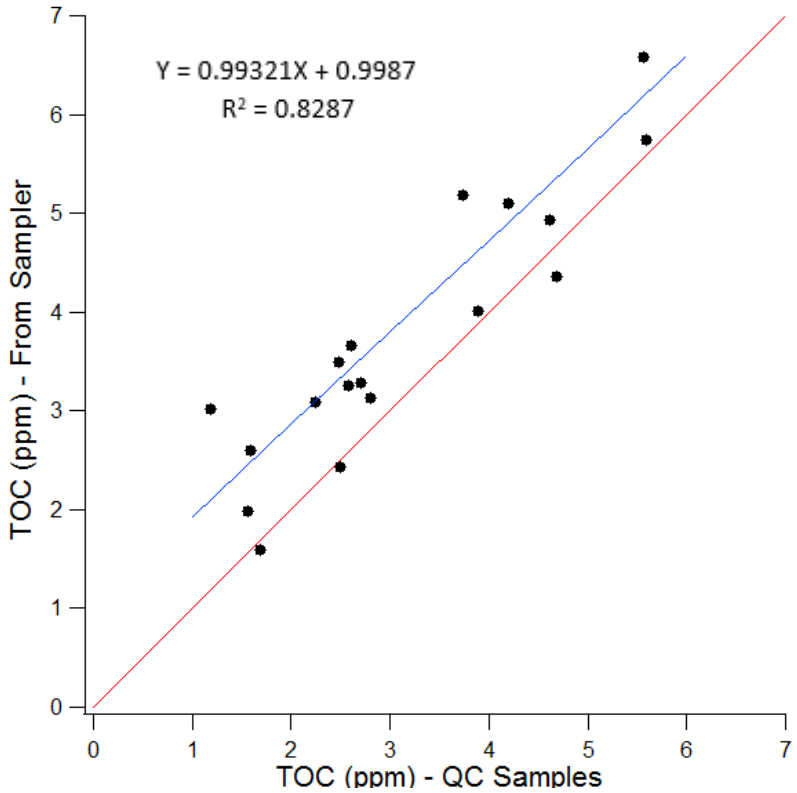

Figure 37 – *QC TOC samples vs. sampler collected TOC samples (From Fig. 36). A 1:1 overlay is shown by the red line. Linear regression for the QC vs. sampler samples is shown by the blue line.*

While the slope estimates a 1:1 line, scatter in the data results in an overall weaker correlation coefficient then expected ($R^2 = 0.8287$, Fig. 37 vs. $R^2 = 0.9987$, Fig. 31). The significant y-intercept of this regression is due to the overestimation of TOC in stored samples, as stated above. This is likely due to a combination of both baseline sampler blank TOC levels in addition to potentially greater than expected TOC spreading. Together, these can potentially explain the systematic overestimation in TOC values. In an effort to help prevent possible increased TOC spreading and carryover within the storage coil, the undiluted 1% HCl acid stock that was typically used for sampling was replaced with 5% HCl. This would allow for a stronger acid concentration throughout the coil hopefully reducing the possibility for TOC adherence while simultaneously all but eliminating any errors potentially associated with alkalinity neutralization and background river conductivity as was discussed in Chapter IV.

In summary with the potential errors discussed in the paragraphs above, this weaker correlation coefficient and larger y-intercept can be further explained by 1) potential spatial variation between TOC values and QC samples collected from the shore (more rocky) vs. TOC samples collected by the DUCS a few meters out at the bottom of the stream (more algae), 2) potential filtration of different fractions of TOC when using different filter treatments used in QC (hydrophobic polypropylene (PPE) 10 μm filters) and DUCS collected samples (hydrophobic 10-μm filters at the sampler inlet), 3) increased sample spreading of the organic fraction in the UCFR than expected (See Figs. 20, 29), and 4) TOC sampler blank contamination.

Data from the SUNA was also offloaded for insight into the CDOM:TOC relationship. Observation of the SUNA indicated an increasing absorbance baseline likely due to bio fouling. This increase was detrended before comparisons (Fig. 38). This data indicated TOC was weakly correlated (R^2 = 0.187, p=38) with CDOM absorbance at 350 nm (Fig. 39). This correlation was stronger (R^2 = 0.578, p=13) prior to a storm event which occurred during this deployment on September 26, 2020 (Fig. 40). This storm event significantly increased the scatter in the CDOM:TOC relationship (R^2 = 0.075, p=25). The CDOM:TOC correlation found over the course of deployment when using QC samples was also examined (R^2 = 0.066, p=18). The overall CDOM correlation may be better correlated with DOC, as TOC is not expected to be as strongly correlated with CDOM as DOC.

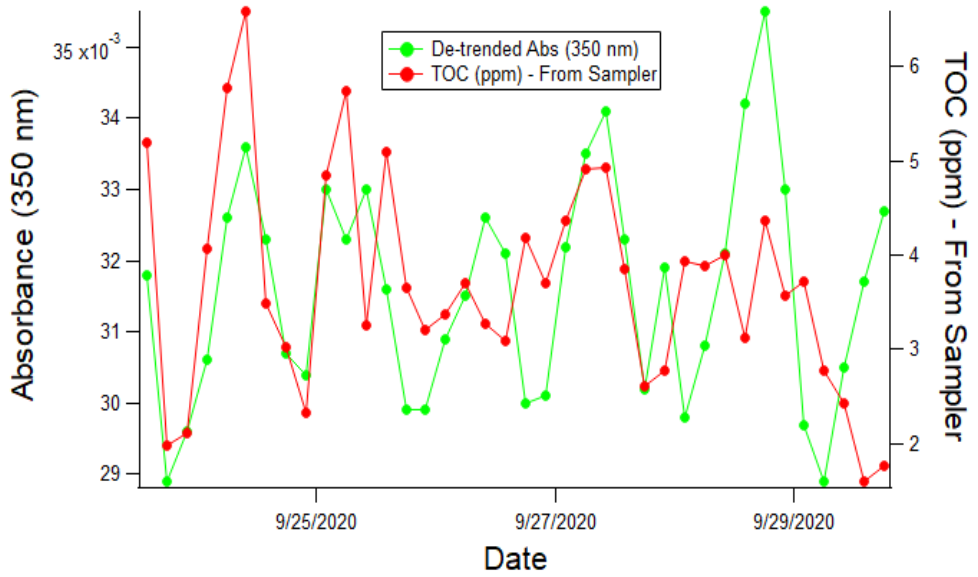

Figure 38 – *Detrended SUNA generated absorbance (350 nm) overlayed against the TOC generated timeseries from the sampler.*

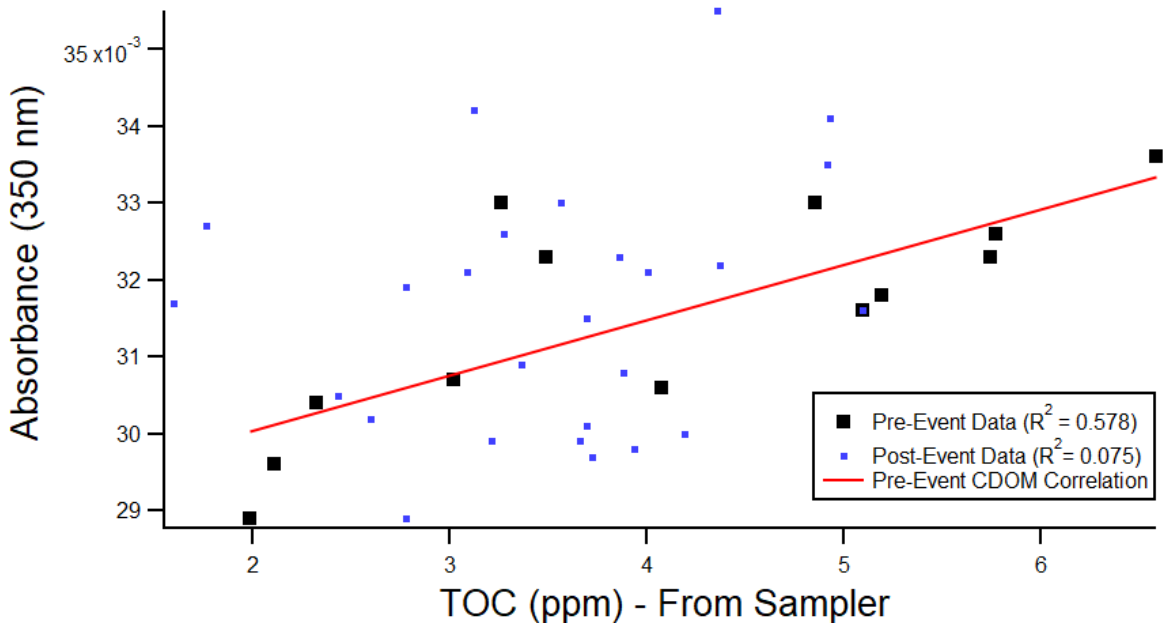

Figure 39 – *Correlation between TOC (ppm) from the sampler and absorbance (350 nm) data from the SUNA (From Fig. 38).*

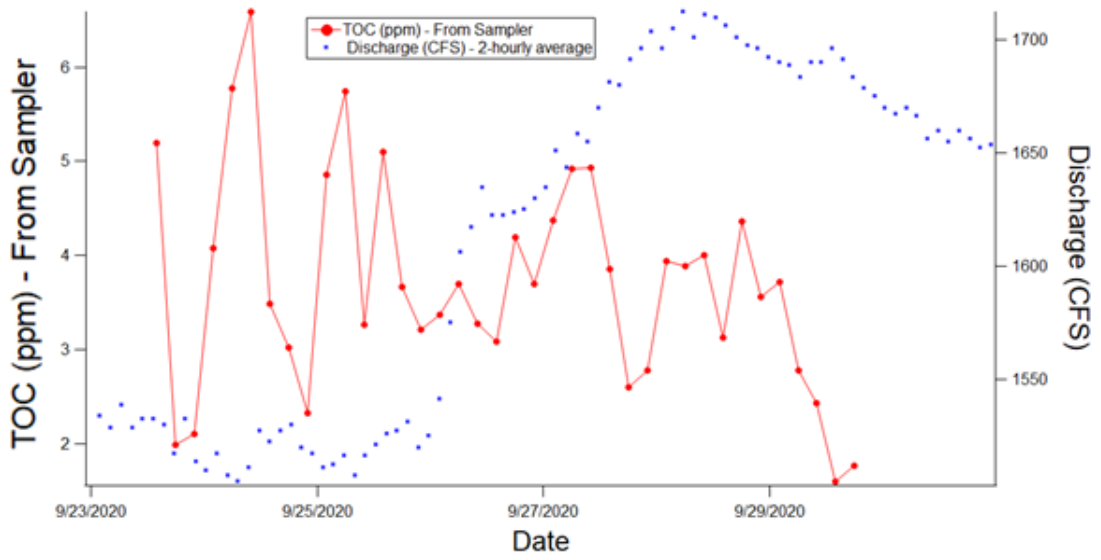

Figure 40 – *TOC data from the sampler deployment overlaid with the discharge data from USGS station 12340500 above Missoula.*

C. DUCS – Field Deployment 3

Following the second deployment, the DUCS and SUNA were prepped for an additional field test to look at the real-world reproducibility of the DUCS. The acid reagent concentration was increased from 1% to 5% to help prevent the possible organic sheering that may have been occurring during the previous deployment. The third deployment took place starting Jan 21, 2021. The location of deployment was at 46°51'47.9"N 113°58'28.4"W near the Hellgate Osprey Nest. The location was moved further upstream due to the icy river banks present at the previous deployment location. During this deployment 36 samples were collected at 2-hour intervals (~3 days) starting at 9:00 UTC. The DUCS was again deployed alongside a SUNA. Temperatures measured during this deployment were significantly lower than during the first and second deployment, with water temperatures reaching as low as 0.01 ºC. These lower temperatures caused significant river ice formation near the DUCS deployment location, with the river surface over the DUCS freezing during deployment (Fig 41).

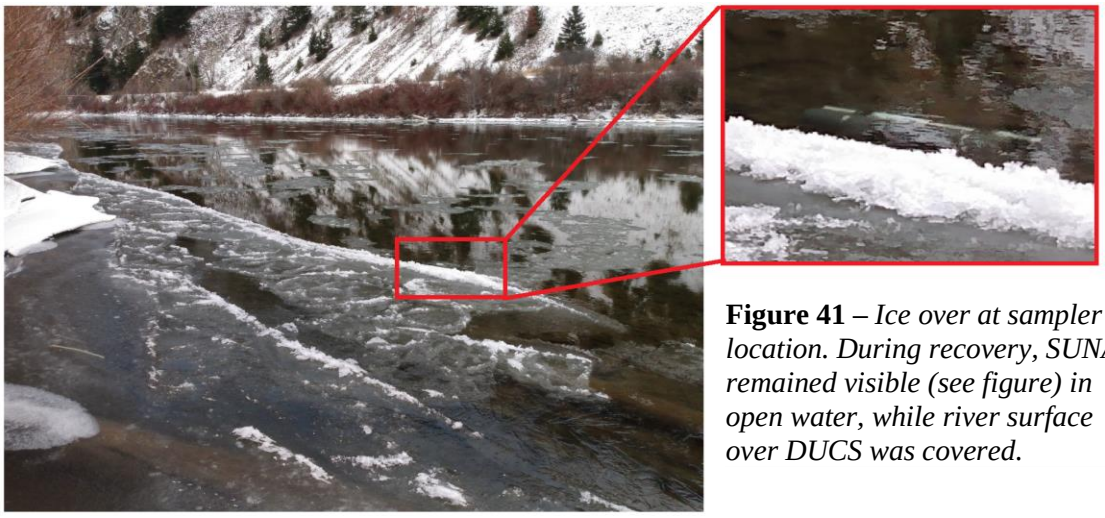

Figure 41 – *Ice over at sampler location. During recovery, SUNA remained visible (see figure) in open water, while river surface over DUCS was covered.*

Following instrument recovery, it was noted that the $CuSO_4$ indicator was near the outer shell of the storage coil which indicated proper sample flow. The $CuSO_4$ indicator was fully dispensed to waste. Sample stored in the storage coil was then dispensed to the small vials for conductivity measurements in 0.5-0.7 mL segments. The conductivity series of this sample set was then generated (Fig. 42). Note the higher conductivity baseline because of the use of 5% HCl compared to the previous deployment (Fig. 35)

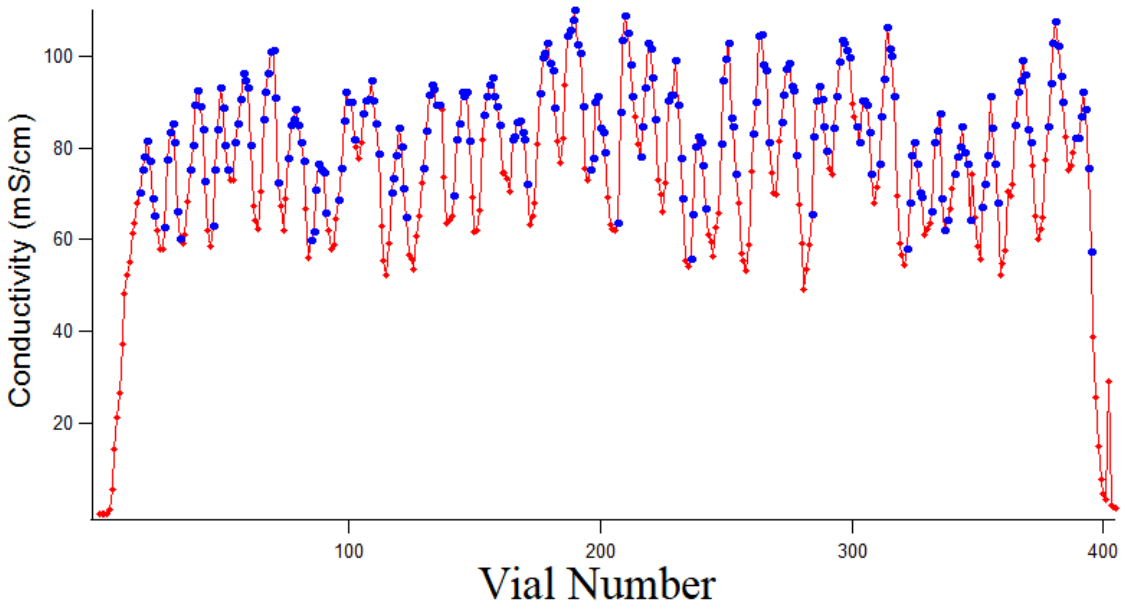

Figure 42 – *Conductivity series for the third deployment sample set. Samples combined from each peak are shown as blue dots on the red conductivity series measured for each vial. Acid reagent for this deployment was 5% HCl.*

From this conductivity series, a total of 36 sample peaks were confirmed to have been collected. The full 36 peaks collected, along with offloaded data from memory, indicated sampling occurred as expected throughout the entire course of deployment. Combined sample from these peaks was then prepared for sample analysis on the Aurora diluting 4 mL of sample collected peaks into 10 mL samples. They were then capped in acid washed and ashed 40 mL amber vials in preparation for DOC analysis. A total of 19 triplicate QC control were collected, filtered, and prepared for analysis on the Aurora. It was a mistake to not take replicate QC samples during the previous field study to quantify the sampling uncertainty, so triplicate QC samples were taken as close in time as possible during this study. QC samples were also taken at the DUCS inlet, as opposed to the river bank, in contrast with the previous deployment. Following sample analysis, the dataset for the third deployment was generated, as shown in Fig. 43.

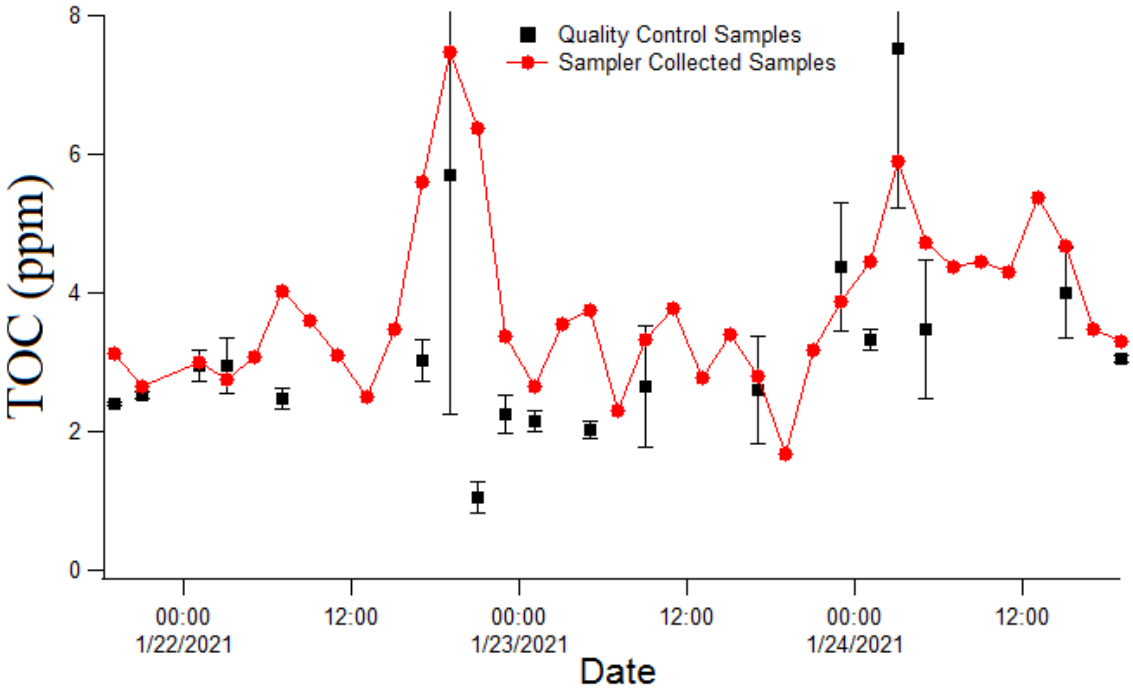

Figure 43 – *Results of samples collected with the DUCS (red circles) and QC samples (black squares + whiskers).*

Compared to the results from the second deployment (Fig. 36), there appears to be no trace of a diel pattern for TOC for this deployment (Fig. 43). The general downward and upward trends in TOC captured by the DUCS were also present in the QC samples. The average sampling accuracy error when comparing between the quality-controlled samples was larger than the second deployment at around 51%. This average error was significantly reduced to 26% when excluding a significant outlier (QC sample 7 had 511% error). When collecting QC samples near the time of this outlier (QC sample 6), it was noted that there was a noticeable film of organic matter on the water surface near the deployment location. Because of this, QC samples for this time were taken both at the inlet, as well as ~ 20 feet upstream away from the organic surface layer. Both sets of QC samples taken during this time showed significant sampling uncertainty. When removing the outlier (QC sample 7) the average accuracy error for this deployment (26%) was more in line to what was observed during the second deployment (30%). Average sampling uncertainty in QC samples was ~16.5%. To further evaluate the accuracy of this dataset, samples from the DUCS with corresponding QC samples were plotted against each other (Fig. 44).

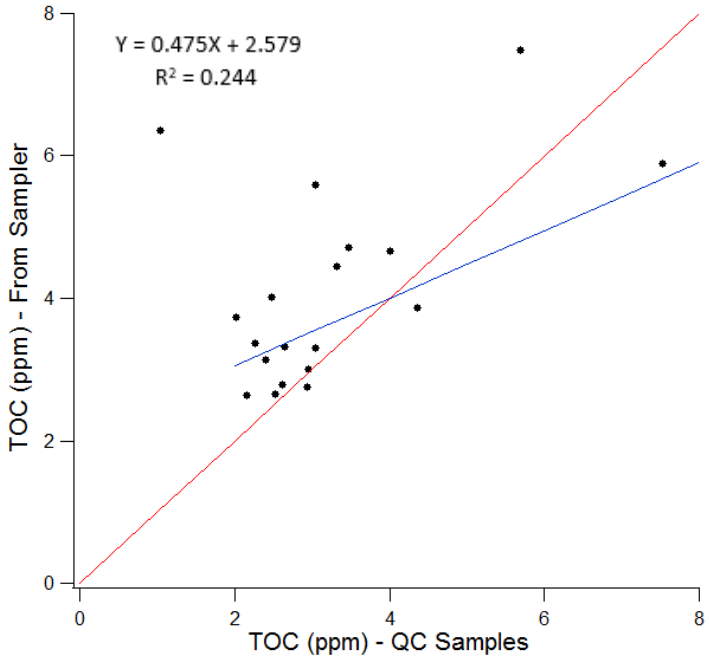

Figure 44 – *QC TOC samples vs. sampler collected TOC samples (From Fig. 43). A 1:1 overlay is shown by the red line. Linear regression for the QC vs. sampler samples is shown by the blue line.*

The scatter in the data resulted in an even overall weaker correlation coefficient than the second deployment (R^2 = 0.244, Fig. 44 vs. R^2 = 0.829, Fig. 37). The range in data for this deployment was also much narrower, however, and this likely influenced this correlation. This relationship was significantly improved (R^2 = 0.52) when removing the most significant outlier discussed above (QC sample 7). The high y-intercept of this regression is again due to the consistent overestimation of TOC (ppm) in DUCS stored samples vs. QC samples, similar to the previous deployment. This can be partially attributed to both blank contamination and the significant sampling uncertainty associated with some of these TOC samples (seen as black squares and error bars, Fig. 43), but there is also the possibility that increasing acid reagent stock from 1% to 5% did not further reduce organic sample spreading. Assuming increasing acid concentration does not resolve organic spreading, this issue could potentially be resolved in future deployments by either spacing samples further apart or using more total volume per sample. Data from the SUNA was also offloaded for insight into the CDOM:TOC relationship, and an overlay of this data with the TOC values seen during the third deployment as shown in Fig. 45.

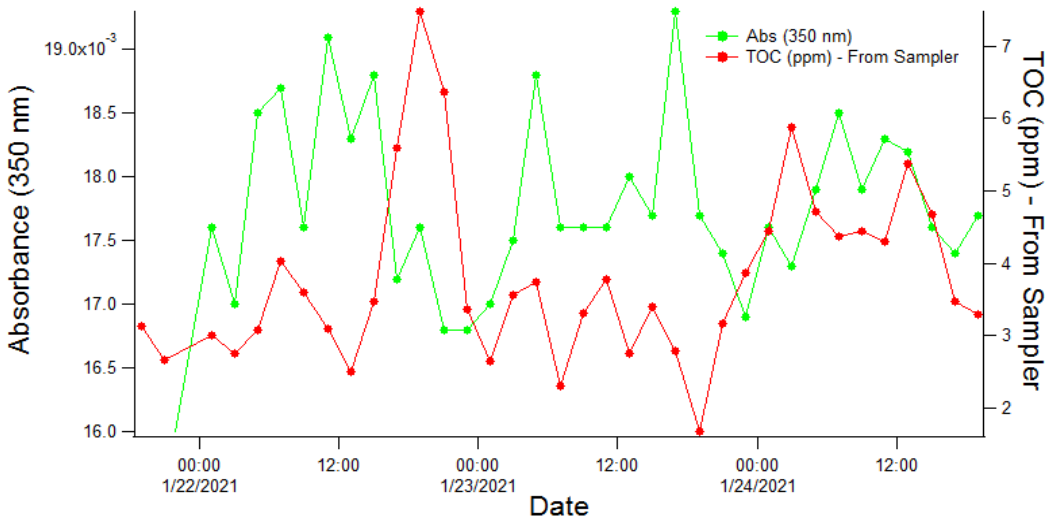

Figure 45 – *SUNA generated absorbance (350 nm) overlayed against the TOC generated timeseries from the DUCS.*

The lack of a clear diel in TOC indicated that daily photosynthesis and nightly respiration did not dominate TOC patterns within the system, and TOC was less interlinked with photosynthesis and respiration pathways than during the second deployment. The comparison between SUNA generated absorbances (350 nm) and TOC (ppm) showed no correlation between TOC and CDOM ($R^2 = 0.00006$), in strong contrast with the previous deployment. This could imply that allochthonous sources of TOC were more significant than autochthonous sources. It should also be noted that the total observed range of absorbances, as well as the average absorbance values (350 nm) were about 50% lower than observed during the second deployment. This may also play a role in the overall weaker correlation seen during the second deployment. The correlation between TOC and absorbance (350 nm) for the third deployment is shown in Fig. 46.

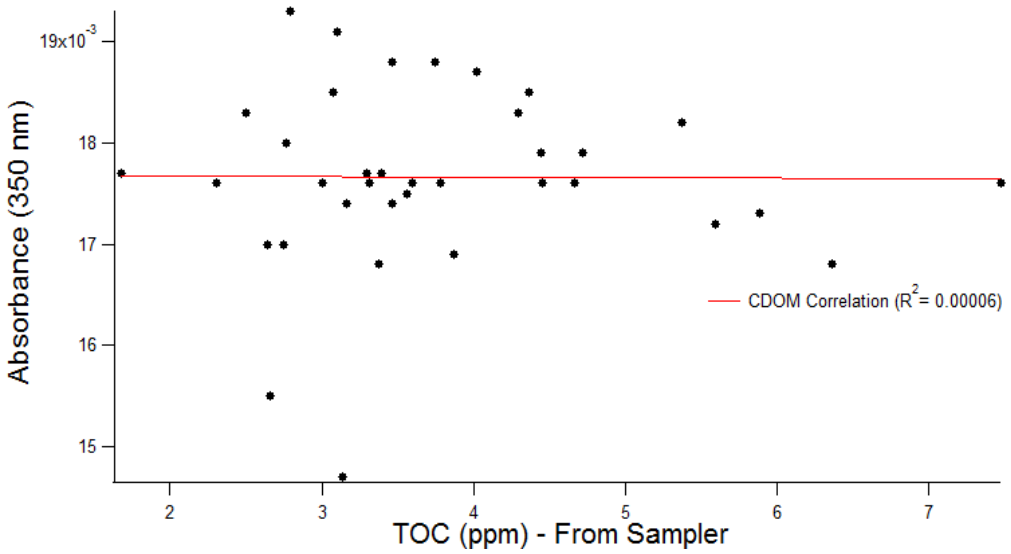

Figure 46 – *Correlation between TOC (ppm) from the DUCS and absorbance (350 nm) data from the SUNA (From Fig. 35).*

D. DUCS – Post Deployment System Optimization

The results from the third deployment indicated that increasing the acid concentration from 1% to 5% likely did not prevent TOC sample blank carryover. To assess differential concentration gradients and how "far" these different gradients will spread into successive samples, as well as to further examine the potential sheering problems described above, a set of lab experiments were carried out. In the first experiment, a series of 0 ppm C (DI), 2.5 ppm C, 5 ppm C, and 10 ppm C standards were prepared for in-lab sampling using 5% HCl. The DUCS then collected these standards as sets (n=5) of samples from the 2.5, 5, 2.5, 10, and DI standards sequentially for storage. Samples were then dispensed from storage and prepared for analysis. The results of this analysis are shown below in Fig. 47.

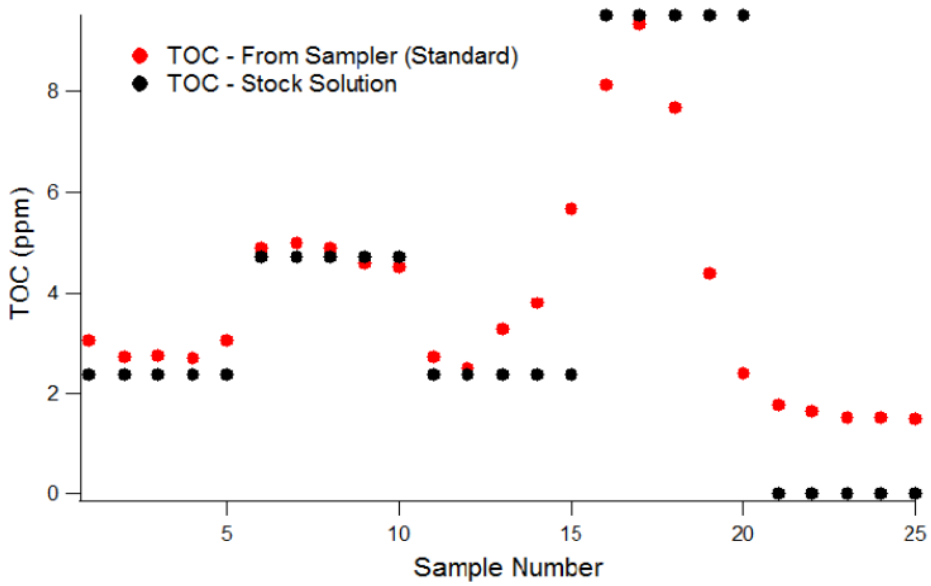

Figure 47 – *Analysis of TOC samples collected in the experiment using the standard sampling method with a 450-m storage coil.*

As discussed above, the standard sampling scheme stores a sample within a set of sequential steps. These steps introduce a sample as a segment of high-conductivity acidified sample with low-conductivity unacidified sample on either side of the acidified sample segment. Samples are collected from the conductivity "peaks" with this method, with collected peaks being ~ 80% sample // 20 % acid reagent by volume. Another possible sampling scheme that was further explored as a potential alternative to the standard sampling method used a "reversed" sampling method.

In this reversed scheme, the acidified sample segments are introduced to the sample coil with undiluted acid reagent, rather than undiluted sample, on either side of each acidified sample segment. Sampling with this approach may prevent the residual carryover between samples seen in Fig. 47. Samples collected using this method would be determined using conductivity "valleys". It was found that using 5% HCl for this step caused all conductivity measurements within the small vials post-sampling to be outside of the linear range of the conductivity probe. However, it was found that these conductivity valleys could be readily resolved for sample collection, similarly to conductivity peaks using the standard scheme, when undiluted HCl acid stock was 3%. Samples collected from valleys using the reversed method were ~ 15 % sample // 85 % acid reagent by volume.

Average conductivity of samples stored using the reversed scheme were ~3x higher than the average conductivity of samples stored using the standard scheme. This indicates that the average acid concentration at any point in the storage coil was higher in the reversed vs. standard schemes, which could potentially reduce organic sample sheering due to organic adhesion to tubing. In the second experiment, a series of 0 ppm C (DI), 2.5 ppm C, 5 ppm C, and 10 ppm C standards were prepared for lab sampling using the standard sampling method with 3% HCl. The DUCS then collected these standards as sets (n=5) of samples from the 2.5, 5, 2.5, 10, and DI standards sequentially for storage. Samples were then dispensed from storage and prepared for analysis. The results of this analysis is shown below in Fig. 48.

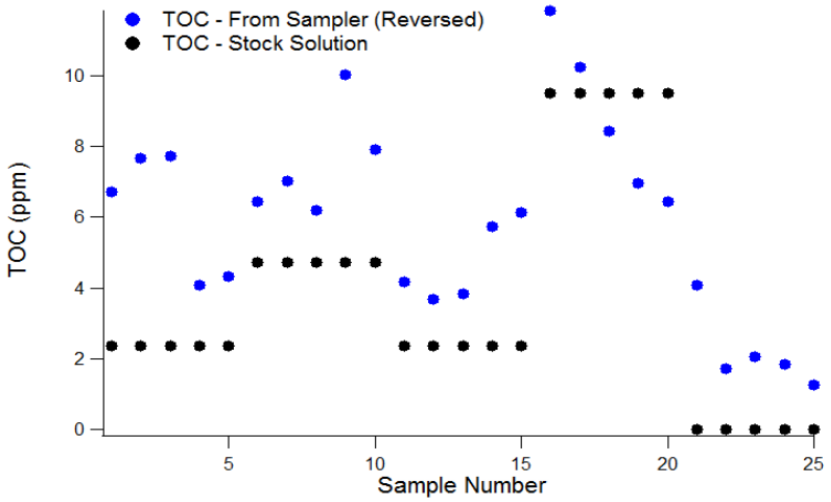

Figure 48 – *Analysis of TOC samples collected in the experiment using the reversed sampling method.*

A graphic overlaying the experimental results presented in Fig. 47 and 48 is shown below in Fig. 49, which will be followed by further discussion.

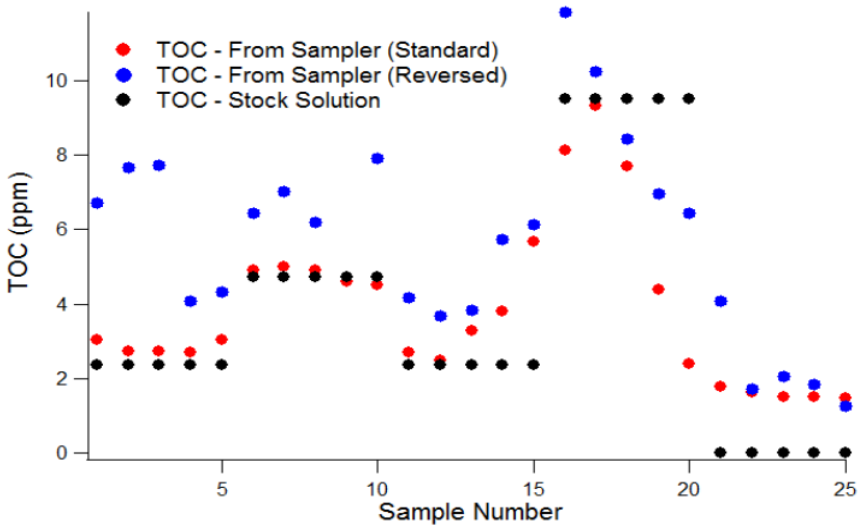

Figure 49 – *Overlay of experimental results comparing the standard and reversed sampling methods.*

When looking at the results of the standard sampling scheme experiment, it was shown that standard scheme samples showed similar behavior to those collected in previous in-lab experimentation (Fig. 31), with sample TOC concentrations tending to be slightly over-estimated.

It should be noted that there was an exception to this generalization as the 10 ppm samples in this experiment were underestimated on average compared to previous experimentation. This variation is likely due to differences in experimental setup. For example, collecting 10 ppm samples surrounded on either side by 2.5 and 0 ppm samples (Fig. 47) caused underestimation due to sample sheering vs. collecting 10 ppm samples from a sample series consisting of only 10 ppm samples which caused overestimation due to blank contamination (Fig. 31). Results from samples collected using the standard scheme experiment were also plotted on the 1:1 graph seen in Fig. 50.

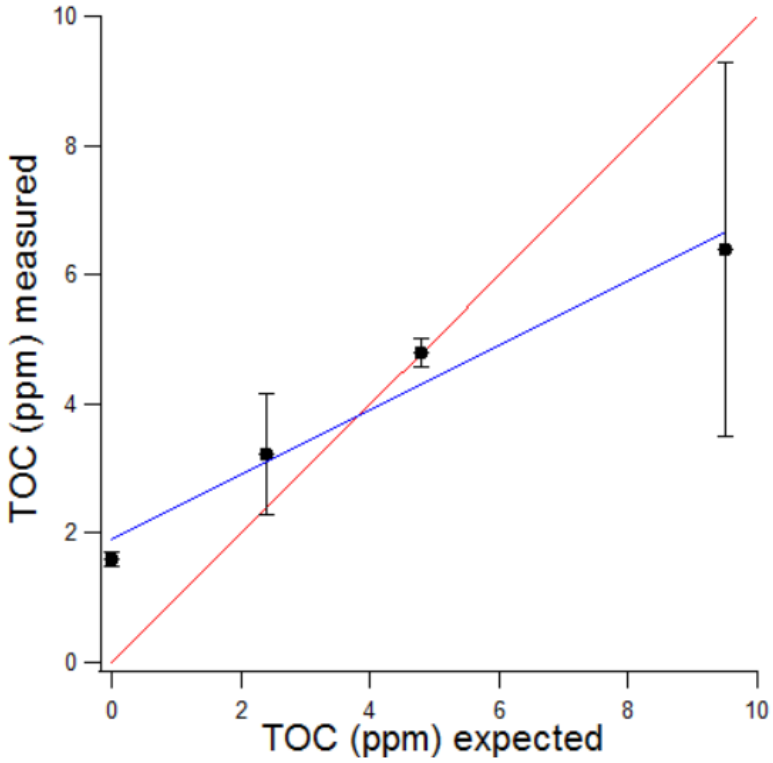

Fig. 50 *- Standard TOC values vs. DUCS collected TOC values (From Fig. 47). A 1:1 overlay is shown by the red line. Linear regression for the standard vs. DUCS samples is shown by the blue line.*

The overall correlation coefficient for this experiment plotted against the 1:1 line was fairly weak with an $R^2 = 0.23$. TOC sample sheering and/or gradient dispersion also appeared to be more pronounced with larger gradient differences than with smaller concentration differences, which is similar behavior to that which was seen during deployments (Figs. 36 and 43). The linear regression

for standard TOC values vs. the DUCS collected values was also very similar to that seen during the third deployment (see linear regressions for Figs. 43 and 50). This correlation coefficient improved dramatically ($R^2 = 0.80$) when removing 3 points closest to the largest concentration gradients (samples 15, 19 and 20 respectively).

This sheering is also much larger than sheering predicted by Gaussian estimations (Fig. 29). This is likely due to an assumption that has been made regarding sample peak spreading. It has been evidenced from conductivity peaks that the relatively inert, inorganic, HCl is unlikely to adhere to tubing walls and cause pronounced concentration gradient spreading - therefore causing a normal distribution of its concentration gradient. It has also been assumed that the concentration gradient spreading for an organic sample plug would follow a normal distribution similar to that of inorganic sample (Fig. 21). However, this appears to have been only the case for shorter lengths of tubing. Over the course of development, the DUCS has been upgraded to storage coils with lengths of 45 m, 135 m, and 450 m to allow for the collection of greater amounts of samples. While concentration gradients caused by sheering for inorganic sample may have continued to follow a normal distribution as storage coil length increased, as indicated by sample conductivity series (see Figs 35 and 42), these experiments indicate this has not the case of organic sample. They indicate that the acidification process did not fully prevent the sheering of the less inert organic sample in the current 450 m tubing length. Since it has been demonstrated that organic sample will follow a normal distribution during storage in shorter tubing lengths, this indicates that the DUCS storage coil length may need to be minimized. Although this decreases the total allowable samples in a single length of coil, this would not be an issue using multiple shorter lengths of coil – and would in fact be preferred if higher sample accuracy and precision were essential. The ideal coil length is yet to be explored.

When looking at the results of the reversed sampling experiment there also appears to be no increased effectiveness in preventing TOC sample sheering (Fig. 49). There was also significantly increased positive scatter in sample TOC values for the reversed scheme samples vs.

those seen collected with the standard scheme. This is likely due to blank contamination coming from the post processing step becoming increasingly detrimental to experimental accuracy when decreasing the sample to acid ratio, which will be further discussed below.

To explain the referenced blank issue, Eq. 3 uses a simple mass balance to compute theoretical Aurora TOC outputs for a sample diluted with acid preservative during sampling and DI during processing. C_S refers to the concentration of the undiluted TOC sample. It should be noted that the expected C_s in a sample can be influenced by sample spreading and dispersion (See Fig. 47), and this effect is not expressed in this Equation. D_1 refers to the dilution factor coming from the acid and is equivalent to the dilution factor equated from Eq. 1. D_2 refers to any dilution factors introduced during post-sampling processing steps. B_1 and B_2 refer to the sampling and processing blank TOC contamination levels, respectively (refer to Chapter IV, Section E). These blanks contribute an additive TOC contamination at both the sampling and processing level. Blank TOC contamination at the sampling level (B_1) is primarily a background TOC contribution over baseline DI during sampling. If acid reagent is contaminated there may be an acid blank effect (B_A) at the sampling level, but Eq. 3 ignores this possibility as acid blank TOC has been shown to not be statistically different than DI, as discussed above. Blank TOC contamination at the processing level (B_2) is the background TOC contribution over baseline DI for all post-sampling processing steps.

$$\mathbf{TOC\ (Aurora)} = (C_S * D_1 + B_1) * D_2 + B_2 \qquad \textit{Eq. 3}$$

From Eq. 3, it can be shown that TOC values output by the Aurora are influenced by blanks at the sampling (B_1) and the processing (B_2) level. Since there is no way of knowing whether contamination in any given sample was introduced at the sampling or processing levels, blank contamination values coming from the processing level (B_2) will have both dilution factors (D_1 and D_2) applied to them. This could create potentially large error when either 1) B_2 is large or 2) the sample to acid ratio in samples collected using the DUCS was very low (as was the case in Fig. 47 b.). It may still be possible to utilize a “reverse” sampling scheme by using a very concentrated

acid to space sample, such that collected samples have a very high sample to acid ratio. It may also be possible to eliminate blank contamination at the processing level.

Table 8 illustrates the potential effects on the accuracy of TOC analysis when 0.1 ppm of blank contamination has been introduced to sample at the sampling (B_1) and/or processing (B_2) levels. In this table theoretical calculations have been included to show the effect blank contamination on 0 (DI) and 5 ppm TOC samples collected using either the standard or reversed sampling schemes discussed above. The associated systematic errors have also been included for each sampling scheme presented. Case 1 shows values assuming there is no blank contamination during sampling or processing. Case 2 shows the values assuming 0.1 ppm contamination is being introduced to sample at the sampling level and 0 ppm is being introduced at the processing level. Case 3 shows the values assuming 0 ppm contamination is being introduced to sample at the sampling level and 0.1 ppm is being introduced at the sampling level. Case 4 shows the back calculated values assuming 0.1 ppm contamination is being introduced to sample at both the sampling and processing levels.

Table 8 – *Theoretical back calculated TOC values (ppm C) for DI and 5 ppm samples collected using the standard or reversed sampling schemes. The different cases represent contamination being introduced at the processing and/or sampling levels.*

Sampling Scheme	Case 1 (B_1=0, B_2=0)	Case 2 (B_1=0.1, B_2=0)	Case 3 (B_1=0, B_2=0.1)	Case 4 (B_1=0.1, B_2=0.1)
DI, *standard*	0.01	0.13	0.42	0.54
5 ppm, *standard*	5.00	5.13	5.42	5.54
DI, *reversed*	0.01	0.52	1.73	2.25
5 ppm, *reversed*	5.00	5.52	6.73	7.25

The results presented in Table 8 provide additional evidence that decreasing the sample to acid ratio causes blank contamination from the post-sampling process to have significantly decreased accuracy. This effect has been noted before. This effect is why post-sampling dilutions had been changed to have a higher sample to acid ratio during the development of the standard method. Errors were also proportionally larger in DI samples compared to 5 ppm samples, in

agreement with past experimental results (Fig. 31). The variability in process blank with the DUCS can more than account for all variability that is seen when using the reversed sampling scheme (Fig. 47 b.). These results indicate that the current sampling scheme utilized by the DUCS may be able to be further optimized. This might involve increasing sample volume through the use of multiple smaller storage coils rather than one larger one, using smaller amounts of more concentrated acids for sample acidification, and/or sampling more quickly to prevent large concentration gradients between successive samples.

To test further the effectiveness in decreasing storage tubing lengths on sampler collected TOC values, an experiment was designed similarly to the experiment presented in Fig. 47. In this experiment, the coil length was changed from the current 450-m coil to a previously utilized 150-m coil. A series of 0 ppm C (DI), 2.5 ppm C, 5 ppm C, and 10 ppm C standards were prepared for lab sampling using the standard sampling method with 5% HCl. The DUCS then collected these standards as sets (n=3) of samples from the 2.5, 5, 2.5, 10, and DI standards sequentially for storage. Samples were then dispensed from storage and prepared for analysis. The results of this analysis are shown below in Fig. 51.

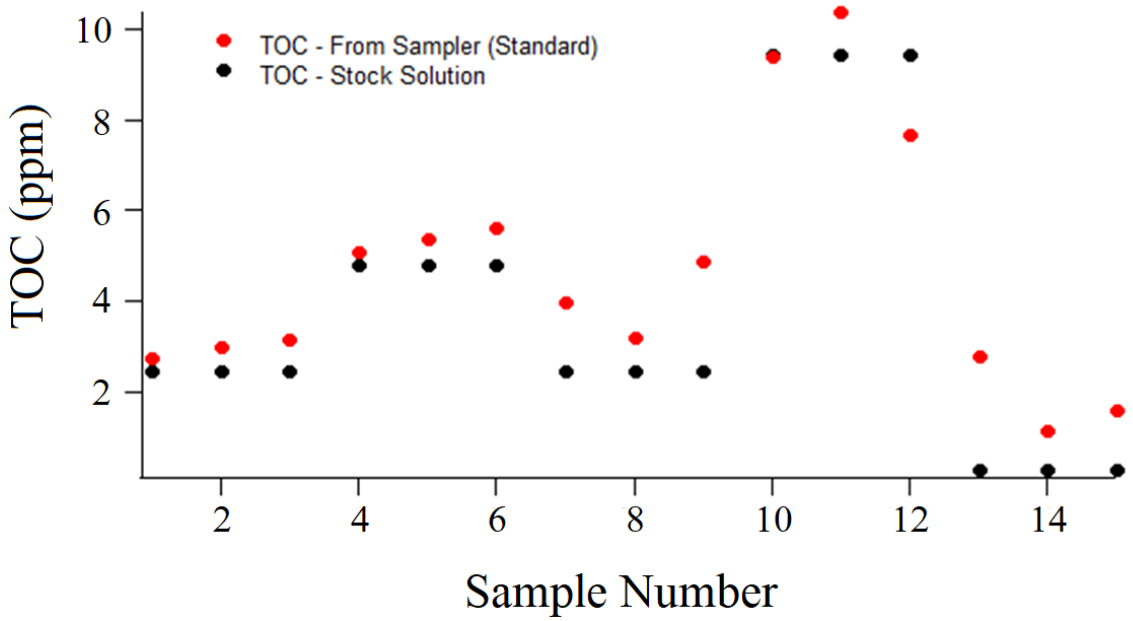

Figure 51 – *Analysis of TOC samples collected in the experiment using the standard sampling method with a 150-m storage coil.*

The overall correlation coefficient for this experiment with the 150-m coil plotted against the 1:1 line was stronger than with the 450-m coil, with an $R^2 = 0.82$. TOC sample sheering and/or gradient dispersion also appeared to be less pronounced with the same large gradient differences in this experiment than during the 450-m coil experiment, as can be seen in the comparison between the 1:1 these coil-length experiments shown below in Fig. 52

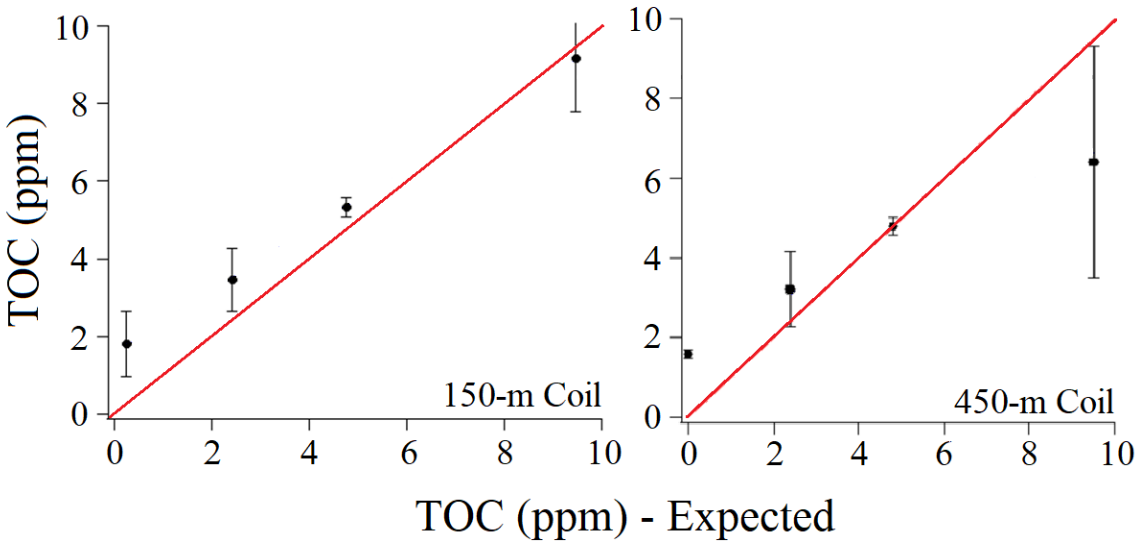

Figure 52 – *Standard TOC values vs. DUCS collected TOC values (From Fig. 47 and 51). 1:1 overlays are shown by the red lines.*

These results indicate improved data quality for TOC when using a shorter length of coil. This provides evidenced that the apparent increased organic sheering seen when using a longer storage coil can be reduced when using a shorter storage coil. Inorganic sheering, determined by the length of the tailing edge of conductivity during conductivity analysis, did not appear to be significantly affected when using a shorter length of storage coil. These results indicate that shorter storage coils may be more well-suited when sampling for organic species, but longer storage coils could potentially be utilized when sampling for inorganic species. More exploration into the ideal coil-length for TOC sampling needs to be explored.

VI. Future Work and Conclusions

A. Future Work

Results from these deployments showed that the DUCS can collect high frequency TOC timeseries. The dynamic nature of TOC in this system provides additional evidence for the need of high frequency sampling technology to better capture the full range of TOC (or DOC) variability within freshwater systems. A single monthly, weekly, or even daily TOC sample does not adequately capture the variability of TOC during these time frames. For example, low frequency data could lead to carbon flux calculations or biologic oxygen demand being significantly misestimated. Through the continued optimization discussed here, the DUCS could be commercialized and used to assess high frequency trends for a wide range of analytes in aquatic systems in the future.

Filtering to the proper size fractions required for dedicated DOC sampling remains an issue. This remains the foremost problem in the implementation of this sampling technology for DOC sample collection. To address this issue, the in-line frit filters described could be utilized with the implementation of a stronger diaphragm pump capable of operating at higher backpressures than the current KNF 1.5 diaphragm pump. This would allow direct in-line filtration at the inlet of DUCS. This issue could also be solved with the implementation of a dedicated pre-inlet sample filtration unit using a different pump as a separate component of the sampler, rather than upgrading the current diaphragm pump. Additionally, organic spreading and blank carryover remain an issue that could potentially be resolved through changing the sample storage scheme.

With further regard to sample storage, the number of allowable samples is dependent on the total length, or volume, of the storage coil used. The system could be adapted to allow for more total samples using a few different methods. A longer length of continuous coil on a single spool of tubing could be used to increase storage volume. This option may be suitable for inorganic sample collection. Experiments have indicated that organic sample spreading appears to increase

as coil length increases. Another option that might be preferable for organic sample would be by using multiple, shorter, storage coil spools that could be switched between through a series of selectable valves. This could potentially solve the issues seen with organic spreading and blank carryover, while still allowing for a large number of total samples.

Current sample collection and preparation from the storage coil has a few very time-consuming or otherwise inefficient steps that could be optimized. The first of these optimizations could be during the sample dispense step from the storage coil. This step requires the user to manually dispense sample from the coil and move them into successive vials to be capped by hand. Flow rates in this step of the process are very slow to prevent sheer and therefore must be manually monitored for long periods of time to ensure proper sample dispensing. Manually collecting samples within the small vials takes ~30 seconds per vial (~0.8 mL). Manually taking conductivity measurements for each small vial takes ~ 45 seconds per vial. Cumulatively, this process takes ~ 8 hours, not including equipment cleaning times, with the current sample storage coil using the standard method of sample preparation. Implementation of a fraction collector to dispense and collect sample during this step would significantly decrease the labor-intensive hours required for this part of the process. Additionally, implementation of an in-line conductivity probe to determine conductivity peaks alongside with a fraction collector could bypass the manual small-vial process altogether. Another possible method of bypassing the small vial process would be through the addition of a pressurized gas canister into the internal plumbing of the DUCS. Using this pressurized gas, individual samples could be separated similarly to samples in segmented flow analysis. This would allow easier determination of sample location within a storage coil, and dilution factors coming from acid could still be used to back calculate undiluted analyte concentrations in each collected sample.

It has been shown experimentally that blank contamination especially during the post-sampling processing is especially detrimental. Eliminating the small vial process would potentially eliminate the step with the highest potential for blank TOC contamination. Additional attention

must be given to minimizing blank contamination levels coming from both the processing and sampling levels, especially for an analyte with a large potential for contamination such as TOC. Blank contamination levels for other possible analytes with the DUCS may not be as detrimental or as likely to occur as blank TOC contamination.

Along the lines of expanding the range of analytes that could be sampled, there should be further exploration into nutrient and metal analysis using the DUCS. Theoretically, any dissolved or suspended analyte sampled from an aquatic system should be viable for use with the DUCS and investigations of this could be undertaken. This may involve the use of a different tracer than conductivity, such as a chromophore, especially if it is to be deployed in a marine ecosystem with larger sample background conductivities.

Requiring sample to be combined into a single larger sample in addition to another secondary dilution to get to the minimum analysis volume required for the Aurora is another part of sample processing that is less than ideal. This process further decreases the sample to blank ratio for analyzed samples (which has been shown to increase uncertainty in low ppm C samples) and introduces an artificially imposed decrease in the total storable samples allowed within the coil. Using a method that allows for smaller sample volumes, either through 1) modification of the Aurora instrument or 2) use of another DOC instrument altogether that would eliminate the need for secondary dilutions post conductivity-measurements. This would allow for more total samples to be collected with the same volume storage coil and would eliminate secondary dilutions. This part of the process is also quite time inefficient, taking ~ 5 mins to perform the secondary dilution on each sample.

As mentioned above, there is another possible sampling scheme for use with the DUCS. The continuous sampling method would involve unspaced “continuous” storage of discrete volumes of sample preserved with acid reagent at frequent intervals. Following each 24 hour interval, an aliquot of unpreserved sample would be injected into the storage coil, breaking continuity in sample collection. This would allow low-conductivity areas to be used to indicate

successive days, rather than successive samples (as with the standard sampling method). This strategy assumes that pumping would be sufficiently reproducible over a 24 hour period that individual sample locations in the tubing would be accurately known. Samples stored in this fashion would be consistently overlapping throughout the length of tubing, similar to sample stored in the continuous samplers described in Chapter. This method of sampling could increase the total amount of samples collected within a specific volume of storage coil by 5 fold. This would be useful, for example, to collect significantly more samples on long-term buoy deployment. Using the continuous method of sampling could also allow for the collection of a single composite sample collected each day. This could allow for a more accurate determination of the median concentration of an analyte in each daily composite sample over the course of a 24 hour period, allowing for more accurate flux calculations. This would come at the loss of the daily temporal data that could be determined from collecting individual samples, however.

B. Conclusions

The sampler (DUCS) described in this thesis used a novel method for chemical sampling in freshwater aquatic systems. Using conductivity as both a sample tracer and a conservative tracer created a sampling technique that, while not commercially viable in its current form, provides a solid backbone on which further work can improve. Data collected during field deployment in the UCFR showed the viability of this sampler's method in generating a high frequency time series in a real world system. Even with the errors seen when TOC sampling with the DUCS in its current form, organic carbon flux calculations from DUCS collected samples could be an improvement over flux calculations generated using single monthly grab samples (Worrall et al., 2013)

With the novel method of sample preservation and tracing with conductivity employed by this research, the prototype developed around this innovation could be used in any freshwater aquatic ecosystem. Eventually, using a tracer besides conductivity (due to the high conductivity of sample in marine environments), the DUCS could be adapted for marine applications. Additionally, the DUCS can collect a potentially unlimited number of samples, in contrast with current commercially available samplers. This limit is controlled by the total storage volume. Increasing total deployment lengths or resolution can be accomplished through a larger storage volumes (i.e., the addition of multiple storage coils that could be switched to using solenoid valves or increasing storage coil lengths), or by increasing the sensitivity of in-lab instrumentation to allow for collection of smaller sample volumes. Modification of these two limiting factors could allow the DUCS to collect long-term, high-resolution datasets when deployed on moorings for periods up to and exceeding a year.

VII. Appendices

A. Appendix A – DOC Sensor Software Controls

This appendix is dedicated to the software that was developed to be used with the benchtop model of the DOC sensor. Both PyKloehn and NoModem .exe software are used together for full operation during degradation tests (Chapter III).

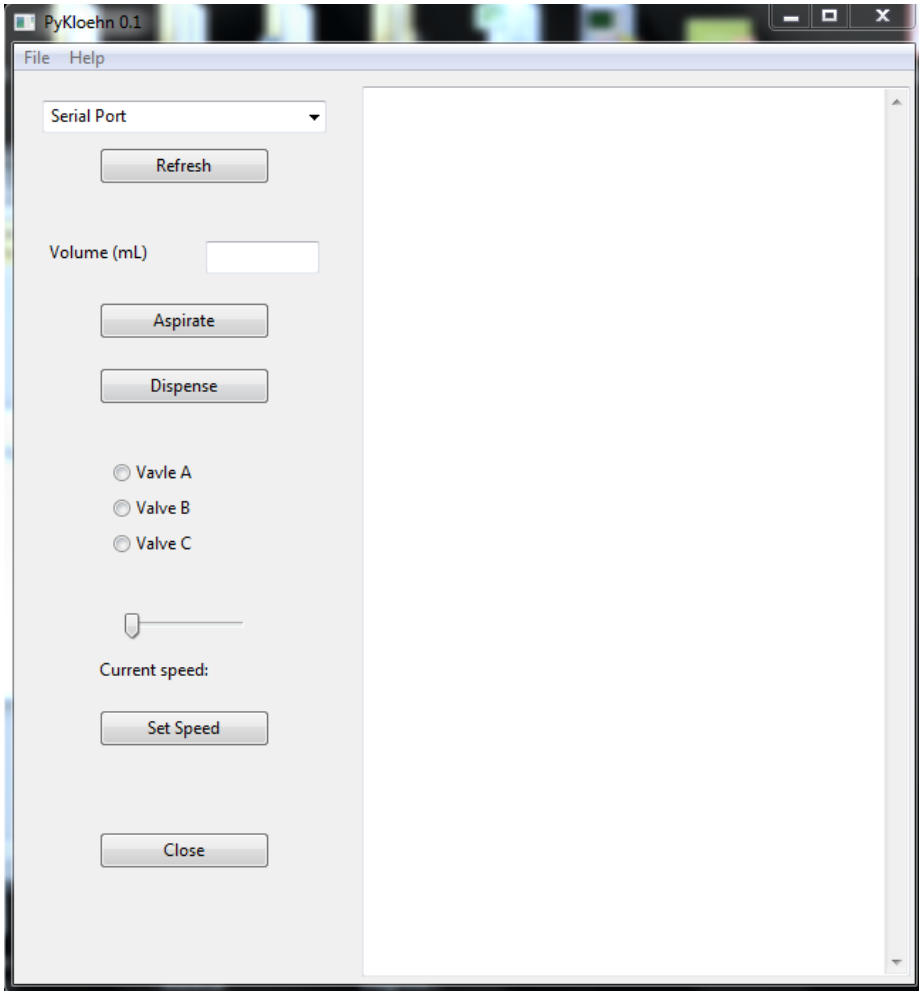

Figure A1– *Computer interface for the PyKloehn software, which was developed by David Podrasky for operation of the Kloehn syringe system. Functions available on the computer interface are discussed below.*

- **Serial Port Selection** – To operate the PyKloehn software, the Syringe Pump must be connected through a USB serial port into the computer of operation. Proper serial port connection must then be chosen using this function. Refreshing the serial port selection upon insertion of the USB serial will show active USB port connections.
- **Volume** – This input allows you to select a value between 0-10, which will set the aspiration or dispense volume on the syringe pump. It should be noted that while the units entered are in mL, this value is only accurate for a 10 mL syringe. Replacing the syringe with a smaller or larger syringe will scale this value proportionally.
- **Valve Set** – Allows user to input one selective valve through which aspiration or dispense mechanics can occur. Although not reflected in Fig. 11 above, additional valve selections between A-F have been programmed into PyKloehn Software. You can aspirate or dispense the chosen volume through set valve by pressing the "*aspirate*" or "*dispense*" inputs.
- **Set Speed** – Allows the user to input a rate of dispense or aspiration. The software is programmed to have a total of 64,000 motor "steps" for a complete volume dispense or aspiration. The software allows for the user to define the number of steps per second the motor will take – which a user can define to be between 40-6400.

Additionally, software was also developed that allows the use of the high-powered UV-LED. The computer interface for this software is shown in Fig. 12 below. This UV-LED must also be connected through serial connection and has the functions described below:

- **t (x)** – This function allows the user to define the length that the UV light will remain on, in seconds. The user can define this to be between 0-36000 seconds.
- **w (x)** – This function allows the user to define the intensity of the UV-LED source on a scale of 1-100 %. The t (x) function must be defined before setting this function as shown in Fig. A2.

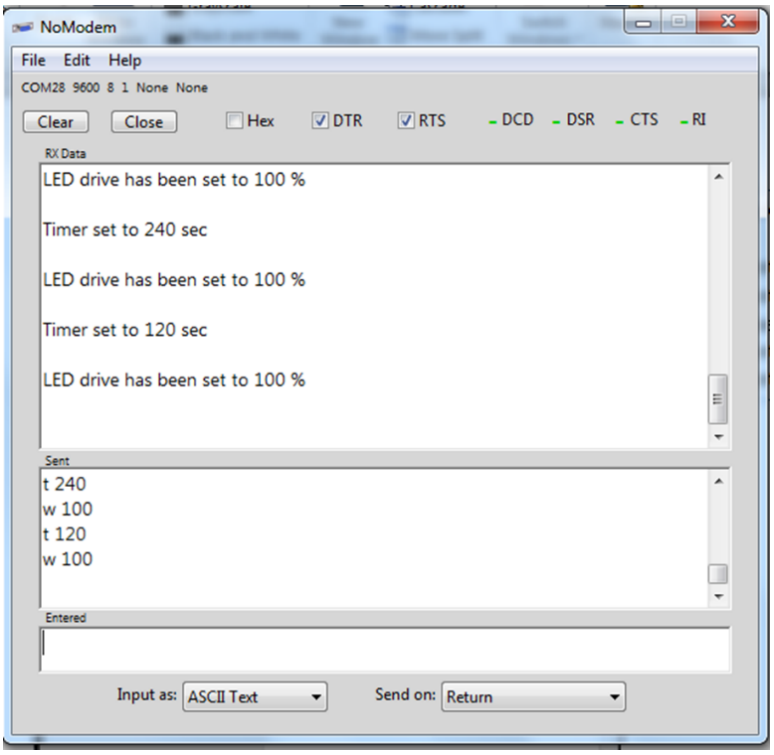

Figure A2– *Computer interface for the NoModem software, which was developed by David Podrasky for operation of the UV-LED. Functions available on the computer interface are discussed above.*

B. Appendix B – DUCS Software Controls and Data Acquisition.

Rather than using dedicated .exe files to control the DUCS (Chapter IV) as in the sensor software described in Appendix A, this sampler employs .tfb files that must be opened and loaded onto the TFX-11 board using TF-TOOLS software. Before loading these programs onto the sampler's computer board, after the desired sub-program has been loaded onto the TFX-11 in TF-TOOLS software, Ctrl + C primes the board for program execution, and program execution can be initiated by pressing Alt + R on the computer interface where the desired subprogram is loaded. Below is a list of subprograms that have been compiled for use with the DUCS as well as their intended functions. These following programs are in the "*DUCS File*s" file on the desktop of the laptop hooked up to the Agilent 8453 in the DeGrandpre lab. A brief description of each subprogram is listed here, followed by a deeper look at the code for these programs. Data is directly offloaded from the TFX-11 board in the TFX software using the data offload function.

DUCS Sampling Sequence – Standard Cleaning Sequence: This subprogram will initiate a 24 hour system flush and cleaning sequence. Prior to any sampling session this subprogram needs to be ran two times, one 24 hour flush with 3 L of 1.0% HCl, followed by one 24 hour flush with DI.

DUCS Sampling Sequence – Visual Indicator Sequence: Prior to initiation of a sampling sequence, this subprogram is ran to load a colored indicator before samples as a visual cue to where sampling began within the coil. A $CuSO_4$ solution is used as the colorimetric indicator in this step, and the sampler inlet should go into this solution.

DUCS Sampling Sequence – Standard Sampling Method: This subprogram will initiate the standard DOC sampling sequence. The pre-designed sequence loaded on this file is programmed to collect a total of 48 samples at a 4-hour sampling interval. To change the total amount of samples or the sampling interval open the subprogram and see edit notes indicated in these sections.

DOC Sampling Sequence – Storage Dispense: Following deployment, this subprogram initiates timed pulses that dispense sample aliquots from DOC storage in continuous succession. Small vials must be dispensed to by hand after initiation of this program.

i. *DUCS Sampling Sequence – Standard Cleaning Sequence*

```
GOSUB QUESTI
PRINT “Re-initialize this program with DI at the inlet”
QUESTI:
  PRINT "This program is for cleaning the sampler tubing and valves, and consists of 2 steps"
  PRINT "an acid rinse with 1% HCl followed by a DI rinse. Begin program w/ acid rinse"
  PRINT "and follow on-screen prompts"
  INPUT "Place inlet of sampler into ~ 3 L of 1% HCl (or DI if on DI rinse) Solution. Make sure
sampler + coil outlets go to waste container. PRESS 1 when ready: "ST
  IF ST=1
  PRINT "Initializing acid flush"

        PCLR 0, 1, 2, 3, 4, 5, 6, 7
        Sleep 50
        Pset 0
Print "This interface will indicate when to begin DI flush on-screen."

for a= 1 to 500  // Mix-coil Flush
sleep 0
sleep 500
next a

PSet 4
sleep 0
sleep 100
```

```
for n = 1 to 29500 // Storage Coil Flush
pset 0
sleep 50
pclr 0
sleep 50
next n
pclr 4

  RETURN
STOP
```

ii. ***DUCS Sampling Sequence – Visual Indicator Loader***

```
GOSUB QUESTI

GOSUB QUESTII

QUESTI:

  PRINT

  INPUT "Attatch Copper Sulfate (CuSO4) visual indicator to sampler inlet. PRESS 1 when loaded: "ST

  IF ST=1

  PRINT "Initializing visual indicator coil-loading"


      PCLR 0, 1, 2, 3, 4, 5, 6, 7

      Sleep 50

      Pset 0

Print "Loading Mixer with Visual Indicator"


for a= 1 to 62

sleep 0

sleep 500

next a


Print "Dispensing Visual Indicator to Storage Coil"


PSet 4

sleep 0

sleep 100
```

```
for n= 1 to 1000
pset 0
sleep 0
sleep 50
pclr 0
sleep 0
sleep 50
next n
PClr 4
Print "Visual Indicator Loaded, Begin Sampling Sequence"
  RETURN

QUESTII:
  PRINT
  INPUT "Attatch DI to sampler inlet. PRESS 1 when loaded: "ST
  IF ST=1
  PRINT "Initializing post-indicator DI plug dispense"

        PCLR 0, 1, 2, 3, 4, 5, 6, 7
        Sleep 50
        Pset 0
Print "Loading Mixer with DI"

for a= 1 to 62
sleep 0
sleep 500
```

```
next a


Print "Dispensing DI to Storage Coil"


PSet 4

sleep 0

sleep 100


for n= 1 to 250

pset 0

sleep 0

sleep 50

pclr 0

sleep 0

sleep 50

next n

PClr 4

Print "Visual Indicator Loaded, Begin Sampling Sequence"

  RETURN

STOP
```

iii. ***DUCS Sampling Sequence – Standard Sampling Sequence***

```
//**************************DOC sampling program – separated samples***************
CBREAK SHUTDOWN // sets CTRL-C destination (Initiates Shutdown)
Sleep 50
GOSUB QUESTI  //  user date entry location
Sleep 50
// **********************************clear I/O pins*********************************
PCLR 0, 1, 2, 3, 4, 6, 7  // Clear everything
        SLEEP 0
        SLEEP 50
PSET 0
        SLEEP 100 // Initiates Pump for Program Run Confirmation
PCLR 0
        SLEEP 100
PSET 5
        SLEEP 0
        SLEEP 50

//*****************************************************************************
//                        separated sample sequence
//*****************************************************************************
Print "Deployment Sleep Initialized"
Sleep 50
GOSUB SETDEPLOYMENT    // define offtime until first sample
```

```
Sleep 50
Print "Sequence Initialized" // Sequence follows as below
Sleep 50
FOR SEQUENCE= 1 to 38  // 38 total samples (~5.5 mL / Sample). Change this value to change
amount of samples.
GOSUB SPACER          // loads unacidified spacer before acidified sample
        SLEEP 0
        SLEEP 50
GOSUB SAMPLE          // loads acidified sample between spacer
        SLEEP 0
        SLEEP 50
GOSUB SPACER          // loads unacidified spacer after acidified sample
        SLEEP 0
        SLEEP 50
PRINT "SAMPLE COMPLETE"
GOSUB GOTOSLEEP       // offtime between samples
        SLEEP 0
        SLEEP 50
NEXT SEQUENCE
//**************************
PCLR 0, 1, 2, 3, 4, 6, 7
        SLEEP 0
        SLEEP 50
GOSUB SHUTDOWN
//**************************
```

```
//*************************************************************************
//                          Spacer Sequence
//*************************************************************************
SPACER
PRINT "Spacer Aspiration Begin"
PCLR 0, 1, 2, 3, 4, 6, 7
        SLEEP 0
        SLEEP 50
PSET 0
//**********************
For a = 1 to 62
SLEEP 0
sleep 500           // flushes coil and loads unacidified sample
next a
//**********************
PRINT "Spacer Aspiration Complete: Spacer Dispense Initialized"
PSET 4
        SLEEP 0
        SLEEP 100
//**********************
FOR n=1 to 125
pset 0              // dispenses unacidified spacer to DOC coil
        SLEEP 0
        sleep 50
pclr 0
        SLEEP 0
```

```
        sleep 60
next n
//**********************
PRINT "Spacer Dispense Successful"
RETURN
//*************************************************************************************
//                    Sample Aspiration/Mixing and Storage
//*************************************************************************************
SAMPLE:
PRINT "Sampling Aspiration Started"
GOSUB QUESTII
PCLR 0, 1, 2, 3, 4, 6, 7
        SLEEP 0
        SLEEP 50
//**********************************
FOR x=1 to 210
PSET 0
        Sleep 0
        SLEEP 5
PCLR 0
        sleep 0
        SLEEP 15
PSET 1
        sleep 0
        SLEEP 25            // alternates between acid RGT / sample to load Mix coil
```

```
PSET 0
        sleep 0
        SLEEP 20
PCLR 0
        sleep 0
        SLEEP 15
PCLR 1
        sleep 0
        SLEEP 25
NEXT x
//**********************************
PRINT "Sample Mix Initialized"
PSET 3, 7
sleep 0
sleep 50
//**********************************
FOR y= 1 to 150
PSET 0
Sleep 10
sleep 0
Pclr 0
sleep 0                 // Sample mixing sequence "closed loop"
Sleep 50
next y
PCLR 3, 7
sleep 0
```

```
sleep 50
PRINT "Dispensing Preserved DOC Sample"
PCLR 0, 1, 2, 3, 4, 6, 7
sleep 0
        SLEEP 50
PSET 4
sleep 0
sleep 50
for b=1 to 70
pset 0
sleep 0
sleep 50                        // sample dispense sequence
pclr 0
sleep 0
sleep 50
next b
//***********************************
PRINT "Sample Dispense Successful"
PCLR 0, 1, 2, 3, 4, 6, 7
        sleep 0
        SLEEP 50
RETURN
//*****************************************************************************
//                      Set TFX-11 RTC (time)
//*****************************************************************************
```

```
QUESTI:
  PRINT
  INPUT "Do you want to set the time and date? PRESS 1 for Yes OR 2 for No: "ST
  IF ST=1
  PRINT
   INPUT "ENTER THE YEAR         (e.g. 2020) "?(5)
   INPUT "ENTER THE MONTH          (1 - 12) "?(4)
   INPUT "ENTER THE DAY OF THE MONTH (1 - 31) "?(3)
   INPUT "ENTER THE HOUR OF THE DAY  (0 - 23) "?(2)
   INPUT "ENTER THE MINUTE         (0 - 59) "?(1)
   INPUT "ENTER THE SECOND         (0 - 59) "?(0)
   STIME //SETS THE HC11 CLOCK
   SETRTC // REAL TIME CLOCK
  RETURN
  ENDIF
  IF ST=2
  RETURN
  ELSE
  PRINT "   THAT IS NOT AN OPTION. TRY AGAIN! "
  GOTO QUESTI
  ENDIF
  PRINT
  RETURN
//*****************************************************************************
//                          Data Storage
//*****************************************************************************
```

```
QUESTII:
READRTC
        RTIME
PRINT #2,?(2),?(1),?(0)
PRINT #2,?(4),?(3),?(5)
Sleep 0
PRINT
sleep 0
SLEEP 50
PCLR 5 // SWITCH THERMISTOR ON
        TEMPSUM! = 0 // INITIALIZE TEMPSUM VARIABLE
        FOR J = 1 TO 50
          G = CHAN(10) // GET TEMPERATURE
          CELLT!=TEMP(G)
       CELLT!=CELLT!/100
   TEMPSUM! = CELLT! + TEMPSUM!
        NEXT J
   PSET 5 // SWITCH THERMISTOR OFF
        CELLT! = TEMPSUM!/50
Sleep 0
myTime$ = str(#2D,?(2),":",#2D,?(1),":",#2D,?(0)) // Hours : Minutes : Seconds String Data
sleep 0
myDate$ = str(#2D,?(4),":",#2D,?(3),":",#2D,?(5)) // Month / Day / Year String Data
sleep 0
myTemp$ = str(#5.2F,CellT!) // 2 decimal place temperature String Data
sleep 0
```

```
myStoreStr$ = str(myTime$," ",myDate$," ",myTemp$,chr(13)) // Data Storage String for
Sample
sleep 0
Store myStoreStr$  // Stores the string of data (listed in code above) in a single data string for
timestamping.
sleep 0
RETURN
//*****************************************************************************
//                          Low Power Modes
//*****************************************************************************
GOTOSLEEP:
// This subroutine defines the offtime inbetween sample intervals
HYB 26
For SAMPLESLEEP=1 to 99 // Define offtime between samples here (1 to n(minutes)). The
DOC sampling sequence has a run
HYB 0                // time associated with it. In this pre-set, this has been accounted for and the
off-time between
HYB 60               // samples (or sampling interval) is every 2 hours (i.e. changing 99 to 39
makes hourly interval).
next SAMPLESLEEP
RETURN
SETDEPLOYMENT:
// This subroutine defines the interval until the first sample will be collected
For STARTSLEEP= 1 to 30 // Define offtime until first sample here (1 to n(minutes)). In this pre-
set, sampling will
HYB 0                // begin 30 minutes after setting the date.
```

```
HYB 60
next STARTSLEEP
RETURN
//*****************************************************************************
//                          SHUTDOWN SEQUENCE
//*****************************************************************************
SHUTDOWN:
PRINT
PRINT "SAMPLING COMPLETE"
PRINT
   PCLR 0,1,2,3,4,6,7 // SHUT DOWN ALL DEVICES
   STOP // STOPS PROGRAM AND GIVES PROMPT
```

iv. *DUCS Sampling Sequence – Storage Dispense*

```
GOSUB QUESTI

QUESTI:

  INPUT " Load DI at the sample inlet Make sure outlet of storage coil is dispensing to small coils.

Outlet must be manually switched between when desired volume has been dispensed to each coil.

PRESS 1 when ready: "ST

  IF ST=1

        PCLR 0, 1, 2, 3, 4, 5, 6, 7

        Sleep 50

PSet 4

sleep 0

sleep 100


for n = 1 to 29500

pset 0

sleep 50

pclr 0

sleep 50

next n

pclr 4


  RETURN

STOP
```

C. Appendix C – Aurora 1030 Instrument Operation Procedure.

**** Note that this is a modified procedure from the standard SOP procedure for the Aurora 1030C located in the Valett lab. For the full in-depth instrument SOP protocol, or if wishing to modify this procedure, reference the original SOP document. ****

Working standards in the appropriate concentration range are prepared on the day they are run by diluting stock DOC solution. Standards run for surface water samples are prepared in 100-mL volumetric flasks and are prepared as 0.2 ppm, 0.5 ppm, 1.0 ppm, 2.5 ppm, 5.0 ppm, 10 ppm, and 15 ppm standards. When running an analysis sequence on this instrument, a known standard sample must also be included in the run sequence to check for instrument drift. The analysis procedure on the Aurora 1030C consists of six fundamental steps, which will be explained below:

1. Employing the Start-up Procedure and checking the setup of the instrument.

- ***i.*** Fill the rinse vessel with frees MilliQ water. Confirm that the waste is below the waste line and that the instrument is properly draining into the plastic tank found underneath the instrument.
- ***ii.*** Turn on the Nitrogen (N_2) gas tank, and make sure there is at least 300 psi remaining in the tank. Adjust delivery pressure to 50 psi.
- ***iii.*** Check the reagent bottles to make sure they are all full and that the contents are being purged by the gas supplied above.
- ***iv.*** Ensure that the computer is turned off. A proper connection to the Aurora requires this at this step.
- ***v.*** Turn the instrument on by initiating power at the two locations. First turn on the autosampler, and then the instrument itself. These are located on the backside of the instrument.
- ***vi.*** Sign into the Aurora, and then turn on the computer.

vii. Once the computer is fully booted, make sure the computer is connected to the instrument by checking to make sure there is a green circle in the bottom corner of the computer interface.

viii. Check to make sure the autosampler is selected for analysis.

ix. Monitor the signal from the NDIR and make sure it stabilizes between 2,000-5,000.

2. Choosing the analysis method

i. The instrument when powered on automatically loads the last analysis method stored on the instrument.

ii. For analysis of sample stored with the DUCS, press *the Editor -> Method* tab and load the "DUCS – Aurora Analysis" method. After confirming the proper analysis method is chosen, confirm needle sampling depth is set to 99% and then proceed to creating the run sequence.

3. Creating the run sequence

i. Press the *Editor -> Sequence tab -> new* button.

ii. Enter an appropriate sequence name for this run (e.g., DOC analysis June-1).

iii. Press *the Add/Insert Sample(s)* button to access the dialog box.

iv. Under sample type, select sample from the dropdown list, and select the method you chose in above.

v. Press OK to enter the *Add/Insert Samples* screen and verify the number of samples that are going to be analyzed this run. Save the sequence

4. Loading and starting the run sequence

i. Press the *Monitor-> Sequence tab -> Load Active Sequence* button to access the dialog box.

ii. Highlight the sequence created in the previous section.

iii. Press the *Load* button to load the sequence for use.

iv. Before initializing the run, confirm all reagent bottles have the required volume for analysis (indicated by lines), and the proper working pressure is being delivered.

v. Press Start to begin the Sequence. Each sample takes about 8 minutes.

5. Transferring sample data and turning off the Aurora instrumentation.

i. To transfer relevant sample and calibration data, before turning off the instrument make sure to copy and paste all pertinent sample information to an excel spreadsheet. To obtain this information follow the path *Monitor -> Result Log*. Once in the Result Log tab you will be able to highlight the entire table of results, copy and paste in to a new excel spreadsheet.

ii. Save the results of this instrument run from this excel file with an appropriate file name (e.g., DOC Analysis 6-1-2020). It should be noted once the instrument is turned off it deletes the sample information. It does however save the method calibration results.

iii. To protect the data and instrument software, use the shutdown function prior to powering off your instrument.

iv. Press the exit button in the upper right-hand corner of the screen. An exit menu will appear with three choices. Choose Shutdown.

v. Press the shutdown button to prepare the instrument to power off. The screen will fade to white.

vi. At this point, power down the instrument. Turn off the power switch on the back of the instrument.

6. Data analysis

i. Once you have an Excel file with calibration and QC data, you can correct the calibration curve for the carbon found in the water used to make the standards.

ii. Determine the amount of organic carbon in the in the reagent grade water plus reagents by the Method of Standard Additions – Plot the concentration of organic carbon for the established standards on the x-axis and the output signal on the y-axis. Generate a

linear regression from the plot. Calculate the concentration of the solution (theoretical total blank = reagent blank + Type I water blank) as the absolute value of the intercept. Note that the intercept is close to the average signal for reagent grade water and should be greater than the one generated for RB. The peak areas of reagent grade water should be < 1000.

iii. Determine the DOC concentration in Type I Water – To determine the C concentration of Type I water, the total signal for water blanks is corrected for the contribution from reagents (RB). To obtain the RB, calculate an average signal for reagent blanks after they become low and stable during warm up (~350). Subtract this value from the mean signal for the total blank (Total Blank = Type I water + reagent). Run the mean value for the water blank through the regression relating to peak magnitude to standard concentration. Typical concentrations for this should be lower than 0.05 ppm.

iv. Correct the observed concentrations of the standards by the amount determined in the above step.

As stated above, there is also concern when analyzing TOC samples that 1) full oxidation of organic matter may not be occurring, and 2) inorganic carbon is not being successfully purged from samples prior to analysis. Validation data provided by Fischer Young has been done on the Aurora examining these two concerns and are seen in figures C1 + C2.

Fig. C1 shows the results of comparing analysis of a readily degradable organic standard (KHP), versus a standard prepared as a mix of many different organic DOC standards. This DOC standard is Sigma DOC standard described in Chapter III. Results of this experimentation showed no statistical differences when evaluating standard curves generated using these standards. This indicates that the Aurora has good oxidation efficiency for less readily degraded organics (such as the humic and fulvic acids in this standard) using its standard method of operation.

DOC vs. KHP Calibration											
	Concentration (ppm)	reps	Area Counts	RSD (%)	Response Factor	R2	R	Area Offset	Mass Offset	Blank Avg	QC Blank Avg
KHP STD	0	3	2337	6.72	0.1909	0.9996	0.9998	4127	-0.7879	1864	0
	0.5	3	23357	1.10							
	2	3	84773	0.73							
	5	3	220529	0.20							
	10	3	428035	0.27							
	15	3	627669	0.57							
DOC STD	0	3	3024	14.94	0.1997	0.9997	0.9998	8054	-1.6082	5247	0
	0.5	3	29155	0.51							
	2	3	88972	0.11							
	5	3	211026	0.30							
	10	3	413401	0.21							
	15	3	604917	0.59							

*Comparing Correlations: Null Hypothesis is retained; No statistical difference

Fig. C1 – *Results of experiments comparing calibration curves generated with a KHP standard, versus those generated by using a less readily degradable DOC standard (described below).*

Fig. C2 shows the results of experimentation examining the effects of inorganic carbon matrix on samples analyzes by the Aurora. This is important as incomplete purging of inorganic carbon can lead to significant overestimation of organic carbon when preforming an analysis. In this experiment, DI with low inorganic carbon concentration (<100 uM) was added to both low (2 ppm C) and high (10 ppm C) DOC standards and analyzed. Additionally, samples prepared using tap water with high inorganic carbon concentration (~3000 uM) was added to the same organic standards and analyzed. Results of this test showed that although there was a statistical difference between samples prepared using these different inorganic carbon matrixes, there is no significant overestimation in samples that have been prepared using tap water. This indicates that the Aurora is effective at doing a full and complete internal inorganic carbon purge during it's standard method of operation.

DIC Carry Over Experiment

Sample Number	Sample ID	Mode	Area Counts	Mass (ug)	Concentration (ppm)	Concentration Corrected for Background (ppm)
1	Tap1	TOC	46021	8.00	1.00	
2	Tap2	TOC	39216	6.70	0.84	
3	Tap3	TOC	39495	6.75	0.84	
4	Tap/LowDOC1	TOC	114019	20.98	2.62	1.73
5	Tap/LowDOC2	TOC	113005	20.79	2.60	1.71
6	Tap/LowDOC3	TOC	113980	20.97	2.62	1.73
7	Tap/HighDOC1	TOC	442631	83.71	10.46	9.57
8	Tap/HighDOC2	TOC	446502	84.45	10.56	9.66
9	Tap/HighDOC3	TOC	444233	84.02	10.50	9.61
10	DI 1	TOC	2372	0.00	0.00	
11	DI 2	TOC	2183	0.00	0.00	
12	DI 3	TOC	2131	0.00	0.00	
13	DI/LowDOC1	TOC	86836	15.79	1.97	1.97
14	DI/LowDOC2	TOC	87544	15.93	1.99	1.99
15	DI/LowDOC3	TOC	86338	15.70	1.96	1.96
16	DI/HighDOC1	TOC	414685	78.38	9.80	9.80
17	DI/HighDOC2	TOC	412709	78.00	9.75	9.75
18	DI/HighDOC3	TOC	416051	78.64	9.83	9.83

LOW DOC = 2 ppm
HIGH DOC = 10 ppm
DI REPRESENTS LOW AT (<100uM)
TAP REPRESENTS HIGH AT (~3000 uM)

Tap/LowDOC vs DI/LowDOC
alpha = 0.05
reject the null; statistical difference

Tap/HighDOC vs DI/HighDOC
alpha = 0.05
reject the null; statistical difference

Fig. C2 – *Results of experiments examining the effects of an inorganic carbon matrix (described below) on both high and low ppm organic C standards.*

D. Appendix D – DUCS Additional Information

The software developed for the DUCS runs on programming that requires tubing to be connected to valves in a specific orientation, and also requires connection of the valves and pump to specific pin I/O outs on the TFX board. Using the DUCS will require a check of tubing and pin outs for proper use of the DUCS. To check for proper electrical connections, make sure the valves and pump I/O pins in Fig. D1 connect to the I/O pins for the similarly numbered valves and pump shown in Fig. D2. It should be noted that there is a I/O connection hub that all back-mounted I/O pins feed into. This hub allows for easy connection to the back mounted board through the connection hub, and this can be found be tracing the wiring coming from any of the back mounted I/Os. Electrical I/O's must match their respective valves or pump exactly, as the dedicated programming was made only for this configuration. In addition, make sure tubing is connected so that valve orientations match those as shown in the in Fig. D3, as improper valve connections will lead to improper sample collection or hardware damage.

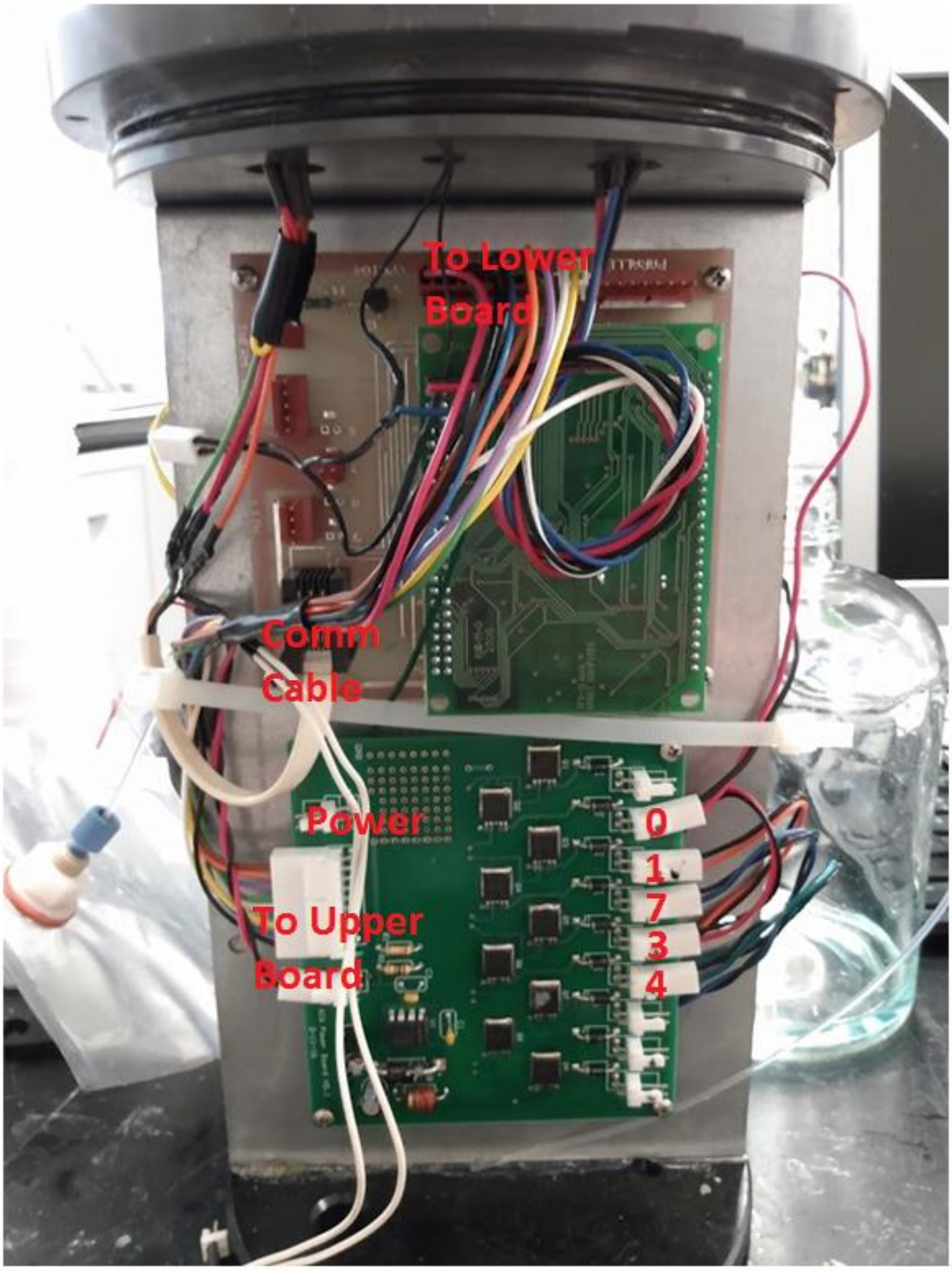

Fig. D1 – *Electrical connection diagram for the sample*

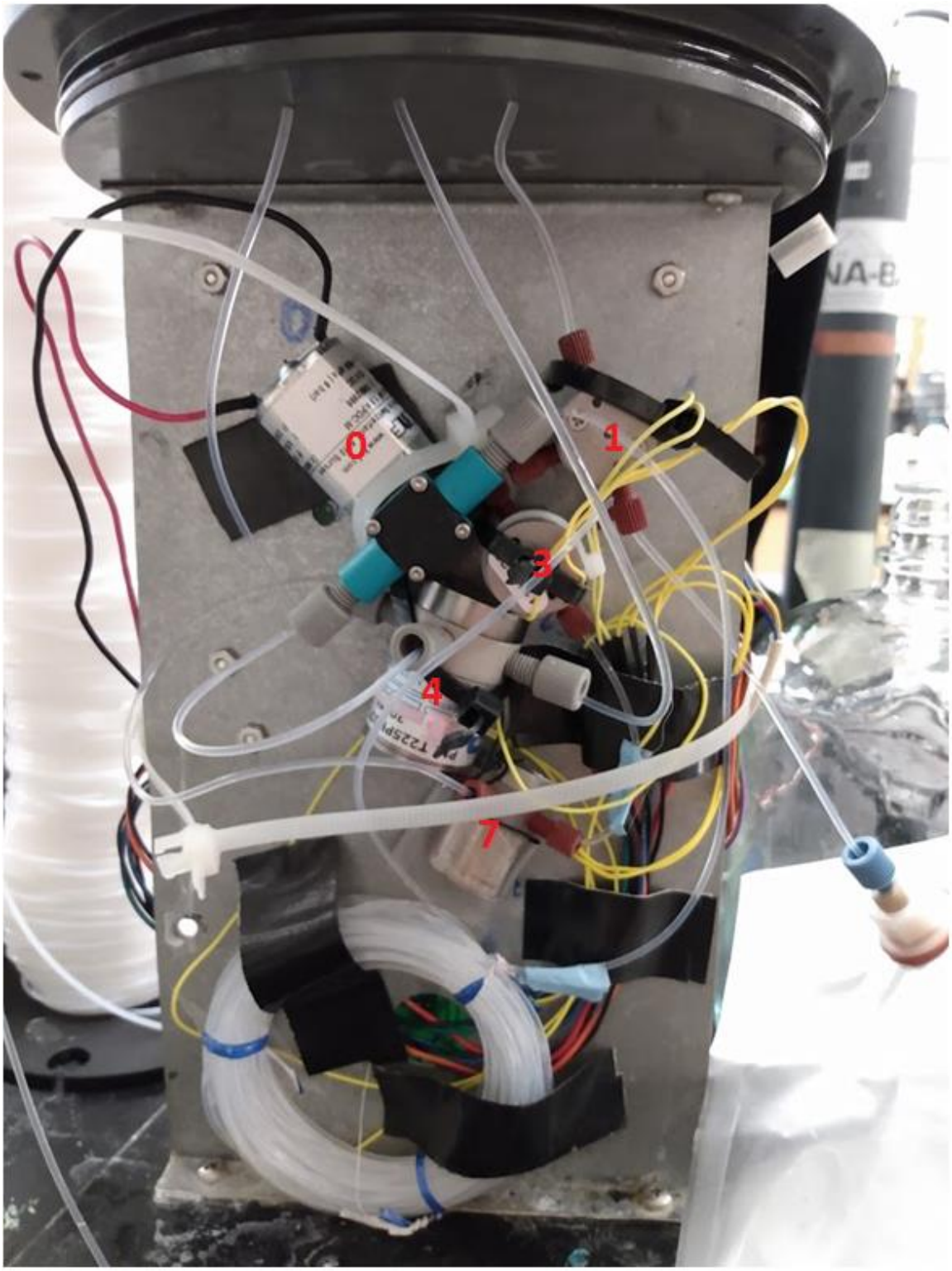

Fig. D2 *– Software specified pin-outs for valves and pump.*

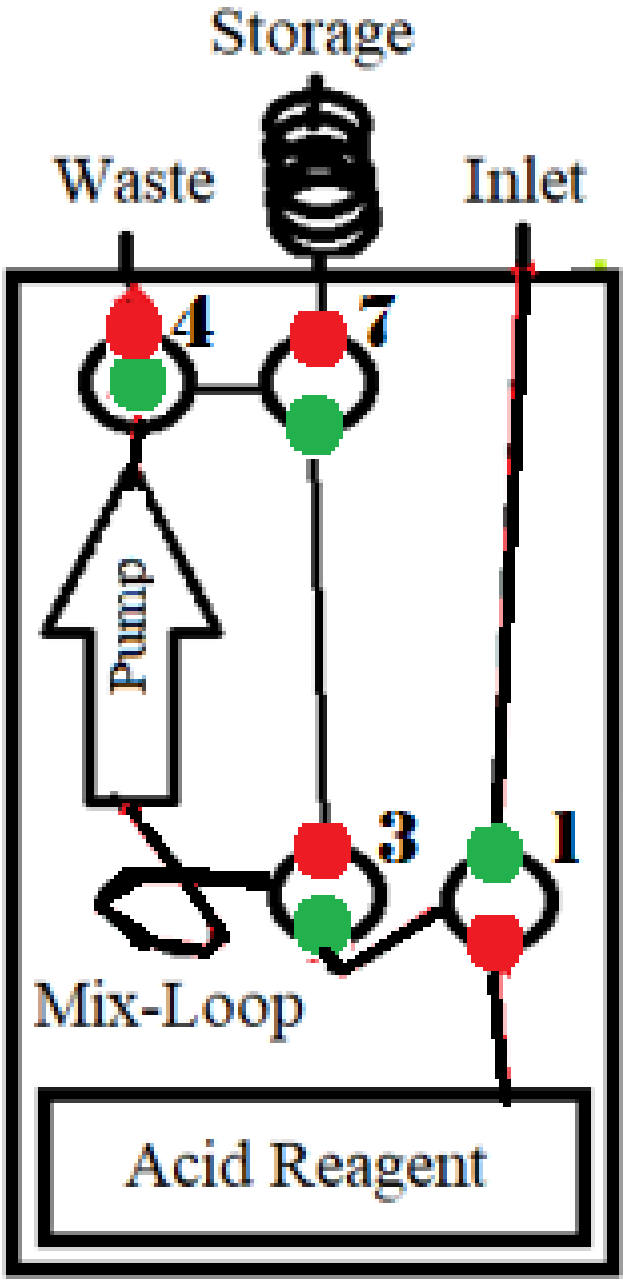

Fig. D3 *– Tubing diagram specifying proper Normally Open (NO) and Normally Closed valve configurations. NO valves are indicated in green and NC valves are indicated in red.*

Table D1 *– A table containing pump models tested and found to not be effective compared to the diaphragm pump in the current sampler setup.*

Pump Model	Manufacturer
1205P1220 - 5TP // 0431667	Bio Chem Valve
1505P12250 - 4EE // 0420812	Bio Chem Valve
LPLX0503100AA // 778260	Lee Co.
MCP-50-7 1/4 - 28 UNF	Takasgo Electric In.

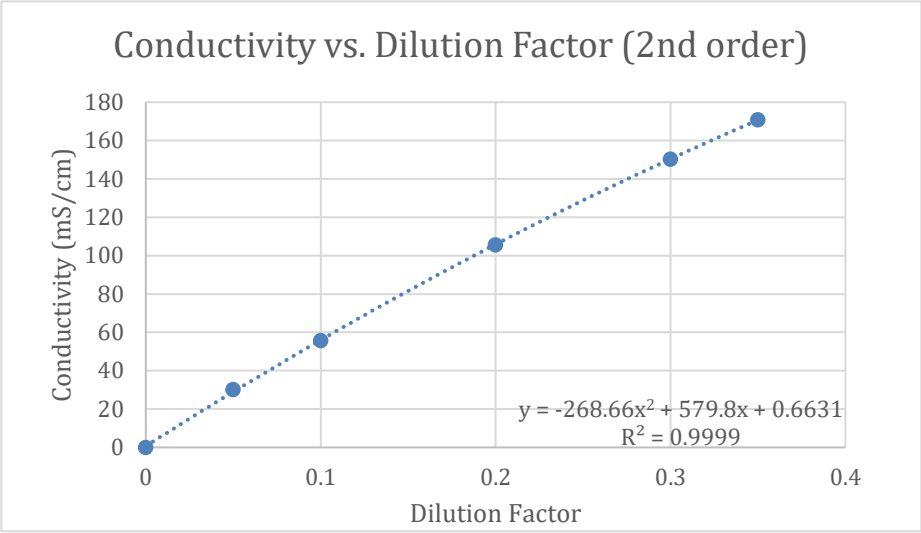

Fig. D4 - *Full range of dilution standard curve for a 5% HCl. The 2nd order polynomial is plotted to show the non-linear nature of conductivity over the full range of dilutions.*

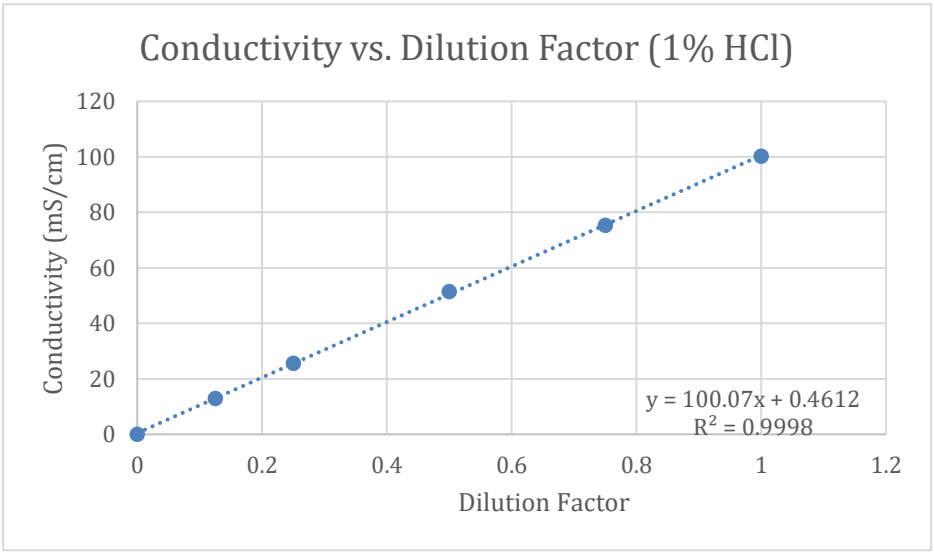

Fig. D5 *– Typical dilution standard curve for 1% HCl as used in early iterations of the sampler's method.*

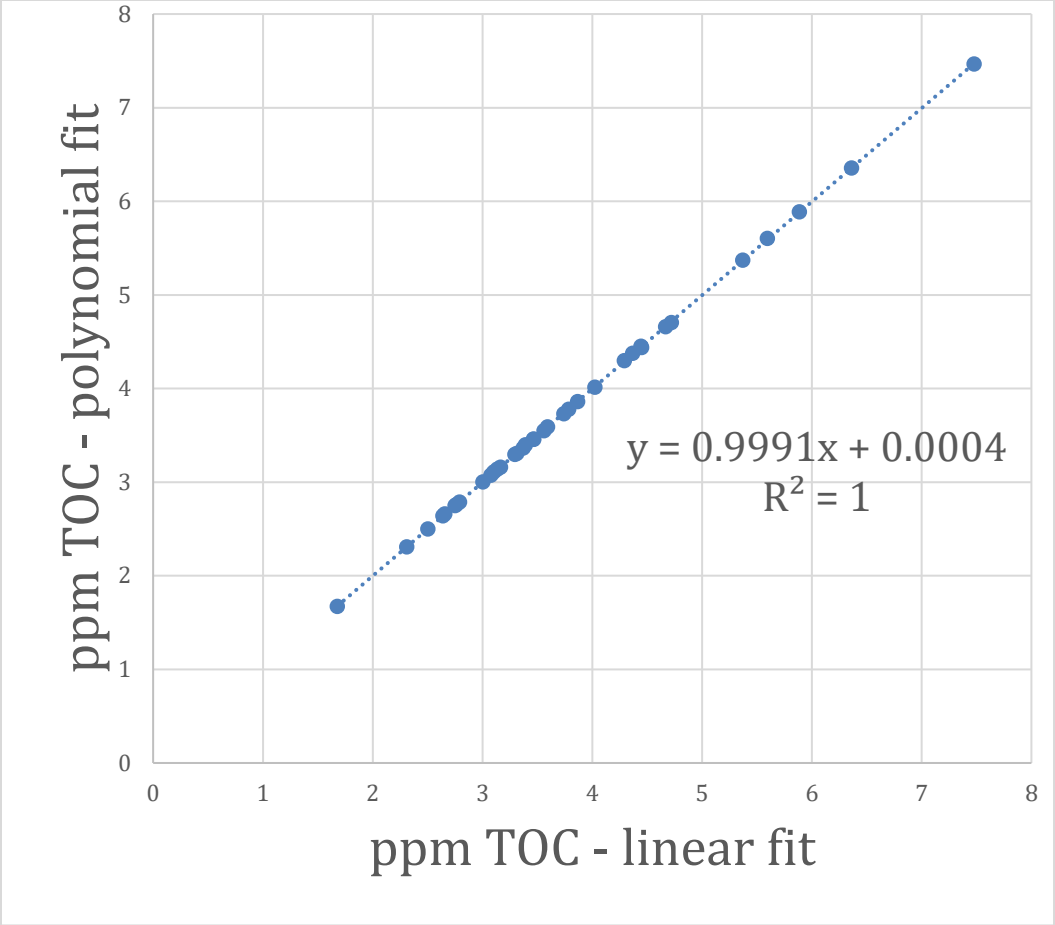

Fig. D6 *– 1:1 plot of TOC values found when dilution factors were found using either a linear or polynomial fit for calculating dilution factors. No statistical difference was found between either of the fits.*

E. Appendix E –Analytical Equipment Instrumental Specs

**Instrument specs in this Appendix were taken from their respective manufacturer's instrument manuals. **

Fig. E1

OI Aurora 1030

Operating Principle	Heated sodium persulfate oxidation
Measurement Technique	Non-dispersive infrared (NDIR) detection
Measurement Range	10 ppb C – 30,000 ppm C (multiple calibration ranges or dilution required)
Instrument Detection Limit (IDL)	2 ppb C
Operator Interface	Color LCD touchscreen display with Windows® CE-based software
Operating Modes	Standalone (Windows® CE), PC-controlled, or LAN/ LIMS network connectivity
Basic Software	Single instrument operation with data transfer to PC
Optional A_{TOC} Software	Network LAN/LIMS operation, data management, custom reports, and 21CFR11 compliance
Autosampler	88 position rotary autosampler designed to fit directly underneath Aurora 1030W analyzer
Sample Injection	Manual syringe, sipper tube, autosampler, or multi-stream at-line sampling module
Certification	CE, EMC: EN61326 / Safety: IEC 61010-11 2001
Reagents Required	Sodium persulfate, 5% phosphoric acid, rinsewater
Sample Injection Volume	10µL – 10mL
Method TC	Acid and persulfate reaction
Method TIC	Acidification with Phosphoric acid and sparging
Method TOC	NPOC by heated persulfate oxidation or TC-TIC
Heating	Adjustable to 100 °C in 1°C increments
Repeatability	2.0% or 2 ppb, whichever is greater
Linearity	±1% FS or 2% relative, whichever is greater
Sample pathway	Color coded Teflon® tubing
Sample handling	Syringe with isolation loop to prevent contamination
Gas Supply	N_2 (99.998%), zero-grade air, or O_2 (99.998%)
Power Supply	Variable voltage, 100-240VAC, 50/60 Hz, 950W
Dimensions – Aurora 1030	42.5 cm H x 49.5 cm W x 41.9 cm D (16.75 in. H x 19.5 in. W x 16.5 in. D)
Dimensions – Aurora 1030 + 1088 Autosampler	26.75 in. H x 19.5 in. W x 23 in. D
Weight – Aurora 1030 + 1088 Autosampler	15.4 kg (34 lbs.), 34.5 kg (76 lbs.) 1030W + 1088

Fig. E2

Mettler Toledo

FiveEasy Cond meter F30

+Cond probe InLab 751-4

Specifications - Cond probe InLab 751-4mm	
Measuring range	0.01 – 100 mS/cm
Temperature Range	0 °C – 100 °C
Connector	Mini-DIN
Cell type	2 platinum poles
Cell Constant	1.0 cm-1
Shaft Material	Glass
Shaft length	120 mm
Shaft Diameter	4 mm
Cable (Length)	1.2 m
Parameter	Conductivity
ISM	No
Temperature probe	NTC 30 kΩ
For portable meter	No
Maintenace-free	Yes
Signal type	Analog
Sample	Small samples

Specifications - FiveEasy Cond meter F30	
Parameter	Conductivity
Channel	Single-channel
Version kit	Meter only
Conductivity measuring range	0.01 µS/cm-200 mS/cm
Conductivity resolution	0.01 – 2
Conductivity accuracy (±)	0.5 %
mV accuracy (±)	0
Temperature Range	0 °C – 100 °C
Temperature Resolution	0.1 °C
Temperature accuracy (±)	0.5 °C
Portable	No
ISM support	No

F. Appendix F – Additional Protocols

i. POC/TOC Standard Preparation Protocol

i. Measure out 0.022g of Brewer's Yeast that has been stored at 0 °C to prevent biologic activity onto an analytical grade balance.

ii. Place weighed Brewer's Yeast into a 1000 mL volumetric flask and dilute to the line with Nanopure water. This will create an unfiltered POC stock solution of ~ 10 mg C/L (ppm).

iii. The solution will then be filtered using vacuum filtration with a Whatman 12-25 μm filter and collected into an acid-washed 1-L glass flask and sealed with airtight cap. Filtration will ensure removal of any particles >100 μm in diameter which must be excluded for analysis on the Aurora. Following subsequent standard preparation steps, the remainder of this stock solution will then be stored at 0 °C to continue suppression of biologic activity.

iv. Using this POC stock solution, an initial set of POC standards will be generated for analysis. From dilution of the primary stock solution, standards with expected concentrations of ~2.5, and 5.0 ppm POC will be prepared. These standards will be prepared using a 100 mL volumetric flask for the ~2.5 ppm POC standard and a 50 mL volumetric flask for the ~5.0 ppm POC standard with delivery of undiluted POC stock being added with a 25 mL acid-washed pipette.

v. A calibration curve will be generated with a KHP-based DOC standard.

vi. Following instrument calibration, the ~2.5 and 5 ppm standards will be analyzed along with an end-of-run and start-of-run DI blank. During oxidation, the CO_2 peak count will be visually monitored to ensure there is a complete return to baseline. Additionally, the reaction chamber should visually be monitored to ensure no particulate buildup within the instrument is occurring.

vii. Initial analysis results are used to check that the CO_2 peak count from the 2.5 and 5.0 ppm POC standard is similar in value to the 2.5 and 5.0 ppm C KHP generated peak counts.

viii. Instrument POC carryover should also be checked at this point by making sure that there is no statistical difference between the pre-run DI blank and the end-of-run DI blank.

ix. Assuming these initial tests look okay, a POC standard curve should then be obtained using triplicate analysis of 0.5, 1, 2.5, and 5 ppm POC standards created from dilution of the stock POC solution. The reproducibility of the triplicate standards in addition to the linearity of the POC calibration curve will then be assessed.

x. If based on the above evaluation of reproducibility and linearity full oxidation of POC is not occurring, vary combustion conditions (*e.g., react time, reagent concentrations*) to allow for a more complete oxidation.

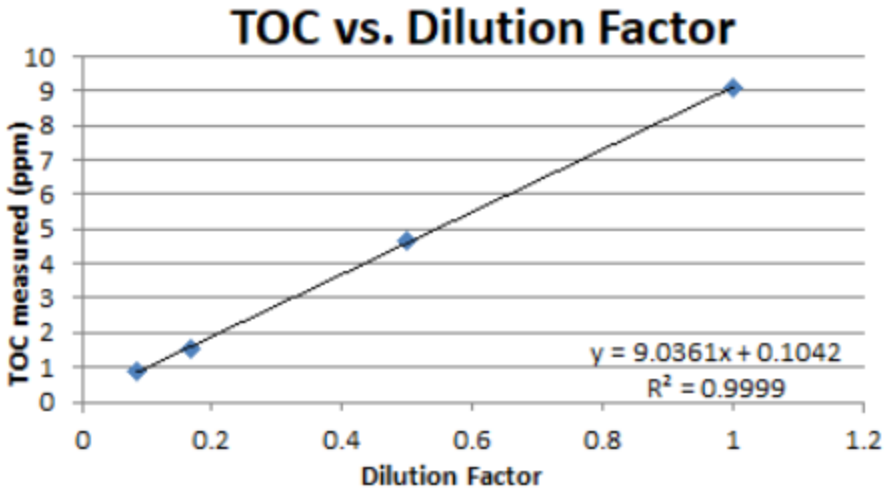

Fig. F1 *– Dilution Factor curve for the POC standard created using the methodology above.*

ii. Small vial cleaning and conductivity analysis procedure.

i. *Dump all liquid out of the small vials. Rinse used vials and caps with 3x with hot tap water, then rinse 3x with DI water.*

ii. Prepare a 1-L bath of 10% HCl. Replace this bath after 3x cleaning sessions.

iii. Place rinsed vials in bath, make sure all vials are fully submerged in solution with no bubbles. This will involve using gloves and manually "sinking" vials.

iv. Let soak in acid-bath for 24 hours, and then remove the small vials and dump the liquid out to waste.

v. Place in an oven at > 100 ^{o}C for 4 hours to dry and ash the small vials.

vi. Load the ashed vials in the small vial holder (Fig F1). When not in use cover with a clean cloth.

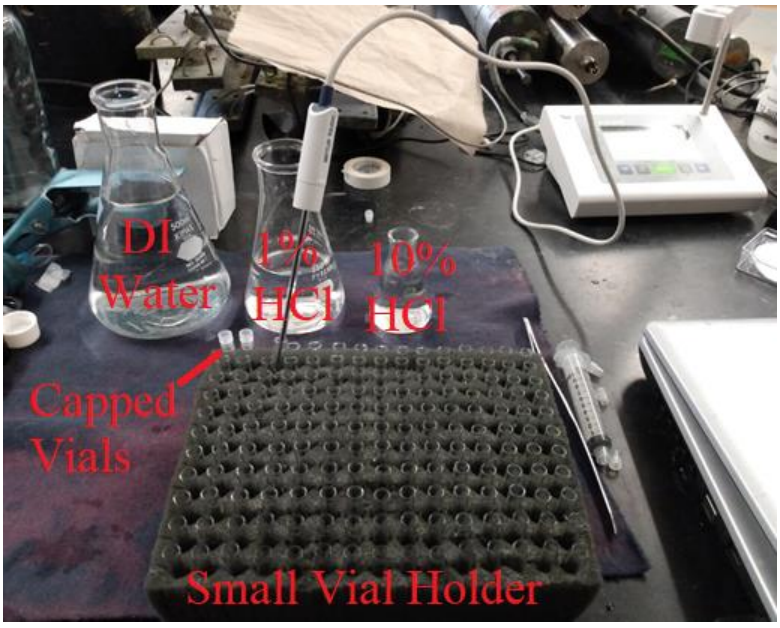

Fig. F2 *– Conductivity probe and meter station setup*

Conductivity Analysis Procedure

i. Following a sample set, the visual indicator will be noticeable on the outer shell of the storage coil. (Fig. F2)

ii. Dispense the visual indicator to waste. After the indicator has been dispensed, initiate the Storage Coil Dispense sequence.

iii. The sampler will start to dispense sample in "pulses" move the outlet to each successive small vial after each pulse. Cap small vials while dispensing to prevent any evaporation of sample, as this step is time consuming.

iv. *Calibrate the conductivity probe and meter using the 12.88 mS/cm single point calibration. Allow 5 minutes for calibration*

v. *Once the small vial holder is fully loaded, start uncapping vials and taking conductivity readings for sample in the small vials.*

Figure F3 *– Visual Indicator on outer shell of coil.*

vi. *The conductivity probe has two small holes at the end where the electrodes are. Set the probe in at an angle so sample flows through these holes to prevent bubbles and get an accurate conductivity reading. Gently swirl the probe in the vial and then wait for a steady (~30 seconds unchanging) reading.*

vii. *Following each conductivity reading, the probe must be cleaned to prevent cross-contamination of sample between vials. Dip the conductivity probe in the 10% HCl for 10 seconds, then move the probe to the 1% HCl solution for 10 seconds, and finally to the DI solution for 10 more seconds (Fig. F1).*

viii. *After soaking the probe in the series of cleaning solutions, it is dried by using the heat gun on low until the meter is reading a signal of < 5 uS/cm. At this point the probe is ready to take another reading.*

This material is based upon work supported in part by the National Science Foundation EPSCoR Cooperative Agreement OIA-1757351. Any opinions, findings, and conclusions or recommendations expressed in this material are those of the author(s) and do not necessarily reflect the views of the National Science Foundation.

VIII. References Cited

Ågren, A., Berggren, M., Laudon, H. & Jansson, M. (2008). Terrestrial export of highly bioavailable carbon from small boreal catchments in spring floods. *Freshwater Biology, vol. 53,* 964–972.

Aiken, G., Kaplan, L. A., Weishaar, J. (2002). Assessment of relative accuracy in the determination of organic matter concentrations in aquatic systems. *Journal of Environmental Monitoring, vol. 4,* 70-74.

Amundson, E. L., Pratt, J. E. & Hemond, H. F. (2000). Gastight sampler for sequential streamflow sampling. *Water Environmental Research, vol. 3,* 377-383.

Asmala, E., Harguchi, L., Jakobsen, H. H., Massicotte, P. & Carstensen, J. (2018). Nutrient availability as major driver of phytoplankton-derived dissolved organic matter transformation in coastal environment. *Biogeochemistry, vol. 137,* 93-104.

Baken, S., Degryse, F., Verheyen, L., Merckx, R. & Smolders, E. (2011). Metal Complexation Properties of Freshwater Dissolved Organic Matter Are Explained by Its Aromaticity and Anthropogenic Ligands. *Environmental Science & Technology, vol. 45 (7),* 2584-2590.

Battin, T. J., Luyssaert, S., Kaplan, L. A., Aufdenkampe, A. K., Richter, A. & Tranvik, L. J. (2009). The boundless carbon cycle. *National Geoscience, vol. 2,* 598–600.

Benner, R. & Hedges J. I. (1993). A test of the accuracy of freshwater DOC measurements by high-temperature catalytic oxidation and UV-promoted persulfate oxidation. *Marine Chemistry, vol. 41,* 161-165.

Benner, R. & Kaiser, K. (2011). Biological and photochemical transformations of amino acids and lignin phenols in riverine dissolved organic matter. *Biogeochemistry, vol. 102,* 209–222.

Bishop, K. H., Grip, H. & O'Neill, A. (1990). The origins of acid runoff in a hillslope during storm events. *Journal of Hydrology, vol. 116,* 35–61.

Bolan, N.S., Baskaran, S. & Thiagarajan, S. (1996). An evaluation of the methods of measurement of dissolved organic carbon in soils, manures, sludges, and stream water. *Communications in Soil Science and Plant Analysis, vol. 27,* 2723-2737.

Buffle, J., Deladoey, P., Zumstein, J. & Haerdi, W. (1982). Analysis of characterization of natural organic matter in freshwater. I. Study of Analytical techniques. *Swiss Journal of Hydrology, vol. 44,* 327–362.

Cai, W. J., Wang, Y. & Hodson, R. E. (1998). Acid–base properties of dissolved organic matter in the estuarine waters of Georgia. *Geochimica et Cosmochimica Acta, vol. 62(3),* 473–483.

Calleja, M. L., Al-Otaibi, N. & Moran, X. A. G. (2019). Dissolved organic carbon contribution to oxygen respiration in the central Red Sea. *Scientific Reports, vol. 9,* 4690.

Carstea, M. E., Popa, C. P., Baker, A. & Bridgeman, J. (2020). In situ fluorescence measurements of dissolved organic matter: A review. *Science of the Total Environment, vol. 45, 699,* 343-361.

Carter, H. T., Tipping, E., Kopriyniak, J. F., Miller, M. P., Cookson, B. & Hamilton-Taylor, J. (2012). Freshwater DOM quantity and quality from a two-component model of UV absorbance. *Water Research, vol. 46,* 4532-4542.

Cauwet, G. (2002). DOM in the coastal zone. *Biogeochemistry of Marine Dissolved Organic Matter. Academic Press, San Diego,* 579–609.

Chavez, F. P., Jannasch, H. W., Johnson, K. S., Sakamoto, C. M., Friedrich G. E., Thurmond, G. D., Harlein, R. A. & Codispoti, L. A. (1991). The MBARI program for obtaining real-time measurements in Monterey Bay. *Oceans, vol. 91,* 327-333.

Coffin, R. B., Connolly, J. P. & Harris, P. S. (1993). Availability of dissolved organic carbon to bacterioplankton examined by oxygen utilization. *Marine Ecology Progress Series, vol. 101,* 9-21.

Cole, J. J., Findlay, S. & Pace, M. L. (1988). Bacterial production in fresh and saltwater ecosystems: A cross-system over-view. *Marine Ecology Progress Series, vol. 43,* 1-10.

Cooper, K. J., Whitaker, F. F., Anesio, A. M., Naish, M., Reynolds, D. M. & Evans, E. L. (2016). Dissolved organic carbon transformations and microbial community response to variations in recharge waters in a shallow carbonate aquifer. *Biogeochemistry, vol. 129,* 215-234.

Cook, S., Peacock, M. & Page, S. (2016). Cold storage as a method for the long-term preservation of tropical dissolved organic Carbon (DOC). *Mires and Peat, vol. 18,* 1-8.

Dafner, E. V. & Wagnersky, P. J. (2002). A brief overview of modern directions in marine DOC studies – Part 1. Methodological aspects. *Journal of Environmental Monitoring, vol. 4,* 48-54.

DeGrandpre, M. D., Hammar, T. R., Smith, S. P. & Sayles, F. L. (1995). In situ measurements of seawater pCO_2. *Limnology and Oceanography, vol. 40 (5),* 969-975.

Dickey, T., Frye, D., Jannasch, H. W., Boyle, E. & Knap, A. H. (1997). Bermuda sensor system testbed. *Sea Technology, vol. 38,* 81-86.

Downing, B. D., Pellerin, B. A., Bergamaschi, B. A., Saraceno, J. F. & Kraus, T. E. C. (2012). Seeing the light: The effects of particles, dissolved materials, and temperature on in situ measurements of DOM fluorescence in rivers and streams. *Limnology and Oceanography: Methods, vol. 10,* 767-775.

Doyle, A., Weintraub, M.N. & Schimel, J.P. (2004). Persulfate digestion and simultaneous colorimetric analysis of carbon and nitrogen in soil extracts. *Soil Science Society of America Journal, vol. 68,* 669-676.

Ekstorm, S. M., Kritzberg, E. S., Kleja, D. B., Larsson, N., Nilsson, P. A., Wilhelm, G. & Bergkvist, B. (2011). Effect of Acid Depostion on Quantity and Quality of Dissolved Organic Matter in Soil-Water. *Environmental Science and Technology.* 4733-4739.

Ensign, S. H. & Paer, H. W. (2006). Development of an unattended estuarine nutrient monitoring program using ferries as data collection platforms. *Limnology and Oceanography, vol. 4,* 399-405

Evans, C. D. & Thomas D. N. (2016). Controls on the processing and fate of terrestrially-derived organic carbon in aquatic ecosystems: synthesis of special issue. *Aquatic Sciences, vol. 78,* 415-418.

Fang, Z., He, C., Li, Y., Chung, K. H., Xu, C. & Shi, Q. (2017). Fractionation and Characterization of Dissolved Organic Matter (DOM) in Refinery Wastewater by Revised Phase Retention and Ion-Exchange Adsorption Solid Phase Extraction Followed by ESI FT-ICR MS. *Talanta, vol. 162,* 466-473.

Ferretto, N., Tedetti, M., Guigue, C., Mounier, S., Raimbault, P. & Goutx, M. (2016). Spatio-temporal Variability of Fluorescent Dissolved Organic Matter in the Rhone River Delta and the Fos-Marseille Marine Area (NW Mediterranean Sea, France). *Environmental Science and Pollution Research International, vol. 5,* 4973-4989.

Freeman, C., Evans, C.D., Monteith, D.T., Reynolds B. & Fenner, N. (2001). Export of organic carbon from peat soils. *Nature, vol. 412,* 785-785.

Gianguzza, A., Pelizzetti E. & Sammartano S. (2013) Chemical Processes in Marine Environments. *Springer Science & Business Media,* 304-311.

Guggenberger, G. (1994). Acidification effects on dissolved organic matter mobility in spruce ecosystems. *Environment International, vol. 20,* 31–41.

Hansell, D. A. (2013). Recalcitrant dissolved organic carbon fractions. *Annual Review of Marine Science, vol. 5,* 421-445.

Harshad, K., Mladenov, N. & Datta, S. (2019). Effects of acidification on the optical properties of dissolved organic matter from high and low arsenic groundwater and surface water. *Science of the Total Environment, vol. 653,* 1326-1332.

Helton, A. M., Wright, M. S., Bernhardt, E. S., Poole, G. C., Cory, R. M. & Stanford, J. A. (2015). Dissolved organic carbon lability increases with water residence time in the alluvial aquifer of a river floodplain ecosystem. *Journal of Geophysical Resaearch: Biogeosciences, vol. 120,* 693-706.

Hood, E., Gooseff, M. N. & Johnson, S. L. (2006). Changes in the character of stream water dissolved organic carbon during flushing in three small watersheds, Oregon. *Journal of Geophysical Research: Biogeosciences, vol. 111,* GO1007 1-8.

Hruška, J., Krám, P., McDowell, W. H. & Oulehle, F. (2009). Increased Dissolved Organic Carbon (DOC) in Central European Streams is Driven by Reductions in Ionic Strength Rather than Climate Change or Decreasing Acidity. *Environmental Science and Technology, vol. 43,* 4320– 4326.

Hunt, C. W., J. E. Salisbury & Vandermark, D. (2011). Contribution of non-carbonate anions to total alkalinity and overestimation of pCO2 in New England and New Brunswick rivers. *Biogeosciences, vol. 8(10),* 3069–3076.

Huntington, T. G., Balch, W. M., Aiken, G. R., Sheffield, J., Luo, L., Roesler, C. S. & Camill, P. (2016). Climate change and dissolved organic carbon export to the Gulf of Maine. *Journal of Geophysical Research: Biogeosciences, vol. 121,* 2700-2716.

Jannasch, H. W., Johnson, K. S. & Sakamoto C.M. (1994). Submersible, osmotically pumped analyzers for continuous determination of nitrate in situ. *Analytical Chemistry. vol. 66,* 3352-3361.

Jannasch, H. W., Wheat, C. G., Plant, J. N., Kastner, M. & Stakes, D. S. (2004). Continuous chemical monitoring with osmotically pumped water samplers: OsmoSampler design and applications. *Limnology and Oceanography: Methods vol. 2,* 102-113.

Jaffe, R., McKnight D., Maie, N., Cory, R., McDowell, W. H. & Campbell, J. L. (2008). Spatial and temporal variations in DOM composition in ecosystems: The importance of long-term monitoring of optical properties. *Journal of Geophysical Research: Biogeosciences, vol. 113,* 15.

Johnson, K. S., Beehler, C. L. & Sakamoto, C. M. (1986). A submersible flow analysis system. *Analytical Chimica Acta, vol. 179,* 245-257.

Jollymore, A., Johnson, M. S. & Hawthorne, I. (2012). Submersible UV-Vis spectroscopy for quantifying streamwater organic carbon dynamics: implementation and challenges before and after forest harvest in a headwater stream. *Sensors (Basel), vol. 12,* 3798–3813.

Kaiser, K., Guggenberger, G., Haumaier, L. & Zech, W. (2001). Seasonal variations in the chemical composition of dissolved organic matter in organic forest floor layer leachates of old-growth Scots pine and European beech stands in northeastern Bavaria, Germany. *Biogeochemistry, vol. 55,* 103–143.

Karanfil, T., Schlautman, M.A. & Erdogan, I. (2002). Survey of DOC and UV measurement practices with implications for SUVA determination. *Journal of American Water Works Association, vol. 94,* 68–80.

Karl, D. M. & Lukas, R. (1996). The Hawaii Ocean Time-series (HOT) program: Background, rational and field implementation. *Deep Sea Research, vol. 43,* 129-156.

Kastner, M. (1995). Long-term continuous monitoring of fluid composition with an osmotically pumped fluid sampler. *International Workshop on Dynamics of Lithosphere Convergence,* Miyagi, Japan.

Khan, E., Babcock, R. W., Viriyavejakul, S., Suffet, I. H. & Stenstrom, M. K. (1998). Biodegradable dissolved organic carbon for indicating wastewater reclamation plant performance and treated wastewater quality. *Water Environment Research, vol. 70 (5),* 1033.

Kieren, K., Chris, B., Stevens, R. & Hannah, D. (2019). Continuous field estimation of dissolved organic carbon concentration and biochemical oxygen demand using dual-wavelength fluorescence, turbidity and temperature. *Hydrological Processes, vol. 31 (3),* 11040.

Kirchner, J. W., Feng, X. H., Neal, C. & Robson, A. J. (2004). The fine structure of water-quality dynamics: the (high-frequency) wave of the future. *Hydrological Processes, vol. 18,* 1353–1359.

Köhler, S. J., Buffam, I., Laudon, H. & Bishop, K. H. (2008). Climate's control of intra-annual and interannual variability of total organic carbon concentration and flux in two contrasting boreal landscape elements. *Journal of Geophysical Research, vol. 113,* 223-230.

Kritzberg, S. A., Pace, M. L., Cole, J. J., Greneli, W. & Bade, D. L. (2004). Autochtonous versus allochthonous carbon sources of bacteria: Results from whole-lake ^{13}C addition experiments. *Limnology and Oceanography, vol. 49(2),* 588-596.

Lai, C., DeGrandpre, M. D. & Darlington, R. C. (2018). Autonomous Optofluidic Chemical Analyzers for Marine Applications: Insights from the Submersible Autonomous Moored Instruments (SAMI) for pH and pCO_2. *Frontiers in Marine Science, vol. 4,* 438.

Li, Y. H. & Gregory, S. (1974). Diffusion of ions in sea water and in deep-sea sediments. *Geochimica et Cosmochimica Acta, vol. 38,* 703-714.

Liang, C., Bruell, C. J., Marley, M. C. & Sperry, K. L. (2003). Thermally Activated Persulfate Oxidation of Trichloroethylene (TCE) and 1,1,1-Trichloroethane (TCA) in Aqueous Systems and Soil Slurries. *Soil Sediment Contamination, vol. 12,* 207-228.

MacKinnon, M. D. (1979). The measurement of the volatile organic fraction of the TOC in seawater. *Marine Chemistry, vol. 8,* 143-162.

Marschner, B. & Kalbitz, K. (2003). Controls of bioavailability and biodegradability of dissolved organic matter in soils. *Geoderma, vol. 113,* 211–236.

Martz, T. R., Dickson, A. G., & DeGrandpre, M. D. (2006). Tracer Monitored Titrations: Measurement of Total Alkalinity. *Analytical Chemistry, vol. 78,* 1817-1826.

Massoth, G. J., Baker, E. T., Feely, R. A., Butterfield, D. A., Embley, R. E., Lupton, J. E., Thomson, R. E. & Cannon, G. A. (1995). Observations of manganese and iron at the CoAxial seafloor eruption site, Juan de Fuca Ridge. *Geophysical Research Letters, vol. 22,* 151-154.

McDonough, L. K., Santos, I. R., Anderson, M. S., O'Carroll, D. M., Rutlidge, H., Meredith, K., Oudone, P., Bridgeman, J., Gooddy, D. C., Sorensen, J. P. R., Lapworth, D. J., MacDonald, A. M., Ward., J & Baker, A. (2020). Changes in global groundwater organic carbon driven by climate change and urbanization. *Nature Communications, vol. 11,* 1279.

McDowell, W. H. (2003). Dissolved organic matter in soils future-directions and unanswered questions. *Geoderma, vol. 113,* 179–186.

Michaels, A. F. & Knap, A. H. (1996). Overview of the U.S. JGOFS Bermuda Atlantic Time-series Study and the Hydrostation S program. *Deep Sea Research, vol. 43,* 157-198.

Moore, S., Gauci, V., Evans., C.D. & Page, S.E. (2011). Fluvial organic carbon losses from a Bornean blackwater river. *Biogeosciences, vol. 8*, 901–909.

Nebbioso, A. & Piccolo, A. (2013). Molecular Characterization of Dissolved Organic Matter 829 (DOM): A Critical Review. *Analytical and Bioanalytical Chemistry, vol. 405*, 109–124.

Park, S. K., Pak K. R., Choi, S. C. & Kim, Y. K. (2004). Evaluation of bioassays for analyzing biodegradable dissolved organic carbon in drinking water. *Journal of Environmental Health, vol. 39*, 103-112.

Piccolo, A. (2001). The Supramolecular Structure of Humic Substances. *Soil Science, vol. 166*, 810-836.

Qualls, R. G. & Haines, B. L. (1992). Factors controlling concentration, export, and decomposition of dissolved organic nutrients in the Everglades of Florida. *Soil Science Society of America Journal, vol. 56*, 578–586.

Rebstock, G.A. (2002). An analysis of a zooplankton sampling gear change in the CalCOFI long-term monitoring program, with implications for copepod population abundance trends. *Progress in Oceanography, vol. 53*, 215-230.

Regier, P. & Jaffe, R. (2016). Short term dissolved organic carbon dynamics reflect tidal, water management, and precipitation patterns in a subtropical estuary. *Frontiers in Marine Science, vol. 3*, 1-13.

Ritson, J. P., Graham, N. J. D., Templeton, M. R., Clark, J. M., Gough, R., Freeman, C. (2014). The impact of climate change on the treatability of dissolved organic matter (DOM) in upland water supplies: A UK perspective. *Science of the Total Environment, vol. 473-474*, 714-730.

Ross, P., Frederick, H., Marco, D. & Alksandra, K. (2013). A comparative study of three different assimilable organic carbon (AOC) methods: Results of a round-robin test. *Water Science & Technology Water Supply, vol. 13*, 1024-1028.

Sando, S. K. & Vecchia, A. V. (2016). Water Quality Trends and Constituent-Transport Analysis for Selected Sampling Sites in the Milltown Reservoir/Clark Fork River Superfund Site in the Upper Clark Fork Basin, Montana, Water Years 1996-2015. *Scientific Investigations Report 2016-5100.*

.

Falcon, Y. S., Salgado, X. A. A., Hernandez, M. D. P., Guerra, A. H. G., Mason, E. & Aristegui, J. (2017) Organic carbon budget for the eastern boundary of the North Atlantic subtropical gyre: major role of DOC in mesopelagic respiration. *Scientific Reports, vol. 7*, 10129.

Saraceno, J. F., Pellerin, B. A., Downing, B. D., Boss, E., Bachand, P. A. M. & Bergamaschi, B. A. (2009). High-frequency in situ optical measurements during a storm event: Assessing relationships between dissolved organic matter, sediment concentrations, and hydrologic processes. *Journal of Geophysical Research, vol. 114*, 11-20.

Saraceno, J. F., Shanley, J. B., Downing, B. D. & Pellerin, B. A. (2017). Clearing the waters: Evaluating the need for site-specific field fluorescence corrections based on turbidity measurements. *Limnology and Oceanography: Methods, vol. 15*, 408-416.

Schiff, S. L., Aravena, R., Trumbore, S. E. & Dillon, P. J. (1990). Dissolved Organic Carbon Cycling in Forested Watersheds: A Carbon Isotope Approach. *Water Resources Research vol. 26 (12),* 2949-2957.

Schulze, W. (2005). Protein Analysis in Dissolved Organic Matter -What Proteins from Organic Debris, Soil Leachate and Surface Water Can Tell Us-a Perspective. *Biogeosciences, vol. 2(1),* 75–86.

Sharp, H. J., Benner, R., Bennett, L., Carlson, C. A., Dow, R. & Fitzwater, S. E. (1993). Re-evaluation of high temperature combustion and chemical oxidation measurements of dissolved organic carbon in seawater. *Limnology and Oceanography, vol. 8,* 45-50.

Smiley, B. P. & Trofymow, J. A. (2017). Historical effects of dissolved organic carbon export and land management decisions on the watershed-scale forest carbon budge of a coastal British Columbia Douglas-fir-dominated landscape. *Carbon Balance and Management, vol. 12,* 15.

Sobczak, W. V. & Raymond, P. A. (2015). Watershed hydrology and dissolved organic matter export across time scales: minute to millennium. *Freshwater Science, vol. 34,* 392–398.

Stewart, A. & Wetzel, R. (1981). Dissolved humic materials: Photodegradation, sediment effects, and reactivity with phosphate and calcium carbonate precipitation. *Archive for Hydrobiology, vol. 92,* 265–286.

Strohmeier, S., Knorr, K. H., Reichert, M., Frei, S., Fleckenstein, J. H., Peiffer, S. & Matzner, E. (2013). Concentrations and fluxes of dissolved organic carbon in runoff from a forested catchment: insights from high frequency measurements. *Biogeosciences, vol. 10,* 905–916.

Tate, C. M. & Meyer, J. L. (1983). The Influence of Hydrologic Conditions and Successional State on Dissolved Organic Carbon Export from Forested Watersheds. *Ecology, vol. 64,* 25–32.

Taylor, G. (1953). Dispersion of soluble matter in solvent flowing slowly through a tube. *Proceedings of the Royal Society, vol. 219,* 186-203.

Thornton, D. C. (2014). Dissolved organic matter (DOM) release by phytoplankton in the contemporary and future ocean. *European Journal of Phycology, vol. 49,* 20-46.

Thurman, E. M. (1985). Organic Geochemistry of Natural Waters. *Springer,* 490-497.

Todres, Z. V. (2003). Organic Ion Radicals: Chemistry and Applications. *Marcel Dekker, Inc. New York,* 8-25.

Tunaley, C., Tetzlaff, D., Lessels, J. & Soulsby, C. (2016). Linking high-frequency DOC dynamics to the age of connected water sources. *Water Resource Research, vol. 52,* 5232-5247.

Ummenhofer, C. C. & Meehl, G. A. (2017). Extreme weather and climate events with ecological relevance: a review. *Philosophical Transactions of the Royal Society London: Biological Sciences, vol. 372,* 1723-1725.

Vaughan, M. C. H., Bowden, W. B., Shanley, J. B., Vermilyea, A., Sleeper, A., Gold, A. J., Pradhanang, S. M., Inamdar, S. P., Levia, D. F., Andres, A. S., Birgand, F. & Schroth, A. W. (2017). High-Frequency Dissolved Organic Carbon and Nitrate Measurements Reveal

Differences in Storm Hysteresis and Loading in Relation to Land Cover and Seasonality. *Water Resources Research, vol. 53(7),* 5345–5363.

Vidon, P. G., Hubbard, H. A., Cuadra, P. E. & Hennessy, M. L. (2012). Storm Dissolved Organic Carbon Dynamics in an Artificially Drained Watershed of the US Midwest. *Air, Soil and Water Research. vol. 5.* 103-115.

Wallace, B. & Purcell, M. (2002) Total organic carbon analysis as a precursor to disinfection byproducts in potable water: Oxidation technique considerations. *Journal of Environmental Monitoring. vol. 4.* 35-42.

Wallin, M. B., Weyhenmeyer, G. A., Bastviken, D., Chmiel, H. E., Peter, S., Sobek, S. & Klemedtsson, L. (2015). Temporal control on concentration, character, and export of dissolved organic carbon in two hemiboreal headwater streams draining contrasting catchments. *Journal of Geophysical Research: Biogeosciences, vol. 120(5),* 1-14.

Wang, A. Z., Bienvenu, D. J., Mann, P. J., Hoering, K. A., Poulsen, J. R., Spencer, R. G. M. & Holmes, R. M. (2013). Inorganic carbon speciation and fluxes in the Congo River. *Geophysical Research Letters, vol. 40,* 511-516.

Weeks, D. A. & K. S. Johnson. (1996). Solenoid pumps for flow injection analysis. *Analytical Chemistry, vol. 68,* 2717-2719.

Westra, S., Fowler, H. J., Evans, J. P., Alexander, L. V., Berg, P., Johnson, F., Kendon, E. J., Lenderink, G. & Roberts, N. M. (2014). Future Changes to the intensity and frequency of short-duration extreme rainfall. *Review of Geophysics, vol. 52,* 522-555.

Winterdahl, M., Laudon, H., Lyon, S. W., Pers, C. & Bishop, K. (2015). Sensitivity of stream dissolved organic carbon to temperature and discharge: Implications of future climates. *Journal of Geophyiscal Research – Biogeosciences, vol. 121,* 126–144.

Worrall, F., Howden, N. J. K., & Burt, T. P. (2013). Assessment of sample frequency bias and precision in fluvial flux calculations – An improved low bias estimation method. *Journal of Hydrology, vol. 503,* 101-110.

Yan, M., Korshin, G., Wang, D. & Cai, Z. (2012). Characterization of dissolved organic matter using high-performance liquid chromatography (HPLC)-size exclusion chromatography (SEC) with a multiple wavelength absorbance detector. *Chemosphere, vol. 87,* 879-885.

Yi, Y., Xiao, M., Mostofa, K. M. G., Xu, S. & Wang, Z. (2019). Spatial Variations of Trace Metals and Their Complexation Behavior with DOM in the Water of Dianchi Lake, China. *International Journal of Environmental Research and Public Health, vol. 16,* 4919.

Zarnetske, J. P., Bouda, M., Abbott, B. W., Saiers, J. & Raymond, P. A. (2018). Generality of Hydrologic Transport Limitation of Watershed Organic Carbon Flux Across Ecoregions of the United States. *Geophysical Research Letters, vol. 45,* 45-50.